2015

Understanding the thermochemical conversion of biomass to overcome biomass recalcitrance

Kwang Ho Kim
Iowa State University

Understanding the thermochemical conversion of biomass to overcome biomass recalcitrance

by

Kwang Ho Kim

A dissertation submitted to the graduate faculty

in partial fulfillment of the requirements for the degree of

DOCTOR OF PHILOSOPHY

Major: Agricultural and Biosystems Engineering

Program of Study Committee:
Robert C. Brown, Co-Major Professor
Xianglan Bai, Co-Major Professor
Kurt Rosentrater
Matthew Darr
Brent Shanks
Young Jin Lee

Iowa State University

Ames, Iowa

2015

DEDICATION

Dedicated to my family for their unwavering support and encouragement over the years.

TABLE OF CONTENTS

ACKNOWLEDGEMENTS

I would like to express the deepest appreciation to my advisor Dr. Robert Brown, for his excellent guidance, caring, support, and providing me with an excellent atmosphere for doing research. He always uplifted my spirit with compliment. I would never have been able to finish my PhD work without his guidance.

I would also like to thank my co-advisor, Dr. Xianglan Bai for guidance and mentorship. Her great passion for her work always inspired me. I would like to thank my committee consisting of Dr. Brent Shanks, Dr. Young-Jin Lee, Dr. Kurt Rosentrater and Dr. Matt Darr, for all of help along the way. I really appreciate valuable discussions, which helped guide me to finishing this work.

I am very thankful for all of the help and discussion with staff at the Bioeconomy Institute, in particular Ryan Smith, Marjorie Rover, Patrick Johnston and Patrick Hall. Also, I am grateful to all of my colleagues at BEI for all of the valuable discussions and help. I was so fortunate to meet and work with them, including Tannon Daugaard, Kaige Wang, Martin Haverly, Mitchell Amundson, Chamila Thilakaratne (Rajeeva), Joseph Polin, Karl Broer, Bernardo Del Campo, Matt Kiefer, Juan Proano, Preston Gable and Longwen Ou.

I would also like to thank my former adviser, Dr. Joon Weon Choi, for the opportunities, guidance and motivation in numerous ways during my Master's work.

Finally, I would like to greatly thank all my family, my parents and brother. They were always supporting me and encouraging me with their best wishes. Also, I would like to thank my fiancée, Jeongah Lee. She was always there cheering me up and stood by me through the good times and bad. She really deserves a big thank you.

ABSTRACT

Thermochemical conversion technologies are promising pathways for producing environmentally benign, sustainable biofuels and value-added chemicals from biomass. However, reaction pathways and chemistry behind these technologies such as pyrolysis and solvolysis of biomass are very complex. Contributing to the complexity are the many factors that could affect the reaction mechanisms. This research focuses on an external effect on thermal decomposition and internal reaction chemistry to provide an insight into the biomass decomposition for better performance.

First, the effect of low concentration of oxygen in sweep gas during biomass pyrolysis in fluidized bed was investigated for practical purpose. It was found that the partial oxidative pyrolysis can increase the yield of pyrolytic sugars. A continuation of the study was performed to produce sugar-rich bio-oil from the biomass passivation of alkali and alkaline earth metals. Partial oxidative pyrolysis of passivated biomass produced approximately 21 wt% hydrolyzable sugars in bio-oil. Additionally, partial oxidative pyrolysis also prevented clogging within the reactor by reducing char agglomerations ensuring continuous operation.

Second, solvolytic conversion of lignin was studied using a micro reactor in the presence of a hydrogen donor solvent. The results showed that hydrogen donor solvents were effective in converting lignin into alkylphenols. It was found that a hydrogen donor solvent could suppress repolymerization reactions by stabilizing the primary products to alkyl-substituted phenols.

Pyrolysis mechanisms of lignin were further studied using methoxy substituted α-O-4 dimeric model compounds. Pyrolysis of aryl-ether linkage primarily involved homolytic cleavage. It was discovered that methoxy group substitution on the aromatic ring increases the reactivity toward C – O homolysis. Additionally, free radicals in the condensed phase of the pyrolysis products were detected by electron paramagnetic resonance spectroscopy, providing information on the presence of oxygen-centered phenoxy and carbon-centered benzyl radicals. Furthermore, methoxy group substitution was revealed to promote oligomerization reactions to form large molecular weight compounds.

Lastly, a quantitative investigation of free radicals in bio-oil and their potential role in condensed-phase polymerization was conducted. It was confirmed that both lignin and cellulose pyrolysis involve homolytic cleavage generating free radicals. Lignin bio-oil fractions contained a significant amount of radicals, which were found to be stable species due to highly delocalized in a π system.

.

CHAPTER 1

INTRODUCTION

The biomass opportunity

Our overdependence on fossil fuels poses risks for the sustainable survival of human society [1]. First of all, fossil fuel reserves are being depleted more rapidly due to an increasing world population. The amount of fossil fuels we consume today is very large, and our consumption is predicted to rise by 60% or so in the next 25 years unless we can replace it on a very large scale [1]. Second, fossil fuel consumption has been attributed to global warming due to the net increase in atmospheric greenhouse gases derived from the burning of fossil fuels. The atmospheric concentration of greenhouse gases will continue to rise to historically unprecedented levels unless the nations around the world work in concert to reduce emission of these gases [2]. Also, geopolitical strife could arise from the competition for limited resources which could lead to economic and energy disruptions, ultimately resulting in international political disputes.

These situations, along with the need for reducing foreign oil dependency and the environmental awareness of world's population has led to a search for alternative primary energy and carbon sources based upon renewable sources [3]. Biomass, especially lignocellulosic material, represents an abundant renewable carbon source. As the only source of renewable carbon, biomass shows great promise for the large-scale economical production of renewable fuels and chemicals [4].

Biomass is an abundant resource that can be produced in agriculture, forestry and aquatic systems. The total energy content from this amount of biomass via heat of

combustion analysis is approximately five times the energy content of the total worldwide crude oil consumption [4]. A recent study that looked specifically at US production capability and showed the potential for the sustainable production of 1.3 billion dry tons per year of biomass from forest and agricultural lands without negatively impacting food, feed and fiber production while still meeting export demands [5].

Biomass: Structures of plant cell wall

The basic structure of all plant cell wall consists of three organic polymers: cellulose, hemicellulose and lignin. Cellulose is the main constituent of biomass. Approximately 40 - 45 % of the dry substance in most biomass is cellulose, located predominantly in the secondary cell wall [6]. Cellulose is a homopolysaccharide composed of β-D-glucopyranose units which are linked together by (1 → 4)-glycosidic bonds, as shown in Figure 1. Cellulose molecules are completely linear and have a strong tendency to form intra and intermolecular hydrogen bonds. Bundles of cellulose molecules are aggregated together in the form of microfibrils, in which highly ordered crystalline regions alternate with less ordered amorphous regions [6, 7]. These microfibrils build up fibrils and finally cellulose fiber.

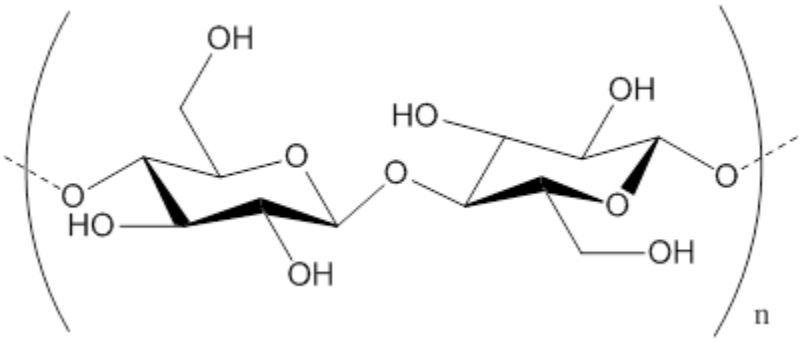

Figure 1. Structure of cellulose

Hemicelluloses belong to a group of heterogeneous polysaccharides which are formed through biosynthetic routes different from that of cellulose. In contrast to cellulose, which is a homopolysaccharide, hemicelluloses are heteropolysaccharides [6]. In hardwoods, the major hemicellulose component is the *O*-acetyl-4-*O*-methylglucuronoxylan (Figure 2), whereas in the softwood species, the *O*-acethylgalactoglucomannan (Figure 3) is the predominant component [3]. Depending on the hardwood species, the xylan content varies within the limits of 15 – 30 % of the dry wood. The amount of galactoglucomannan, in softwood is about 20 % [6]. Hemicellulose is thought to bind non-covalently to the surface of cellulose fibrils. It acts as an amorphous matrix material, holding the stiff cellulose fibrils in place [8]. Due to its non-crystalline nature, hemicellulose is more susceptible to depolymerization than cellulose.

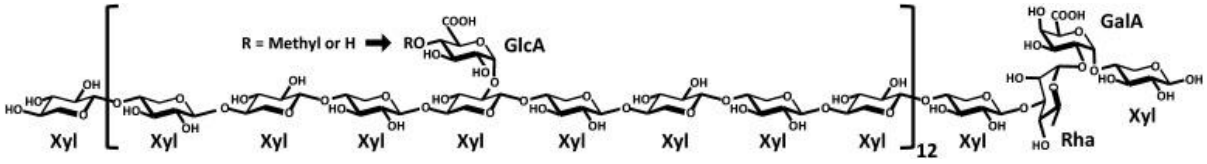

Figure 2. Structure of glucuronoxylan [9]

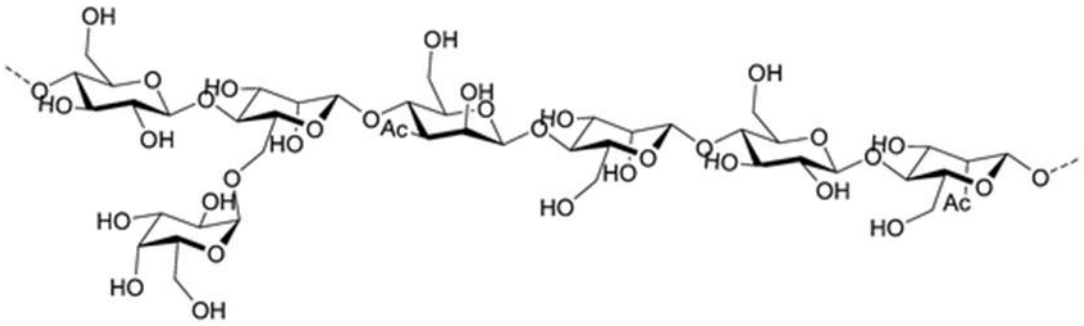

Figure 3. Structure of galactoglucomannan [8]

Lignin, a heterogeneous aromatic polymer, is the second most abundant biopolymer after cellulose [10]. Lignin is synthesized in the plant cell wall via phenylpropanoid pathway. Based on their aromatic ring substitution pattern, lignin is designated as *p*-hydroxyphenyl (H unit), guaiacyl (G unit) and syringyl (S unit). The three monolignols are shown in Figure 4. Significantly, many of the monolignol and lignin-forming pathway steps apparently also evolved during transition of plants to the land habitat. To put this pathway into the broader context of carbon allocation from photosynthesis, woody gymnosperm stems generally have lignin contents ~28 – 30 %, whereas those in woody angiosperms are of lower amount ~20 – 24 % [4, 11].

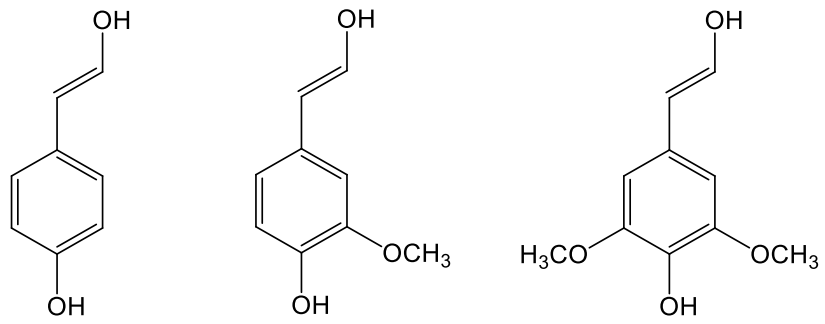

Figure 4. Three monolignols acting as source materials for biosynthesis of lignin (p-coumaryl alcohol, coniferyl alcohol and sinapyl alcohol; from left to right)

There are several linkage types in lignin structure, including β-O-4, 5-5, β-5, 4-O-5, and β-β, of which the β-O-4 linkage is dominant. Table 1 shows the proportions of different types of linkages in lignin. As indicated, the dominant linkage in both softwood and hardwood is the β-O-4 linkage. The identification and quantification of the various structures and linkages in lignin is a considerable challenge as the lignin molecule is very complex [12]. In any case, lignin represents a significant commitment and designation of the total carbon

taken up during photosynthesis; indeed, the lignins are some of the most metabolically expensive of all plant products formed [13].

Table 1. Proportions of different types of linkages connecting the phenylpropane units in lignin [6]

Linkage type	Dimer structure	Percent of the total linkages	
		Softwood	Hardwood
β-O-4	Arylglycrol- β-aryl ether	50	60
α-O-4	Noncyclic benzyl aryl ether	2-8	7
β-5	Phenylcoumaran	9-12	6
5-5	Biphenyl	10-11	5
4-O-5	Diaryl ether	4	7
β-1	1,2-Diaryl propane	7	7
β-β	Linked through side chains	2	3

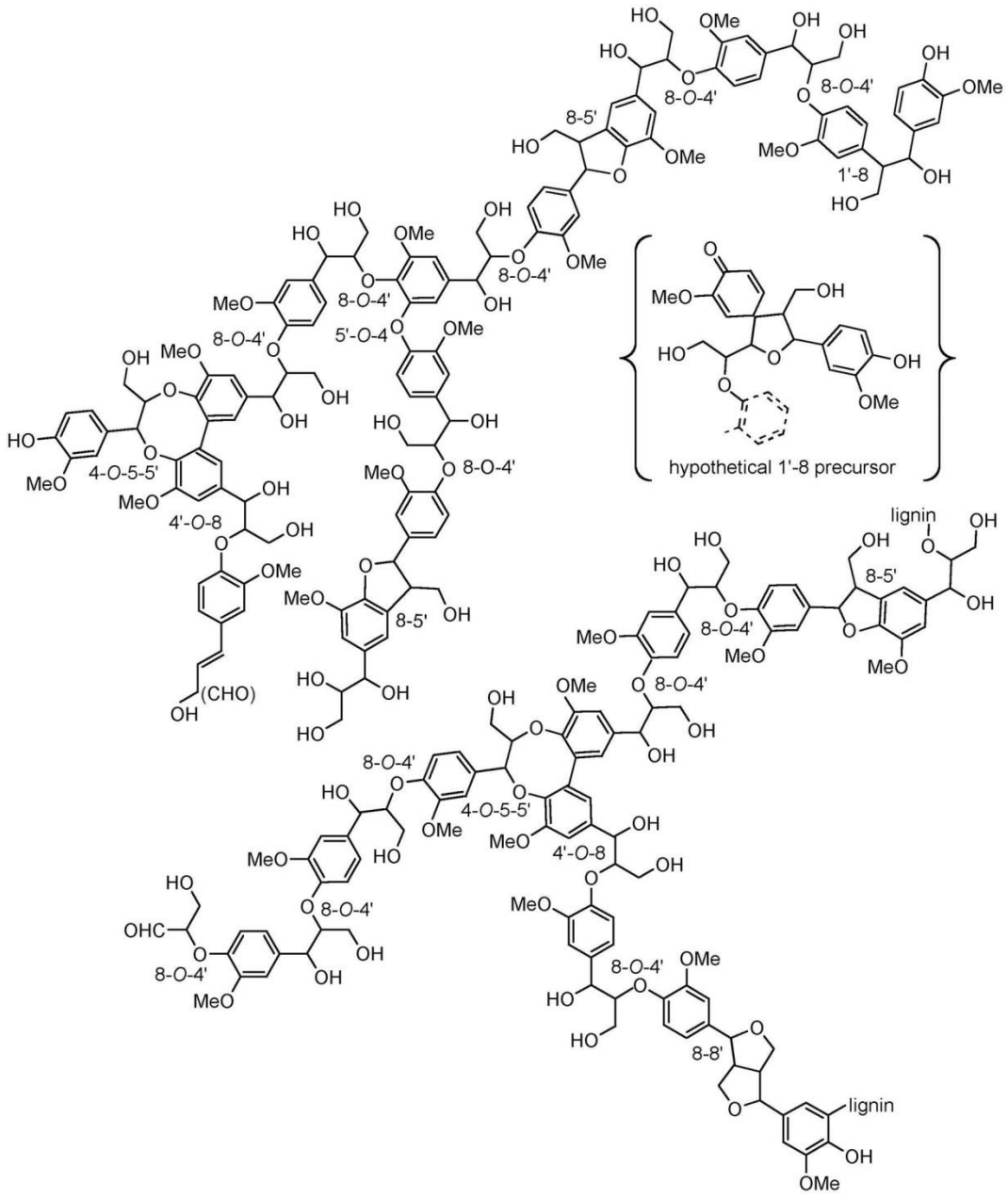

Figure 5. A structural segment of lignin proposed by Brunow et *al*. [14]

Biorefinery opportunity: Thermochemical processing of biomass

The reliability, affordability and environmental impact of energy supplies have become a critical issue for the world's economy [3]. Due to world population growth, primary energy consumption has increased and will continue to increase in the future. As

mentioned above, lignocellulosic biomass is potentially convertible to energy, fuels and green chemicals. The integrated production of biofuel, through advanced processes of separation and conversion while minimalizing carbon cycle impact, defines the biorefinery concept [3]. The term “biorefinery” is a refinery utilizing biomass as a feedstock to produce gaseous and liquid fuels, specialty or commodity chemicals, or other products commonly produced in petrochemical refineries, where the feedstocks are mainly fossil fuels [15]. Several new processes are being developed for usage in a biorefinery. Among them, the thermochemical platform is one of the most promising conversion technologies that can be adopted in a biorefinery.

Thermochemical processes

Thermochemical processing of biomass uses heat and catalysts to transform plant polymers into fuels, chemicals or electric power [16]. This contrasts with biochemical processing of biomass, which utilizes enzymes and microorganisms for the same purpose. Thermochemical routes can be categorized as combustion, gasification, fast pyrolysis, hydrothermal processing and hydrolysis to sugars [16].

Thermal gasification is the conversion of solid, carbon-rich materials at elevated temperatures (typically 750 – 1500 ˚C) and under oxygen-starved conditions into syngas, a flammable gas mixture of carbon monoxide, hydrogen, methane, nitrogen, carbon dioxide and smaller quantities of hydrocarbons [2]. One of the most attractive features of gasification is its flexibility of application, including thermal power generation, hydrogen production and synthesis of fuels and chemicals. This offers the prospect of gasification-based energy

refineries, producing a mix of energy and chemical products or allowing the staged introduction of technologies as they reach commercial viability [16].

Fast pyrolysis is the rapid thermal decomposition of organic compounds in the absence of oxygen to produce liquids, gases and char [17]. The distribution of products depends on the biomass composition and other reaction conditions including residence time, temperature, etc. The resulting bio-oil is a complex mixture of oxygenated organic compounds including carboxylic acids, alcohols, aldehydes, saccharides and phenolic compounds. This bio-oil has been used as fuel for both boilers and gas turbine engines, although its production cost, corrosiveness and instability during storage have impeded its commercial deployment [16]. Bio-oil can be upgraded to transportation fuels through a combination of steam reforming of light oxygenates in the bio-oil to provide hydrogen and hydrocracking lignin oligomers and carbohydrate to synthetic diesel fuel or gasoline [18-20].

Solvolysis is pyrolysis in the presence of a solvent. The process is known as direct liquefaction although this overlooks the prospects for also fractionating or gasifying biomass via solvolysis [2]. A variety of solvents can be employed, their physical and chemical properties determining the temperature and pressures at which the processes operate. Because water is a major constituent of biomass, it is frequently used as a solvent, in which case solvolysis is referred to as hydrothermal processing.

Thermochemical conversion characteristics of biomass components

Carbohydrates are the major constituents of biomass. Understanding the pyrolytic behavior of carbohydrates is important as the interest in utilizing bio-oil obtained from fast pyrolysis of biomass for fuels and chemicals is growing. There have been many works on

pyrolysis of cellulose to elucidate products distribution and reaction mechanisms, and so on [21-25]. Patwardhan et *al*. [26] investigated the product distribution of fast pyrolysis of several glucose-based carbohydrates. They revealed that levoglucosan, a major pyrolysis product from cellulose, and low molecular weight compounds are formed through competitive pyrolysis reactions rather than sequential pyrolysis reaction. Also it was found that the oligomerization of levoglucosan and decomposition of primary products such as 5-hydroxymethyl furfural and furfural were the major secondary reactions [24].

The pyrolysis behavior of hemicellulose is different from cellulose pyrolysis. First of all, it starts to decompose lower temperature than cellulose, around from 220 to 315 ˚C [27]. And the primary pyrolysis products obtained from hemicellulose are furfural, formic acid, acetic acid and some mono- or disaccharides [28]. Patwardhan et *al.* revealed that decarboxylation is one of the preliminary steps of hemicellulose decomposition [28] releasing acetic acid [29]. Additionally, they found that the yield of low molecular weight species was enhanced by increasing the pyrolysis temperature.

Lignin is quite challenging to thermally decompose compared to carbohydrates. This is because of its structural complexity, very hydrophobic character, and its relative intractability due to difficulties of efficiently solubilize [4]. And their striking abilities to self-associate [30] due to the strong electronic stabilization energies between the various subunits in the adjacent biopolymeric chains [4]. Also, lignin depolymerization is challenging given the broad distribution of bond strengths among the various C – O and C – C linkages in lignin and the tendency for low-molecular-weight species to undergo recondensation, often to more recalcitrant species [31]. Thus, several so called lignin model compounds have been studied due to the structural complexity of linin. For example, the characteristics of thermal

decomposition of monomeric model compounds such as guaiacol [32], catechol [33, 34] and dimeric model compounds [35-37] were investigated. Usually, lignin thermally decomposes from 160 to 900 ˚C, and the generated solid residue is very high (~40 wt%) [27]. However, simple model compounds cannot provide representative results due to the variation and complication in lignin structure. Therefore, more in-depth studies are necessary to better understand its properties during thermal decomposition.

Dissertation organization

This dissertation is composed of five chapters in addition to the introduction (Chapter 1) and conclusions (Chapter 7). Chapter 2 and 3 discuss oxidative pyrolysis of biomass. Chapter 2 focuses on pyrolysis with small amounts of oxygen in carrier gas and its effect on the product distribution and chemical properties. Oxygen is usually excluded from pyrolysis reaction to prevent oxidation of biomass. However, it's difficult to achieve a fully inert environment because the void space in biomass contains air. Thus, the main goal of this study was to understand the effect of oxygen on pyrolysis of biomass.

Chapter 3 explores the effect of oxygen in sweep gas on passivated biomass to produce sugar-rich bio-oil. Previously, it was demonstrated that the yield of monosaccharides increased dramatically by passivation of the alkali and alkaline earth metals (AAEMs) to thermally stable salts. Combining this idea with previous work (Chapter 2), an extensive investigation was performed to produce sugar-rich bio-oil and is the focus of Chapter 3.

Chapter 4 discusses lignin solvolysis with assistance of hydrogen-donor solvents. When thermally decomposed, lignin fragments tend to form large molecular weight compounds, undesirable products. This leads to the hypothesis that lignin can produce

phenolic monomers in presence of hydrogen-donor reagents which are believed to prevent secondary repolymerization during reactions.

Chapter 5 discusses the mechanisms of lignin pyrolysis using model dimers. Methoxy-substituted three dimeric model compounds were chosen to understand the effect of methoxyl group on lignin pyrolysis. An electron paramagnetic resonance spectroscopy was used to elucidate the existence of free radicals produced from homolytic cleavage of lignin model dimers. The empirical evidence of free radicals supports our assumption that aryl ether linkages, the most frequent linkage type in lignin structure, involve in homolytic cleavage generating free radicals.

Chapter 6 is dedicated to the analysis of free radicals in bio-oils. Specifically, a quantitative analysis of free radicals in bio-oils produced from biomass components is performed. Also, their potential role in condensed-phase polymerization is discussed in this chapter. Although there have been many previous works on the chemical composition of bio-oil, few studies have focused on the free radicals, from its formation to thermal reactivity in bio-oil. Thus, it’s believed that this work could provide further insight into the chemistry of biomass pyrolysis.

REFERENCES

[1] B.E. Rittmann, Opportunities for renewable bioenergy using microorganisms, Biotechnol Bioeng 2008;100:203-12.

[2] R.C. Brown, T.R. Brown, Why are We Producing Biofuels?: Shifting to the Ultimate Source of Energy, Brownia LLC, 2012.

[3] P. Bajpai, Biorefinery in the Pulp and Paper Industry, Academic Press, 2013.

[4] M.E. Himmel, Biomass recalcitrance: deconstructing the plant cell wall for bioenergy, Wiley-Blackwell, 2009.

[5] R.D. Perlack, L.L. Wright, A.F. Turhollow, R.L. Graham, B.J. Stokes, D.C. Erbach, Biomass as feedstock for a bioenergy and bioproducts industry: the technical feasibility of a billion-ton annual supply, in, DTIC Document, 2005.

[6] E. Sjöström, Wood chemistry: fundamentals and applications, 2nd ed., Academic Press, Inc., San Diego, 1993.

[7] D. Klemm, B. Philipp, T. Heinze, U. Heinze, W. Wagenknecht, General Considerations on Structure and Reactivity of Cellulose: Section 2.1–2.1. 4, Wiley Online Library, 1998.

[8] A. Brandt, J. Grasvik, J.P. Hallett, T. Welton, Deconstruction of lignocellulosic biomass with ionic liquids, Green Chem 2013;15:550-83.

[9] B.R. Urbanowicz, M.J. Pena, S. Ratnaparkhe, U. Avci, J. Backe, H.F. Steet, M. Foston, H.J. Li, M.A. O'Neill, A.J. Ragauskas, A.G. Darvill, C. Wyman, H.J. Gilbert, W.S. York, 4-O-methylation of glucuronic acid in Arabidopsis glucuronoxylan is catalyzed by a domain of unknown function family 579 protein, P Natl Acad Sci USA 2012;109:14253-58.

[10] A.M. Boudet, A new view of lignification, Trends Plant Sci 1998;3:67-71.

[11] K.V. Sarkanen, C.H. Ludwig, Lignins: occurrence, formation, structure and reactions, Lignins: occurrence, formation, structure and reactions. 1971.

[12] J. Zakzeski, P.C.A. Bruijnincx, A.L. Jongerius, B.M. Weckhuysen, The Catalytic Valorization of Lignin for the Production of Renewable Chemicals, Chem Rev 2010;110:3552-99.

[13] N.G. Lewis, E. Yamamoto, Tannins—their place in plant metabolism, in: Chemistry and significance of condensed tannins, Springer: 1989, pp. 23-46.

[14] G. Brunow, I. Kilpeläinen, J. Sipilä, K. Syrjänen, P. Ka, Oxidative coupling of phenols and the biosynthesis of lignin, 1998.

[15] P. Axegård, The future pulp mill–a biorefinery, in: First international biorefinery workshop, Washington, 2005.

[16] R.C. Brown, Thermochemical processing of biomass: conversion into fuels, chemicals and power, John Wiley & Sons, 2011.

[17] A.V. Bridgwater, G.V.C. Peacocke, Fast pyrolysis processes for biomass, Renew Sust Energ Rev 2000;4:1-73.

[18] S. Czernik, R. French, C. Feik, E. Chornet, Hydrogen by catalytic steam reforming of liquid byproducts from biomass thermoconversion processes, Ind Eng Chem Res 2002;41:4209-15.

[19] D.C. Elliott, Historical developments in hydroprocessing bio-oils, Energ Fuel 2007;21:1792-815.

[20] M.M. Wright, D.E. Daugaard, J.A. Satrio, R.C. Brown, Techno-economic analysis of biomass fast pyrolysis to transportation fuels, Fuel 2010;89:S11-S19.

[21] J. Piskorz, P. Majerski, D. Radlein, A. Vladars-Usas, D.S. Scott, Flash pyrolysis of cellulose for production of anhydro-oligomers, J Anal Appl Pyrol 2000;56:145-66.

[22] H. Kawamoto, M. Murayama, S. Saka, Pyrolysis behavior of levoglucosan as an intermediate in cellulose pyrolysis: polymerization into polysaccharide as a key reaction to carbonized product formation, J Wood Sci 2003;49:469-73.

[23] Z.Y. Luo, S.R. Wang, Y.F. Liao, K.F. Cen, Mechanism study of cellulose rapid pyrolysis, Ind Eng Chem Res 2004;43:5605-10.

[24] P.R. Patwardhan, D.L. Dalluge, B.H. Shanks, R.C. Brown, Distinguishing primary and secondary reactions of cellulose pyrolysis, Bioresource Technol 2011;102:5265-69.

[25] D.K. Shen, S. Gu, The mechanism for thermal decomposition of cellulose and its main products, Bioresource Technol 2009;100:6496-504.

[26] P.R. Patwardhan, J.A. Satrio, R.C. Brown, B.H. Shanks, Product distribution from fast pyrolysis of glucose-based carbohydrates, J Anal Appl Pyrol 2009;86:323-30.

[27] H.P. Yang, R. Yan, H.P. Chen, D.H. Lee, C.G. Zheng, Characteristics of hemicellulose, cellulose and lignin pyrolysis, Fuel 2007;86:1781-88.

[28] P.R. Patwardhan, R.C. Brown, B.H. Shanks, Product Distribution from the Fast Pyrolysis of Hemicellulose, ChemSusChem 2011;4:636-43.

[29] D.K. Shen, S. Gu, A.V. Bridgwater, Study on the pyrolytic behaviour of xylan-based hemicellulose using TG-FTIR and Py-GC-FTIR, J Anal Appl Pyrol 2010;87:199-206.

[30] S. Sarkanen, D.C. Teller, C.R. Stevens, J.L. McCarthy, Lignin. 20. Associative interactions between kraft lignin components, Macromolecules 1984;17:2588-97.

[31] A.J. Ragauskas, G.T. Beckham, M.J. Biddy, R. Chandra, F. Chen, M.F. Davis, B.H. Davison, R.A. Dixon, P. Gilna, M. Keller, P. Langan, A.K. Naskar, J.N. Saddler, T.J. Tschaplinski, G.A. Tuskan, C.E. Wyman, Lignin Valorization: Improving Lignin Processing in the Biorefinery, Science 2014;344:709.

[32] Wahyudiono, M. Sasaki, M. Goto, Thermal decomposition of guaiacol in sub- and supercritical water and its kinetic analysis, J Mater Cycles Waste 2011;13:68-79.

[33] M.J. Wornat, E.B. Ledesma, N.D. Marsh, Polycyclic aromatic hydrocarbons from the pyrolysis of catechol (ortho-dihydroxybenzene), a model fuel representative of entities in tobacco, coal, and lignin, Fuel 2001;80:1711-26.

[34] E.B. Ledesma, N.D. Marsh, A.K. Sandrowitz, M.J. Wornat, An experimental study on the thermal decomposition of catechol, P Combust Inst 2002;29:2299-306.

[35] H. Kawamoto, S. Horigoshi, S. Saka, Pyrolysis reactions of various lignin model dimers, J Wood Sci 2007;53:168-74.

[36] T. Nakamura, H. Kawamoto, S. Saka, Pyrolysis behavior of Japanese cedar wood lignin studied with various model dimers, J Anal Appl Pyrol 2008;81:173-82.

[37] P.F. Britt, A.C. Buchanan, M.J. Cooney, D.R. Martineau, Flash vacuum pyrolysis of methoxy-substituted lignin model compounds, J Org Chem 2000;65:1376-89.

CHAPTER 2

THE EFFECT OF LOW-CONCENTRATION OXYGEN IN SWEEP GAS DURING PYROLYSIS OF RED OAK USING A FLUIDIZED BED REACTOR

A paper published in *Fuel*

Kwang Ho Kim, Xianglan Bai, Marjorie Rover, Robert Brown

Abstract

Partial oxidative pyrolysis of red oak was studied in a laboratory-scale, continuous fluidized bed reactor. The concentration of oxygen in sweep gas was between 0.525 % and 8.40 % (v/v), corresponding to equivalence ratios of 0.034 to 0.539. The influence of oxygen on the distribution and properties of pyrolysis products was investigated using various analytical methods, including GC-MS/FID, IC, HPLC and FT-IR. It was found that total bio-oil yield was not affected by varying oxygen concentration (61.2 – 64.8 g/100 g biomass) although the water content of the bio-oil increased. The elemental carbon content of bio-oil and biochar decreased with increasing oxygen concentration, being converted to non-condensable gases mainly CO and CO2. As expected, the presence of high concentration of oxygen in the sweep gas stream had detrimental effects on the pyrolysis products, including increase in water and oxygen content. However, the results also revealed that a small amount of oxygen in the sweep gas (0.525 to 1.05 %, v/v) improved the yield of hydrolyzable sugars and total yield of phenolic monomers. The bio-oil produced under oxidative pyrolysis also contained less acid and pyrolytic lignin. Oxygen increased the surface area of biochar. The results of this study suggest that carefully controlled partial oxidative pyrolysis can improve

the quality of bio-oil from fast pyrolysis, increasing the content of sugars and phenolic monomers.

Keywords: oxidative pyrolysis; bio-oil; levoglucosan; phenolic monomers; biochar

Introduction

Biomass resources present opportunities to produce liquid fuels and chemicals as alternatives to petroleum-based products [1]. As a carbon-neutral renewable source, biomass presents a promising approach to sustainable energy production. Among several thermochemical biomass conversion technologies, fast pyrolysis is attractive because it can transform a variety of recalcitrant biomass feedstocks into liquid fuels and other value-added products. Bio-oil produced from fast pyrolysis of biomass can be used directly as an energy source or it can be further upgraded into a higher quality fuel. For example, bio-oil can substitute for fuel oil in many applications, including boilers, furnaces, engines and turbines for electricity generation [2, 3]. Bio-oil has also been studied for production of hydrogen [4] and platform chemicals, including BTX (benzene, toluene and xylene) by catalytic upgrading [5, 6]. Fast pyrolysis produces gas, liquid and char as final products in different proportions. While it is well known that product distribution mainly depends on pyrolysis temperature and residence time [7], other experimental parameters also can influence the outcome of pyrolysis. Although fast pyrolysis of biomass is usually operated in an inert environment, several studies have investigated the effect of reactive gases on product distribution and properties of bio-oil and biochar. Marker et *al*. [8] studied hydropyrolysis of biomass using a fluidized bed reactor operated in 14-35 bar of hydrogen to produce gasoline and diesel fuels. Mante et *al*. [9] investigated the influence of recycling non-condensable gases including CO,

CO_2 and H_2 as a part of sweep gas on pyrolysis of biomass and reported increased liquid yield and decreased char/coke yield compared to use of inert sweep gas.

It has been previously reported that oxygen can promote devolatilization reactions during pyrolysis [10-12]. Butt [11], investigating the influence of molecular oxygen during low-temperature (290-295°C) fast pyrolysis of pine, reported a positive influence on increasing the yield of monomeric phenols. However, the total yield of phenolic monomers was very low (0.02-0.64%) due to the low pyrolysis temperatures where lignin only partly depolymerizes. Amutio et *al*. [13] used oxygen to achieve autothermal operation of a conical spouted bed pyrolyzer but found it decreased the yield of organic compounds in the bio-oil by 6%. Previous studies of oxidative pyrolysis used thermogravimetric analyzers to simulate fast pyrolysis and employed relatively high concentrations (approximately 5 – 21 vol%) of oxygen in the sweep gas [10, 14-16]. Oxygen is usually excluded from pyrolyzers to the extent practical to prevent oxidation of biomass and pyrolysis products and formation of light gases and water. However, achieving a fully inert environment is difficult in continuous pyrolyzers because the void space in bulk biomass contains air. Thus, understanding the effect of oxygen on pyrolysis of biomass is important in predicting product yields. In order to better understand the effects of low concentrations of oxygen in the sweep gas of biomass pyrolyzers, we introduced a relatively small amount of oxygen to a laboratory-scale fluidized bed pyrolyzer. The influence of molecular oxygen on the distribution, compositions and properties of the resulting pyrolysis products was assessed in detail.

Materials and methods

Feedstock

Northern red oak *(Quercus Rubra)* used in this study was obtained from Wood Residuals Solutions (Montello, WI). Bark-free chips were ground and sieved to a constant size (250-400 μm) and then air dried to around 7-8 wt.% moisture content. Ultimate and proximate analyses of the red oak are presented in Table 1.

Table 1. Ultimate and proximate analysis of red oak

Ultimate analysis (wt. %)	
Carbon	46.13
Hydrogen	6.38
Oxygen[1)]	47.34
Nitrogen	0.15
Proximate analysis (wt. %)	
Moisture content	7.74
Volatiles	80.39
Fixed carbon	11.46
Ash	0.64

[1)] Determined by difference

Pyrolysis

Fast pyrolysis of red oak was performed using a laboratory-scale, continuous fluidized bed reactor. A schematic diagram of the reactor is shown in Fig. 1. The reactor consisted of a feeder, an injection auger, and a stainless steel reactor 0.34 m in height and 38.1 mm in diameter. The plenum, which was designed to preheat nitrogen sweep gas and provide a uniform supply of nitrogen through the porous distributor plate, was 0.17 m in height with an inner diameter of 38.1 mm. Silica sand with average diameter of 520 μm was used as a heat carrier. The feed rate of biomass was 100 g/h. For the control run, nitrogen sweep gas was introduced into the plenum at 8 standard liters per minute (SLPM) and purged

through the feed system at 2 SLPM leading to a total flow rate of 10 SLPM. All pyrolysis experiments were performed at 500 °C. The calculated vapor residence time in the reactor was estimated to be 1.2 sec.

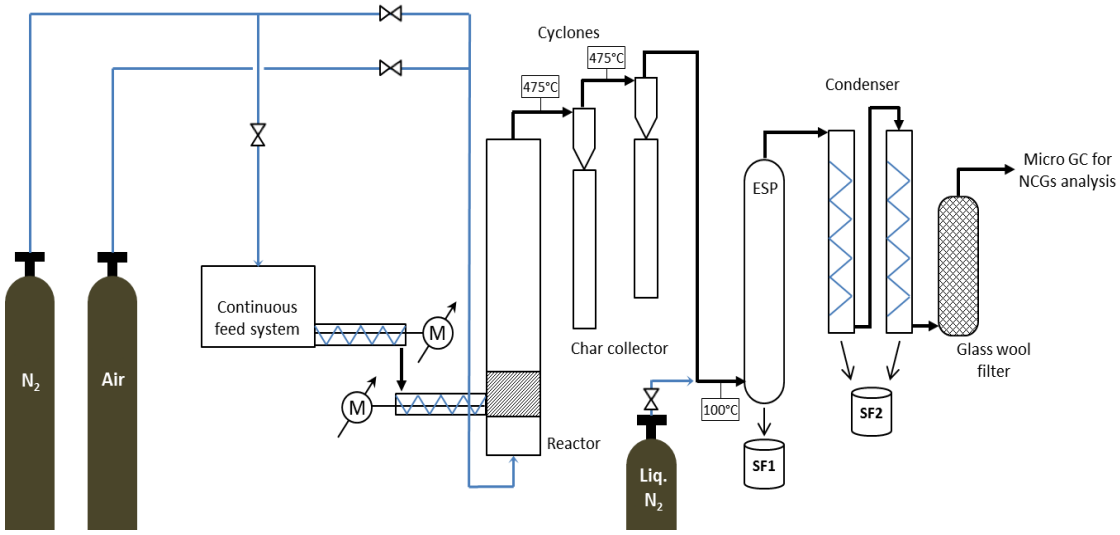

Figure 1. Schematic diagram of a fluidized bed reactor

For oxidative pyrolysis tests, oxygen was admitted to the plenum in the amount of 0.5 - 4 SLPM while maintaining total flow rate of sweep gas (nitrogen and oxygen) at 10 SLPM. Thus, the inlet concentration of oxygen ranged from 0 to 8.40 vol%, which corresponded to 3.4 – 53.9% of stoichiometric oxygen for combustion of the biomass feed. Since oxygen participates in the pyrolysis reactions, mass yields are reported on the basis of biomass processed (g/100 g biomass) instead of percentages to avoid any confusion when yields exceed 100%.

The effluent from the reactor passed through two cyclones in series to remove char and ash particles. A novel bio-oil recovery system was used to quickly quench the pyrolysis vapor [17]. It consisted of two stages with heavy ends collected in an electrostatic

precipitator (ESP) and the light ends collected in a condenser, the resulting bio-oil fractions referred to as SF1 (stage fraction 1) and SF2 (stage fraction 2), respectively. Liquid nitrogen was sprayed into the pyrolysis vapor stream just ahead of the ESP, which collected the aerosols formed from the heavy ends. The remaining pyrolysis vapor passed into a tubular heat exchanger where it was chilled to -10°C causing water and light oxygenates to condense as an aqueous phase.

The yield of char was determined by weighing the particulate matter captured by the cyclones. The yield of bio-oil was determined by weighing the bio-oil recovery system before and after a run, which accounted for bio-oil that remained inside pipes and vessels. The composition of non-condensable gases (NCG) in the exhaust stream was measured with a micro-GC (Varian CP-4900) calibrated for nitrogen (N_2), hydrogen (H_2), carbon monoxide (CO), methane (CH_4), carbon dioxide (CO_2), ethylene (C_2H_4), ethane (C_2H_6), propane (C_3H_8). The yield of NCG was calculated using a drum-type gas meter (Ritter, Germany) and the ideal gas law.

Characterization of pyrolysis products

Several analytical methods were adopted to characterize the bio-oil. CHN elemental analysis of the bio-oil and biochar was performed using an elemental analyzer (Elementar, vario MICRO cube) with oxygen content determined by difference. The higher heating value (HHV) of bio-oil and biochar was determined theoretically using an equation developed by Demirbas based on elemental compositions [18]. Water content in bio-oil was measured using a Karl-Fischer Titrator (KEM, MKS-500) with Hydranal-composite 5K solution. The acidity of bio-oil was determined as modified acid number (MAN) with titrator (Metrohm,

798 MPT Titrino) using N,N-dimethylformamide and methanol as solvents [19]. MAN value was expressed as mg KOH / g of bio-oil.

Identification and quantification of chemical compounds in bio-oil were performed using a Varian CP-3800 gas chromatography equipped with Saturn 2200 mass spectrometry and mass spectrometry (MS)/flame ionization detector (FID). Authentic compounds of the chemicals identified in bio-oil using GC/MS were calibrated in GC/FID for the compounds quantification. The capillary column used was a Phenomenex ZB-1701 (60 m × 0.25 mm × 0.25μm). Injection temperature was 275 °C and oven temperature was programmed to hold at 35 °C for 3 minutes, ramp to 280 °C at 3 °C/min and then hold for additional 4 minutes. In this work, 9 carbohydrates derivatives and 15 lignin derivatives were identified and quantified using a GC-MS/FID system after calibrating authentic compounds. Ion chromatography (DIONEX, ICS-3000) was used to quantify acetate, glycolate, propionate and formate without pretreatment. Authentic chemicals of these compounds were calibrated in the system prior to the analysis for quantification. The yield of hydrolyzable sugar in bio-oil was measured using an Ulitmate 3000 series high performance liquid chromatography (HPLC, Dionex) after hydrolysis of SF1 bio-oil with 4 % of sulfuric acid at 125 °C for 45 minutes. The HPLC system is precalibrated for cellobiosan, glucose, xylose, sorbitol and levoglucosan, the yield of each sugar in the hydrolyzed sample was obtained accordingly. Pyrolytic lignin was extracted from each SF1 bio-oil and quantified using the method described by Scholze and Meier [20].

Biochar was also characterized after degassing at 300 °C for 12 hours under vacuum. Fourier transform infrared spectroscopy (FT-IR) of biochar was conducted with a Nicolet iS10 (Thermo Scientific) instrument. Each sample was scanned 32 times at a resolution of 4

cm^{-1} and an interval of $1cm^{-1}$. The normalized spectra were obtained with the region of wavenumber ranging from 700 cm^{-1} to 4000 cm^{-1}. Brunauer-Emmet-Teller (BET) surface area of the biochar was measured using a NOVA 4200e surface area analyzer (Quantachrome Instruments).

Statistical analysis

The effect of oxygen concentrations on products distribution and the yields of GC detectable compounds and hydrolyzable sugars were evaluated by analysis of variance (ANOVA). One-way ANOVA was performed to test the null hypothesis that the average values for varying oxygen concentrations are not significantly different. The ANOVA model equation is in the following.

$$y_{ij} = \mu_j + \epsilon_{ij}$$

where y_{ij} are observations, μ_j is the mean of the observations for the jth treatment group and ϵ_{ij} are normally distributed zero-mean random errors. SAS Institute's SAS 9.3 statistical software was used to perform ANOVA test. The value of the *F*-statistic and the *p*-value were reported in this study. Parameters with *p*-values less than 0.05 were considered significant with 95% confidence. Duplicate pyrolysis tests were conducted at each condition and their respective average yields of pyrolysis products are reported in this paper. All reported analytical results of bio-oil and biochar are the average of triplicate measurements of each test.

Results and discussion

Products distributions

The mass yields of products from the partial oxidative pyrolysis of red oak are shown in Fig. 2. The average bio-oil yield for the control runs (i.e. 0 % oxygen) was 63.3 g/100 g biomass with standard deviation of 3.32. The yields of bio-oils, interestingly, produced from oxidative pyrolysis were similar, ranging from 61.2 to 64.8 g/100 g biomass over oxygen concentrations used in this study. The difference from the control case is statistically insignificant (*F=0.27, p=0.9129*) over the entire oxygen range. The yield of NCG increased from 13.2 to 55.3 g/100 g biomass (*F=116.7, p=<.0001*), whereas biochar yield decreased from 13.1 to 9.1 g/100 g biomass (*F=4.41, p=0.0494*) with increasing oxygen concentration in the range tested.

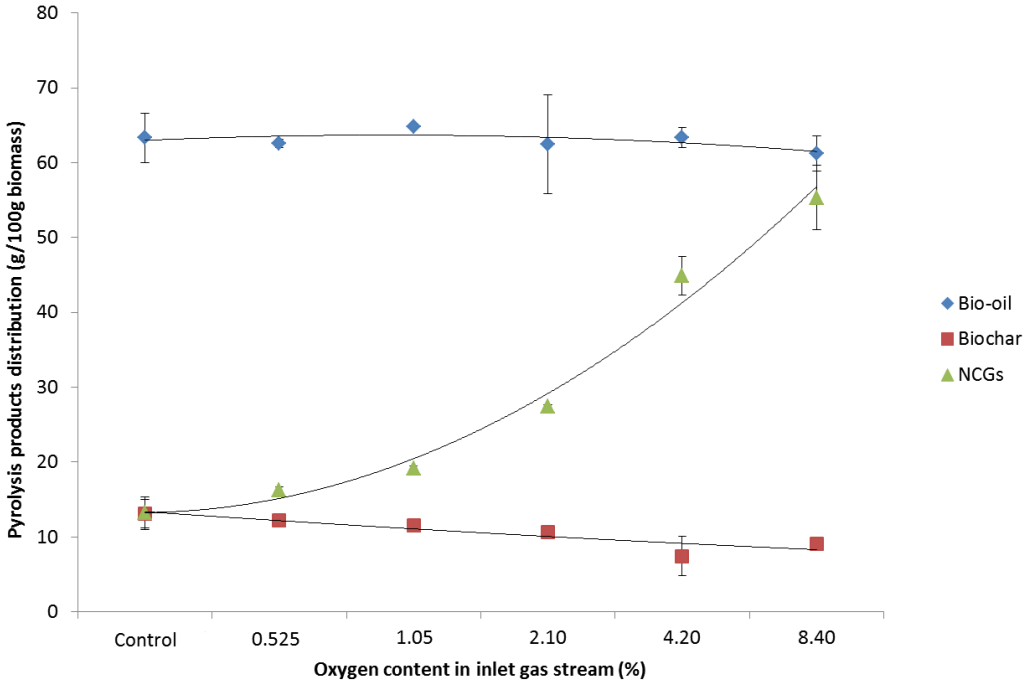

Figure 2. The distributions of pyrolysis products

The two fractions of bio-oil (SF1 and SF2) were analyzed separately. Each fraction of bio-oil had a distinct appearance. In all tests, SF1 was black and viscous, whereas SF2 was a watery and lightly tinted red. However, the distribution between the two bio-oil fractions was dependent on the amount of oxygen present during pyrolysis. Fig.3 shows the fractional yield of SF1 and SF2. The yield of heavy fraction decreased from 29.6 to 19.5 g/100 g biomass (*F=12.28, p=0.0042*) whereas the yield of the aqueous fraction increased from 33.7 to 41.7 g/100 g biomass (*F=5.18, p=0.0347*) with increasing oxygen concentration from 0 to 8.4 % (v/v). This result indicates a shift from high molecular weight products to low molecular weight products with increasing oxygen.

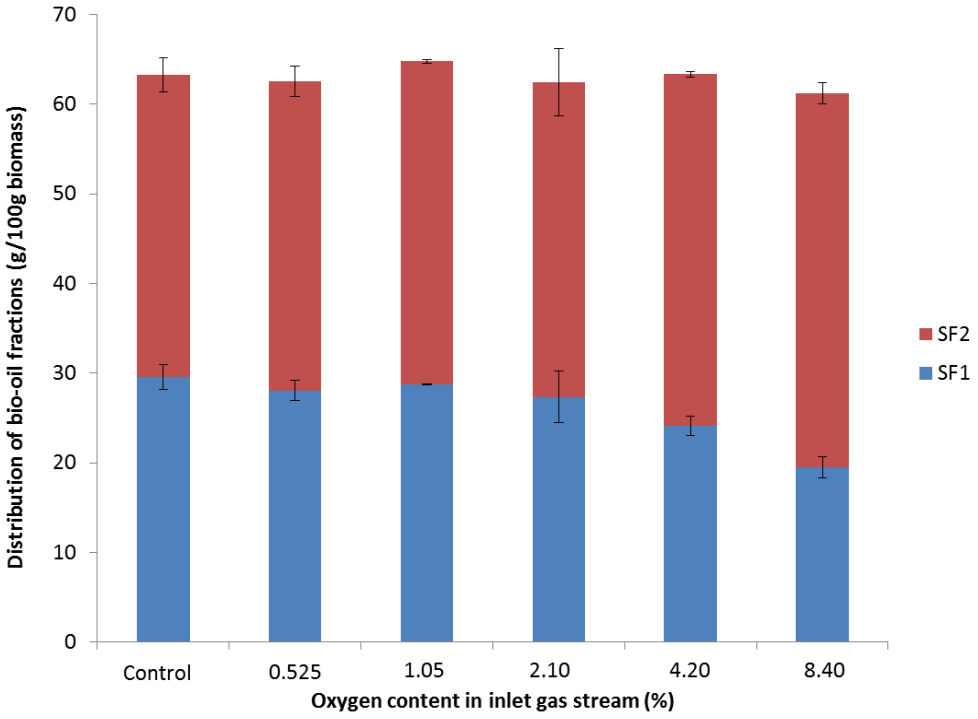

Figure 3. The fractional yield of each bio-oil fraction

Total carbon mass balance for the pyrolysis products as a function of oxygen concentration was also calculated, and the result is shown in Fig. 4. Total carbon balance of 83-90 wt.% was achieved. The carbon content of both bio-oil and biochar monotonically decreased with increasing oxygen concentration during pyrolysis. Bio-oil produced under an inert gas environment contained 53 wt.% of carbon whereas carbon content for bio-oil from pyrolysis with 8.4 % (v/v) of oxygen was significantly reduced to 33 wt.% (*F=15.76, p=0.0021*). Similarly, the carbon content of the biochar decreased from 21 to 14 wt.% (*F=7.02, p=0.0172*) for the same condition. On the other hand, carbon content of the NCG significantly increased (*F=140.43, p=<.0001*), as might be expected since oxygen converts reduced carbon compounds to oxidized gases. It is, however, important to note that when oxygen concentration in the sweep gas was sufficiently low (below 2.1 % (v/v)), the effect neither on the distribution of carbon content nor the yields of SF1 and SF2 was significant.

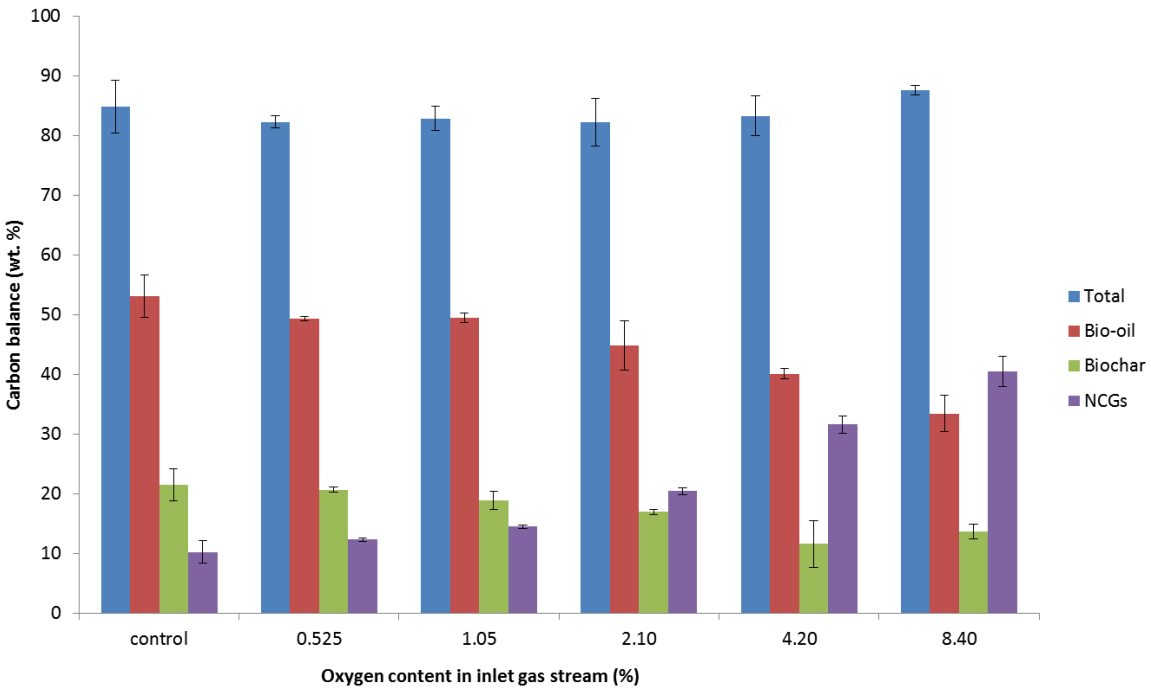

Figure 4. Carbon balance analysis of pyrolysis products

Chemical composition and properties of bio-oil

Water content, MAN, elemental composition and calorific value of bio-oils are summarized in Table 2. The water content in SF1 obtained from the control run was about 6 wt.%. This result did not change much for oxidative pyrolysis conditions. Most of the water produced during pyrolysis was collected in SF2, which increased as the oxygen concentration in the gas stream increased. Such distinct distribution of water in SF1 and SF2 bio-oil is attributed to the unique bio-oil collection system employed in this study [19]. The water content in whole bio-oil (representing the combined bio-oil from SF1 and SF2) for the control trials was 32 wt.%. Water content of whole bio-oil increased to 53 wt.% as oxygen content of the sweep gas increased to 8.4 % (v/v).

As shown in Table 2, the MAN of SF1 was relatively unaffected by oxygen content during pyrolysis, ranging from 26 to 33 mg KOH/g bio-oil. In the case of SF2, however, MAN decreased from 100 to 57 mg KOH/g bio-oil with increasing oxygen, as would be expected from the decreasing amount of acetic acid produced under oxidative conditions.

Elemental composition of bio-oil is presented in Table 2. Increasing oxygen concentrations in the sweep gas led to slight decreases in the carbon and hydrogen as well as an increase in the oxygen content in SF1, which are shown to be statistically significant. In SF2, carbon content significantly decreased while oxygen and hydrogen content increased with increasing oxygen concentrations in the sweep gas. The substantial amount of water produced from a partial oxidation reaction during pyrolysis was collected primarily in SF2, which led to overall lower carbon and higher oxygen content in the SF2.

Table 2. The properties of bio-oils

	Based on	control	0.525% O_2	1.05% O_2	2.10% O_2	4.20% O_2	8.40% O_2
Water content (wt.%)	**SF1**	6.41	6.78	6.46	5.37	6.04	8.71
	SF2	54.27	61.98	62.10	67.61	74.07	73.54
	Bio-oil[1)]	31.91	37.15	37.42	40.33	48.14	52.90
MAN (mg KOH/g)	**SF1**	29.79	31.99	32.15	30.65	25.95	33.05
	SF2	96.00	99.99	95.02	76.29	56.84	57.19
Elemental composition (wt.%)	**SF1**						
	C	57.61	57.62	56.40	56.05	56.85	53.58
	H	6.36	6.30	6.24	6.26	6.19	5.13
	O[2)]	35.92	35.96	37.26	37.59	36.84	41.17
	N	0.11	0.12	0.10	0.11	0.12	0.11
	SF2						
	C	22.04	19.08	18.41	15.28	12.21	11.90
	H	9.15	9.24	9.24	9.47	9.77	9.87
	O[2)]	68.81	71.38	72.35	75.25	78.02	78.23
	N	n.d.	n.d.	n.d.	n.d.	n.d.	n.d.
Higher heating value[3)] (MJ/kg)	**SF1**	22.80	22.71	22.02	21.87	22.16	18.90
	SF2	9.80	8.50	8.18	7.01	5.98	5.99

[1)] Bio-oil indicates the sum of SF1 and SF2. Water yield in bio-oil is determined based on the water content of SF1 and SF2 and their respective yields.
[2)] Determined by difference
[3)] Determined by theoretical calculation

The chemistry of fast pyrolysis is complex [21], producing hundreds of chemicals. A large number of them cannot be identified or quantified due to the lack of commercially available compounds. In this study, 15 lignin derivatives (phenolic monomers) and 13 carbohydrates derivatives were identified and quantified using IC and GC-MS/FID. Table 3 shows the yield of each compound on a biomass basis.

Table 3. Compositional analysis of bio-oils determined by IC and GC-FID[1)].

	Compounds (g/100 g biomass)	control	0.53% O_2	1.05% O_2	2.10% O_2	4.20% O_2	8.40% O_2
carbohydrates	**Acetic acid**[2)]	3.04±0.42	2.72±0.01	2.89±0.21	2.26±0.17	1.89±0.09	1.97±0.18
	Glycolic acid[2)]	0.38±0.11	0.29±0.03	0.34±0.05	0.30±0.07	0.23±0.01	0.20±0.01
	Formic acid[2)]	0.45±0.12	0.43±0.01	0.47±0.01	0.43±0.06	0.39±0.04	0.42±0.06
	Propionic acid[2)]	0.27±0.15	0.14±0.00	0.21±0.04	0.17±0.08	0.11±0.01	0.12±0.04
	Acetol	1.52±0.46	1.00±0.15	0.91±0.05	0.83±0.19	0.60±0.04	0.45±0.16
	Dimethoxytetrahydrofuran	0.38±0.16	0.16±0.03	0.22±0.01	0.25±0.06	0.22±0.01	0.18±0.06
	Furfural	0.35±0.11	0.22±0.04	0.19±0.02	0.15±0.04	0.12±0.02	0.14±0.06
	2-Furanmethanol	0.10±0.09	0.01±0.00	0.01±0.00	0.01±0.00	0.00±0.00	0.01±0.01
	5-methyl furfural	0.06±0.03	0.03±0.01	0.03±0.00	0.03±0.01	0.02±0.00	0.05±0.03
	2-(5H)Furanone	0.44±0.17	0.33±0.04	0.36±0.05	0.31±0.02	0.22±0.02	0.23±0.03
	Methylcyclopentenolone	0.22±0.08	0.11±0.03	0.09±0.01	0.08±0.01	0.05±0.01	0.03±0.01
	5-HMF	0.16±0.02	0.20±0.07	0.17±0.02	0.17±0.02	0.11±0.01	0.07±0.01
	Levoglucosan	2.54±0.08	3.37±0.59	3.32±0.18	3.43±0.61	2.43±0.28	2.36±0.20
	Sum of carbohydrates derivatives	**9.88±0.41**	**9.02±0.96**	**9.18±0.07**	**8.39±0.53**	**6.37±0.22**	**6.22±0.41**
Lignin	**Phenol**	0.04±0.03	0.02±0.00	0.02±0.00	0.02±0.01	0.01±0.00	0.03±0.00
	2-methoxyphenol	0.15±0.07	0.08±0.02	0.09±0.01	0.10±0.02	0.09±0.00	0.13±0.05
	2-methoxy-4-methylphenol	0.09±0.03	0.06±0.01	0.06±0.01	0.05±0.01	0.04±0.00	0.03±0.00
	4-ethyl-2-methoxyphenol	0.02±0.01	0.01±0.01	0.01±0.00	-	-	-
	2-methoxy-4-vinylphenol	0.16±0.02	0.14±0.02	0.13±0.02	0.13±0.01	0.12±0.01	0.07±0.00
	Eugenol	0.04±0.01	0.03±0.01	0.03±0.00	0.02±0.00	0.02±0.00	0.01±0.00
	2,6-dimethoxyphenol	0.37±0.07	0.36±0.08	0.36±0.00	0.29±0.06	0.27±0.02	0.16±0.02
	Isoeugenol	0.24±0.08	0.20±0.07	0.20±0.03	0.21±0.04	0.17±0.05	0.11±0.01
	4-methyl-2,6-dimethoxyphenol	0.26±0.06	0.30±0.09	0.27±0.01	0.22±0.04	0.21±0.00	0.12±0.01
	Vanillin	0.10±0.02	0.13±0.04	0.13±0.00	0.16±0.05	0.16±0.04	0.21±0.02
	4-hydroxy-3-methoxyacetophenone	0.05±0.00	0.08±0.03	0.07±0.00	0.09±0.03	0.08±0.01	0.07±0.01
	2,6-dimethoxy-4-(2-propenyl) phenol	0.21±0.02	0.20±0.08	0.18±0.02	0.14±0.00	0.15±0.02	0.07±0.00
	2,6-dimethoxy-4-(1-propenyl) phenol	0.72±0.05	0.91±0.44	0.87±0.02	0.64±0.24	0.56±0.02	0.24±0.01
	4-hydroxy-3,5-dimethoxybenzaldehyde	0.24±0.01	0.36±0.13	0.40±0.01	0.45±0.00	0.60±0.09	0.68±0.02
	4-hydroxy-3,5-dimethoxyacetophenone	0.14±0.00	0.19±0.07	0.11±0.05	0.18±0.03	0.17±0.00	0.03±0.01
	Sum of lignin derivatives	**2.84±0.37**	**3.05±1.10**	**2.93±0.02**	**2.69±0.28**	**2.66±0.16**	**1.94±0.11**
	Sum of total	***12.7±0.77***	***12.1±2.05***	***12.1±0.09***	***11.1±0.81***	***9.0±0.06***	***8.2±0.53***

[1)] Include SF1 and SF2 bio-oil

[2)] Measured by ion chromatography (IC)

Phenolic monomers originating from the lignin were quantified with GC/FID. The yield of vanillin, 4-hydroxy-3,5-dimethoxybenzaldehyde, 4-hydroxy-3-methoxyacetophenone, and 4-hydroxy-3,5-dimethoxyacetophenone increased while others decreased with increasing oxygen concentration. It is noteworthy that vanillin and 4-hydroxy-3,5-dimethoxybenzaldehyde contain aldehyde functional group and 4-hydroxy-3-methoxyacetophenone and 4-hydroxy-3,5-dimethoxyacetophenone contain ketone functional group in their side chains. The amount of aldehyde and ketone functional groups is normally small in the phenolic monomers from fast pyrolysis. This suggests that oxygen reacted with vinylphenol and methylphenol to produce phenolic monomers containing aldehyde and ketone functional groups. Namboodiri et *al*. [22] reported that the vinyl group of styrene can be converted into ketone functional group by selective oxidation reactions. Many studies have reported vanillin production from oxidation of lignin [23-25]. In the present study, total yield of phenolic monomers was higher than the control case when 0.525 and 1.05 % (v/v) of oxygen was added to the sweep gas. Overall, the addition of oxygen up to 1.05% (v/v) had a positive effect on the production of phenolic monomers, but further increases in oxygen reduced their yield ($F=1.26$, $p=0.3891$).

In addition to the phenolic monomers identified and quantified by chromatographic techniques, pyrolytic lignin, consisting of non-volatile phenolic oligomers, was also extracted from each SF1 sample and quantified. As shown in Table 4, the pyrolytic lignin yield of the control bio-oil was 15.8 g/100 g biomass. The yield significantly decreased to 9.5 g/100 g biomass ($F=17.96$, $p=0.0015$) as oxygen concentration increased from 0 to 8.40 % (v/v). The strong reactivity of molecular oxygen likely promoted formation of NCG from lignin or lignin-derived oligomers.

Table 4. The yield of pyrolytic lignin in bio-oils

g/100 g biomass	control	0.525% O_2	1.05% O_2	2.10% O_2	4.20% O_2	8.40% O_2
Pyrolytic lignin	15.75 ± 0.29	13.75 ± 1.32	12.30 ± 0.25	11.23 ± 0.23	10.94 ± 0.70	9.48 ± 0.94

The yields of carbohydrate derivatives are shown in Table 3. The yields of acids decreased with increasing oxygen concentration in the sweep gas. The yield of acetic acid, a dominant acid in bio-oil, was approximately 3 g/100 g biomass in the control case, decreasing to 2 g/100 g biomass at an oxygen concentration of 8.40 % (v/v). Previously, Meyer et *al*. [26] reported that the major products of acetic acid oxidation were CO, CO_2, CH_4 and H_2, suggesting that carboxylic acids produced from primary pyrolysis are further decomposed via reaction with oxygen. Yields of other light oxygenates such as acetol and furfural, originating from decomposition of cellulose and hemicellulose, also decreased with increasing oxygen (*F=17.87, p=0.0015*).

Levoglucosan, the major thermal depolymerization product of cellulose, increased with increasing oxygen in the range of 0.525 - 2.10 % (v/v). The yield of levoglucosan was 2.5 g/100 g biomass in the control run, but increased to 3.4 g/100 g biomass at 2.10 % (v/v) oxygen concentration. As the oxygen concentration was further increased, the yield of levoglucosan began to level off, suggesting an optimum concentration of oxygen for maximum levoglucosan yield (*F=3.64, p=0.0737*). These results are surprising, contradicting previous observations in the literature [13, 27]. Oxygen is thought to both catalyze polymerization [28] and increase decomposition [29] of levoglucosan. Oxygen

concentrations of 0.525, 1.05 and 2.10 % (v/v), corresponding to equivalence ratios of 0.034, 0.067 and 0.135, increased levoglucosan yields compared to the non-oxidative control trials. Amutio et *al*. [13], who observed monotonic decreasing levoglucosan yields with increasing oxygen, operated at significantly higher equivalence ratios (0.15 and 0.25), which might explain the difference with the present study. The ability of oxygen to promote the production of levoglucosan has several potential explanations. First, oxygen might break down the lignin sheath surrounding cellulose fibers, allowing levoglucosan produced from depolymerizing cellulose to escape. While lignin thermally decomposes over a wide range of temperatures up to 700 °C, cellulose depolymerizes at relatively low temperatures [30]. If levoglucosan is not able to readily evaporate and escape the pyrolyzing biomass, it will repolymerize to oligosaccharides followed by dehydration to char and light gases [31, 32]. Small amounts of oxygen are likely to oxidize the lignin sheath, forming small pores that allow levoglucosan vapors to escape from the interior of the cell wall [33].

Another possibility is that oxygen reacts with naturally occurring alkali and alkaline earth metals (AAEM) in biomass to form oxides. AAEM, coordination bonded to plant polysaccharides, is well known to catalyze scission of pyranose and furanose rings during pyrolysis, producing light oxygenated compounds instead of sugars [35]. Physical removal or conversion of AAEM into thermally stable compounds is known to mitigate ring scission and enhance sugar formation [34]. Oxidation of AAEM will produce thermally stable oxides, hydroxides, or carbonates [35], which are expected to be less catalytically active than AAEM that directly bonded to biomass. The amount of AAEM in biomass is usually much less than 1 wt%, thus requiring little oxygen to oxidize it. Higher levels of oxygen than required to oxidized AAEM might be expected to decompose cellulose and reduce levoglucosan yields.

In addition to levoglucosan, bio-oil contains several other sugars, including five-/six-membered monosaccharides and oligosaccharide. These non-volatile sugars cannot be detected and quantified by the GC/MS-FID system, so in order to understand the effects of oxygen on total sugars in bio-oil, the total sugars were quantified using a HPLC after hydrolysis of SF1. Levoglucosan and other sugars were converted to monomeric forms (mainly glucose) through acid-catalyzed hydrolysis. Along with other sugars such as xylose and sorbitol, the non-volatile sugars were quantified and the result is presented in Table 5. The influence of oxygen concentrations on total sugar yields was significant (*F=7.37, p=0.0153*). Compared to the control case, total hydrolyzable sugar increased by 16 and 2.5 % for 0.525 and 1.05 % (v/v) oxygen, respectively. Further increases in oxygen concentrations reduced the total sugar yield.

Table 5. Sugars in bio-oil after acid hydrolysis

g/100 g biomass	Control	0.525% O_2	1.05% O_2	2.10% O_2	4.20% O_2	8.40% O_2
cellobiosan	0.10±0.00	0.12±0.04	0.09±0.00	0.09±0.00	0.09±0.02	0.07±0.00
glucose	4.28±0.06	4.62±0.09	4.48±0.26	4.28±0.23	4.30±0.05	3.39±0.13
xylose	1.47±0.10	1.38±0.01	1.36±0.00	1.22±0.01	1.27±0.01	0.95±0.04
sorbitol	1.67±0.24	2.72±0.31	1.83±0.35	1.92±0.01	1.83±0.07	1.61±0.10
levoglucosan	0.31±0.02	0.24±0.11	0.26±0.10	0.25±0.06	0.23±0.01	0.27±0.07
Total	7.83±0.71	9.08±0.56	8.03±0.72	7.76±0.32	7.72±0.15	6.29±0.35

It can be seen that the yields of glucose and sorbitol increased and decreased in similar trends with a statistical significance (*F=14.43, p=0.0027 for glucose; F=6.67, p=0.0194 for sorbitol*). The yield of xylose, however, decreased with increasing oxygen concentrations (*F=33.14, p=0.0003*). Hemicellulose and lignin are covalently linked in a matrix surrounding cellulose [36]; thus, xylose is likely to be more susceptible than cellulose

to reaction with molecular oxygen in the sweep gas. Sorbitol, on the other hand, is derived from cellulose and thus might be expected to show yield response similar to that of levoglucosan.

Composition of non-condensable gases

The NCG yield of the control pyrolysis experiment was 13.2 g/100 g biomass (Fig. 5). CO and CO_2 were the two major gases with yields of 5 and 7 g/100 g biomass, respectively. Small amounts of CH_4, C_2H_4 and H_2 were produced, but the sum of the yields of these three gases was less than 1 g/100 g biomass. As expected, the formation of CO_2 and CO was accelerated with increasing oxygen concentrations due to the partial oxidation reaction and stronger cracking reaction caused by the oxygen molecules. The yields of CO_2 and CO significantly increased from 7 to 38 g/100 g biomass ($F=82.75$, $p=<.0001$) and from 5 to 18 g/100 g biomass ($F=111.01$, $p=<.0001$), respectively. When 8.40 % (v/v) oxygen was added to the sweep gas stream, the total yield of NCG including CO_2, CO, CH_4, C_2H_4 and H_2 was 57 g/100 g biomass.

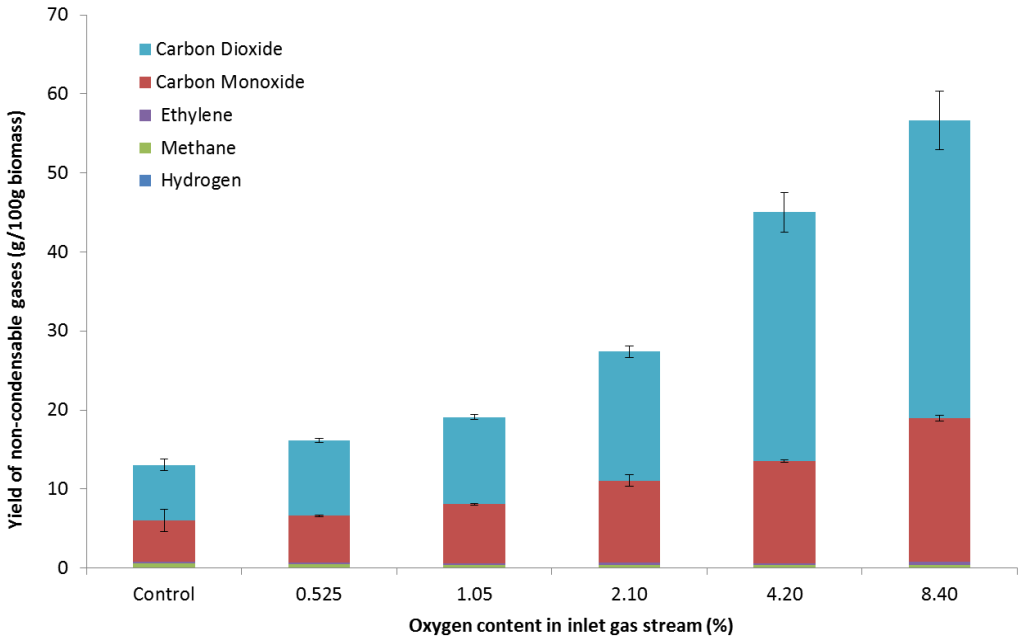

Figure 5. The composition of non-condensable gases (NCG)

Properties of biochar

The elemental composition, heating value, BET surface area and FT-IR of biochar samples were investigated as a function of oxygen concentration during pyrolysis. As shown in Table 6, the content of carbon and hydrogen in biochar decreased as oxygen concentration in the sweep gas increased. The higher heating value of biochar decreased from 27.74 to 23.15 MJ/kg with statistical significance over the range of increasing oxygen content of the sweep gas. As shown in Table 6, BET surface area of biochar increased statistically significantly from 2.4 m^2/g in the control run to 93.1m^2/g when 4.20 % (v/v) of oxygen was added, as might be expected for oxygen diffusing into nascent pores in the char before reacting. BET surface area decreased when oxygen concentration further increased probably

because the rate of oxidation became much faster than the rate of pore diffusion, limiting oxidation to the outer surface of char particles [13].

Table 6. The properties of biochars

		control	0.525% O_2	1.05% O_2	2.10% O_2	4.20% O_2	8.40% O_2
Elemental composition (wt.%)	C	77.14	77.88	75.31	73.70	72.09	69.40
	H	3.44	3.32	3.32	3.18	2.90	2.92
	O[1)]	19.20	18.59	21.17	22.88	24.74	27.40
	N	0.22	0.22	0.21	0.24	0.28	0.28
Higher heating value[2)] (MJ/kg)		27.74	27.92	26.66	25.66	24.42	23.15
BET surface area (m^2/g)		2.4 (1.1)[3)]	2.5 (1.3)	10.3 (4.8)	22.8 (15)	93.1 (77.4)	77.6 (63.5)

[1)] Determined by difference
[2)] Determined by theoretical calculation
[3)] The value in parenthesis indicates micropore surface area (pore diameter less than 2 nm)

The FT-IR spectra of biochars were analyzed (Fig. 6). The spectra were characterized by several principal bands. The stretch bands at 1240 cm^{-1} were assigned to aromatic CO- and phenolic –OH vibration. Other important absorbance peak at 1600 cm^{-1} and 1712 cm^{-1} are assigned to aromatic C=O and aromatic COOH / C=O stretching, respectively [37]. These bands, representatives of the highly condensed aromatic structure of biochar, appeared with high intensities for all samples. Some other peaks including COOH / CHO at 1410 cm^{-1} and aliphatic C-H at 3000-2860 cm^{-1} also appeared. As shown in the figure, the band at 1712 cm^{-1} attributed to the aromatic carboxyl/carbonyl group and the band at 1600 cm^{-1} attributed to the aromatic C=O appeared with higher intensity for the biochar produced in oxidative pyrolysis conditions. This indicates that oxidation of the functional groups to carboxyl or carbonyl

groups occurred during oxidative pyrolysis. These findings are consistent with the increased occurrence of phenolic monomers with ketone and aldehyde functional groups in bio-oil as oxygen in the sweep gas increased.

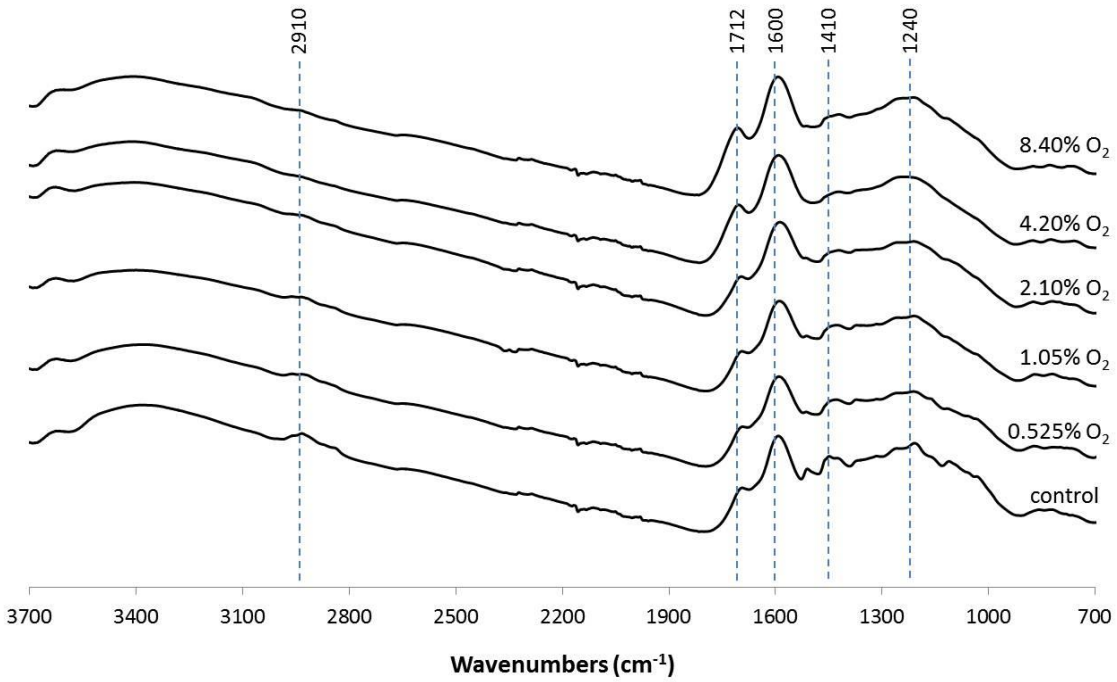

Figure 6. FT-IR spectra of biochar samples

Conclusion

Fast pyrolysis of red oak was performed in a fluidized bed reactor with oxygen added to the sweep gas in concentrations ranging from 0 to 8.40 % (v/v) to. The yields of bio-oil in all cases of partial oxidative pyrolysis were in the range of 61 - 65 g/100 g of biomass, which was similar to the control run without oxygen. However, the total yield of organic compounds in the bio-oil decreased and water content increased as oxygen in the sweep gas increased. The yield of NCG increased from 13 to 55 g/100 g biomass with increasing

oxygen, which was mainly attributed to enhanced production of CO_2 and CO by the reaction of the added oxygen with the pyrolyzing biomass. These results were similar to those of previous researchers. However, the present study also revealed that yields of levoglucosan and total hydrolyzable sugars increased compared to pyrolysis in the absence of oxygen. The results showed that a small amount of oxygen in the sweep gas (0.525 to 1.05 %, v/v) improved the yield of hydrolyzable sugars. The yield of total monomeric phenols also increased over this oxygen range. Although the carbon balance of bio-oil decreased under oxidative conditions, it was statistically insignificant in the optimum oxygen concentration range discussed above. The bio-oil produced from oxidative pyrolysis was also less acidic and contained less pyrolytic lignin. It can be concluded that in general oxygen is detrimental to thermal depolymerization of biomass, small amounts of oxygen can be beneficial to the production of sugars and monomeric phenols.

Acknowledgement

The financial support of Phillips 66 is gratefully acknowledged. The authors thank Dustin Dalluge for assistance in operating fluidized bed reactor. Authors also thank Bernardo del Campo for assistance in performing the experiment and analyzing the biochar BET surface area.

REFERENCES

[1] S.R. Collinson, W. Thielemans, The catalytic oxidation of biomass to new materials focusing on starch, cellulose and lignin, Coordin Chem Rev 2010;254:1854-70.

[2] J. Leech, Running a dual fuel diesel engine on crude pyrolysis oil, Biomass Gasification and Pyrolysis: State of the Art and Future Prospects 1997:495-97.

[3] S. Czernik, A.V. Bridgwater, Overview of applications of biomass fast pyrolysis oil, Energ Fuel 2004;18:590-98.

[4] A. Lea-Langton, R.M. Zin, V. Dupont, M.V. Twigg, Biomass pyrolysis oils for hydrogen production using chemical looping reforming, International Journal of Hydrogen Energy 2012;37:2037-43.

[5] T.R. Carlson, G.A. Tompsett, W.C. Conner, G.W. Huber, Aromatic production from catalytic fast pyrolysis of biomass-derived feedstocks, Topics in Catalysis 2009;52:241-52.

[6] T.P. Vispute, H. Zhang, A. Sanna, R. Xiao, G.W. Huber, Renewable chemical commodity feedstocks from integrated catalytic processing of pyrolysis oils, Science 2010;330:1222-27.

[7] D. Mohan, C.U. Pittman, P.H. Steele, Pyrolysis of wood/biomass for bio-oil: A critical review, Energ Fuel 2006;20:848-89.

[8] T.L. Marker, L.G. Felix, M.B. Linck, M.J. Roberts, Integrated Hydropyrolysis and Hydroconversion (IH2) for the Direct Production of Gasoline and Diesel Fuels or Blending Components from Biomass, Part 1: Proof of Principle Testing, Environ Prog Sustain 2012;31:191-99.

[9] O.D. Mante, F.A. Agblevor, S.T. Oyama, R. McClung, The influence of recycling non-condensable gases in the fractional catalytic pyrolysis of biomass, Bioresource Technol 2012;111:482-90.

[10] Y. Chen, J. Duan, Y.H. Luo, Investigation of agricultural residues pyrolysis behavior under inert and oxidative conditions, J Anal Appl Pyrol 2008;83:165-74.

[11] D. Butt, Formation of phenols from the low-temperature fast pyrolysis of Radiata pine (Pinus radiata) - Part I. Influence of molecular oxygen, J Anal Appl Pyrol 2006;76:38-47.

[12] D. Butt, Formation of phenols from the low-temperature fast pyrolysis of Radiata pine (Pinus radiata) - Part II. Interaction of molecular oxygen and substrate water, J Anal Appl Pyrol 2006;76:48-54.

[13] M. Amutio, G. Lopez, R. Aguado, J. Bilbao, M. Olazar, Biomass Oxidative Flash Pyrolysis: Autothermal Operation, Yields and Product Properties, Energ Fuel 2012;26:1353-62.

[14] M. Amutio, G. Lopez, R. Aguado, M. Artetxe, J. Bilbao, M. Olazar, Kinetic study of lignocellulosic biomass oxidative pyrolysis, Fuel 2012;95:305-11.

[15] R. Bilbao, J.F. Mastral, M.E. Aldea, J. Ceamanos, The influence of the percentage of oxygen in the atmosphere on the thermal decomposition of lignocellulosic materials, J Anal Appl Pyrol 1997;42:189-202.

[16] D.K. Shen, S. Gu, B.S. Jin, M.X. Fang, Thermal degradation mechanisms of wood under inert and oxidative environments using DAEM methods, Bioresource Technol 2011;102:2047-52.

[17] D.L. Dalluge, Y.S. Choi, B.H. Shanks, R.C. Brown, Contact and Indirect Contact Heat Exchange in Levoglucosan Recovery from Cellulose Fast Pyrolysis, Bioresource Technol 2013 (submitted).

[18] A. Demirbas, Calculation of higher heating values of biomass fuels, Fuel 1997;76:431-34.

[19] A.S. Pollard, M.R. Rover, R.C. Brown, Characterization of bio-oil recovered as stage fractions with unique chemical and physical properties, J Anal Appl Pyrol 2012;93:129-38.

[20] B. Scholze, D. Meier, Characterization of the water-insoluble fraction from pyrolysis oil (pyrolytic lignin). Part I. PY-GC/MS, FTIR, and functional groups, J Anal Appl Pyrol 2001;60:41-54.

[21] K.H. Kim, I.Y. Eom, S.M. Lee, D. Choi, H. Yeo, I.G. Choi, J.W. Choi, Investigation of physicochemical properties of biooils produced from yellow poplar wood (Liriodendron tulipifera) at various temperatures and residence times, J Anal Appl Pyrol 2011;92:2-9.

[22] V.V. Namboodiri, R.S. Varma, E. Sahle-Demessie, U.R. Pillai, Selective oxidation of styrene to acetophenone in the presence of ionic liquids, Green Chem 2002;4:170-73.

[23] A.L. Mathias, A.E. Rodrigues, Production of Vanillin by Oxidation of Pine Kraft Lignins with Oxygen, Holzforschung 1995;49:273-78.

[24] J.D.P. Araujo, C.A. Grande, A.E. Rodrigues, Vanillin production from lignin oxidation in a batch reactor, Chem Eng Res Des 2010;88:1024-32.

[25] H.R. Bjorsvik, Fine chemicals from lignosulfonates. 1. Synthesis of vanillin by oxidation of lignosulfonates, Org Process Res Dev 1999;3:330-40.

[26] J.C. Meyer, P.A. Marrone, J.W. Tester, Acetic acid oxidation and hydrolysis in supercritical water, Aiche J 1995;41:2108-21.

[27] D.S. Scott, J. Piskorz, D. Radlein, P. Majerski, Process for the production of anhydrosugars from lignin and cellulose containing biomass by pyrolysis, in, US Patents (5395455 A), 1995.

[28] Y. Houminer, S. Patai, Thermal polymerization of levoglucosan, Journal of Polymer Science Part A-1: Polymer Chemistry 1969;7:3005-14.

[29] F. Shafizadeh, The chemistry of pyrolysis and combustion, in: R.M. Rowell (Ed.) The Chemistry of Solid Wood, American Chemical Society: 1984, pp. 489-529.

[30] B.B. Uzun, A.E. Putun, E. Putun, Composition of products obtained via fast pyrolysis of olive-oil residue: Effect of pyrolysis temperature, J Anal Appl Pyrol 2007;79:147-53.

[31] X. Bai, P. Johnston, S. Sadula, R.C. Brown, Role of levoglucosan physiochemistry in cellulose pyrolysis, J Anal Appl Pyrol 2013;99:58-65.

[32] X. Bai, P. Johnston, R.C. Brown, An experimental study of the competing processes of evaporation and polymerization of levoglucosan in cellulose pyrolysis, J Anal Appl Pyrol 2013;99:130-36.

[33] R.K. Sharma, J.B. Wooten, V.L. Baliga, X.H. Lin, W.G. Chan, M.R. Hajaligol, Characterization of chars from pyrolysis of lignin, Fuel 2004;83:1469-82.

[34] N. Kuzhiyil, D. Dalluge, X. Bai, K.H. Kim, R.C. Brown, Pyrolytic Sugars from Cellulosic Biomass, ChemSusChem 2012;5:2228-36.

[35] M.J. Wornat, R.H. Hurt, N.Y.C. Yang, T.J. Headley, Structural and Compositional Transformations of Biomass Chars during Combustion, Combust Flame 1995;100:133-45.

[36] F. Helm Richard, Lignin-Polysaccharide Interactions in Woody Plants, in: Lignin: Historical, Biological, and Materials Perspectives, American Chemical Society: 1999, pp. 161-71.

[37] Y. Chun, G.Y. Sheng, C.T. Chiou, B.S. Xing, Compositions and sorptive properties of crop residue-derived chars, Environ Sci Technol 2004;38:4649-55.

CHAPTER 3

PARTIAL OXIDATIVE PYROLYSIS OF ACID INFUSED RED OAK USING A FLUIDIZED BED REACTOR TO PRODUCE SUGAR RICH BIO-OIL

A paper published in *Fuel*

Kwang Ho Kim, Robert Brown, Xianglan Bai

Abstract

Acid infusion of lignocellulosic biomass as a pretreatment prior to fast pyrolysis has been shown to significantly increase the yield of sugar in the products. However, under these conditions char formation increases forming large agglomerates that clog the reactor and eventually interrupt operation of the system. In the present study, partial oxidative pyrolysis of acid infused red oak was performed in a fluidized bed reactor at 500 °C with the concentration of oxygen in the sweep gas ranged from 0 - 8.4 vol% in an effort to mitigate char agglomeration. The addition of oxygen reduced char agglomeration by up to 88.9 % compared to the control run during pyrolysis ensuring continuous run of the reactor. Moreover, the addition of oxygen increased the total sugar content in the bio-oil to as high as 20.6 g/100 g biomass. Stage fraction 1 (heavy fraction) of bio-oil obtained from oxidative condition contained up to 67 % of hydrolysable sugar and it was less acidic compared to standard pyrolysis.

Keywords: acid infusion pretreatment, oxidative pyrolysis, bio-oil, agglomeration, levoglucosan and sugar

Introduction

Conversion of cellulosic biomass into sugars suitable for fermentation to alcohol fuels has been one of the leading challenges in developing advanced biofuels. Enzymatic hydrolysis of cellulose to sugars has been studied by the recalcitrance of biomass to biological degradation. Sugars can also be produced from fast pyrolysis of biomass. However, the detrimental catalytic effect of naturally occurring alkali and alkaline earth metals (AAEM) found in most biomass must be mitigated prior to pyrolysis in order to increase sugar content in bio-oil. It is known that AAEM strongly catalyzes pyranose ring scission by forming coordinate bonds with the oxygen atoms of vicinal hydroxyl groups of the glucose ring. This leads to homolytic scission of the ring during pyrolysis resulting in the formation of low molecular compounds [1].

Removing AAEM by hot water or diluted acid washing has been found to effectively increase the sugar yield in bio-oil [2-8]. It was also found that the pretreatment conditions, for example the concentration of the acid, temperature and pretreatment time, could influence the yield of levoglucosan in bio-oil when the dilute-acid washed biomass is pyrolyzed [9]. An infusion of small amount of acid into biomass prior to pyrolysis also has been proven to dramatically improve levoglucosan yields in bio-oil [9-11. According to our previous study [9], this is because AAEM reacts with acid to form thermally stable salts that are less catalytically active during pyrolysis. The addition of optimum concentration of acid was also found to buffer the system to promote the depolymerization of cellulose. Compared to removing AAEM in biomass by acid washing, this method does not produce acidic waste water that has to be neutralized before disposal and also reduces the corrosion issue during the pretreatment process. Therefore, it appeared to be a more economically-efficient way to

produce sugars from biomass based on fast pyrolysis. However, pyrolysis of acid infused biomass in continuous reactors often causes char agglomeration inside the reactor [11]. If the pyrolysis is conducted in fluidized bed reactors, such char agglomerates reduce fluidization of the reactor bed and eventually result in clogging the reactors. Zhou et *al*. speculated that the agglomeration is possibly related to the formation of viscous liquid intermediates promoted under acidic condition [11].

On the other hand, although fast pyrolysis is conducted in the absence of oxygen due to high reactivity of oxygen for cracking, carefully controlled partial-oxidative pyrolysis could be beneficial to the selective depolymerization of biomass [12-14]. Recently, we found that introducing a small amount of oxygen during fast pyrolysis of biomass in a fluidized reactor improved sugar production when the oxygen concentration was carefully controlled [14]. The addition of the controlled amount of oxygen also promoted the depolymerization of lignin to smaller compounds and reduced the formation of phenolic oligomers. It was also found that the surface area of biochar greatly increased even when a very low concentration of oxygen was present, suggesting many micropores are created inside of biomass. It is possible that the increased diffusivity through the pores facilitates the volatiles escaping from biomass matrix. Therefore, we hypothesize that partial oxidative pyrolysis of acid infused biomass possibly mitigates the issue with char agglomeration occurring during non-oxidative pyrolysis. The hypothesis is tested in the present study by conducting partial oxidative pyrolysis of acid infused red oak in a fluidized bed reactor with varied oxygen concentrations in the sweep gas. To our best knowledge, this is the first time acid-infused biomass has been pyrolyzed under partial-oxidative conditions for increasing sugar in bio-oil.

Methods and materials

Feedstock

Red oak *(Quercus Rubra)* wood chips obtained from Wood Residuals Solutions (Montello, WI) were ground and sieved to a constant size (250 – 400 μm). Sulfuric acid (H_2SO_4, Fisher Scientific, ACS Plus, purity: 96.6 %) was then infused to the red oak with concentration of 0.004 g H_2SO_4/g dry red oak. Our previous study showed that this level of acid infusion produced the maximum yield of levoglucosan during pyrolysis [9]. Briefly, 4 g of H_2SO_4 was dissolved in 3 L of deionized water and mixed with 1kg of red oak. After stirring for 2 h, the damp biomass was dried in an oven at 40 °C until the biomass appeared uniformly dry at 6 – 10 % moisture. Actual moisture content of the infused red oak was measured before the pyrolysis experiments. Ultimate and proximate analyses of the feedstock are presented in Table 1.

Table 1. Ultimate and proximate analysis of red oak

Ultimate analysis (wt. %)	
Carbon	46.39
Hydrogen	5.35
Oxygen[1)]	48.15
Nitrogen	0.05
Sulfur	0.06
Proximate analysis (wt. %)	
Moisture content	5.08
Volatiles	86.22
Fixed carbon	8.54
Ash	0.21

[1)] Determined by difference

Partial oxidative pyrolysis of acid infused red oak

Partial oxidative pyrolysis of acid infused red oak was performed using a laboratory-scale, continuous fluidized bed reactor. The specification and design of the fluidized bed reactor have been described elsewhere [14]. Briefly, this system consisted of a biomass feeder, an injection auger, a stainless steel reactor, two cyclones, an electrostatic precipitator (ESP), and a condenser. All pyrolysis experiments were performed at 500 °C. Pyrolysis experiments performed with acid infused red oak but in the absence of oxygen are referred to as "control" cases throughout the study. For the control case, nitrogen sweep gas was added to the reactor at 8 standard liters per minute (SLPM) and purged through the feed system at 2 SLPM leading to a total flow rate of 10 SLPM. For the oxidative pyrolysis experiments, oxygen was added to the reactor in amounts between 1 - 4 SLPM while maintaining the total flow rate of sweep gas at 10 SLPM. Thus, the inlet concentrations of oxygen in the sweep gas ranged from 0 to 8.4 vol%, which corresponded to 0 - 54 % of stoichiometric oxygen for combustion of the biomass feed. The bio-oil recovery system consisted of two stages with the heavy ends collected in an ESP and the light ends collected in a condenser [14]. The resulting bio-oil fractions are referred to as SF1 (stage fraction 1) and SF2 (stage fraction 2), respectively.

Characterization of reaction products

The yields of SF1 and SF2 bio-oils were determined by weighting the condensers and the bio-oil collection bottles. The yield of char agglomerates was measured gravimetrically by measuring the difference of the weights of the sand and the agglomerates collected from

the reactor after each test. The composition of non-condensable gases (NCG) in the exhaust stream was measured with a micro-GC (Varian CP-4900). Before analysis, it was calibrated for nitrogen (N_2), hydrogen (H_2), carbon monoxide (CO), methane (CH_4), carbon dioxide (CO_2), ethylene (C_2H_4), ethane (C_2H_6) and propane (C_3H_8). The yield of NCG was calculated using a drum-type gas meter (Ritter, Germany) and the ideal gas law.

Carbon mass balance of the reaction products was determined using the methods described in following: carbon mass balance of bio-oil and char was calculated by the results of elemental carbon analysis and the yields of bio-oil and char; elemental composition (carbon, hydrogen, nitrogen and oxygen) of bio-oil and char was measured using an elemental analyzer (Elementar, vario MICRO cube); the char agglomerates were grounded to powder prior to the elemental analysis to exclude the fluidizing sand that agglomerated with char; carbon mass balance of NCG was calculated by the yields of NCG and their molecular formulas.

Water content of bio-oil was measured using a Karl-Fischer Titrator (KEM, MKS-500) with a Hydranal-composite 5K solution. The acidity of bio-oil was determined through modified acid number (MAN) with titrator (Metrohm, 798 MPT Titrino) using N,N-dimethylformamide and methanol as reagents. MAN value was expressed as mg KOH/g of bio-oil.

The volatile content of bio-oil was determined with a Varian CP-3800 gas chromatograph (GC) equipped with flame ionization detector (FID). The column coupled with GC was a Phenomenez ZB-1701 (60 m × 0.25 mm × 0.25 μm). Methanol solution containing approximately 10 wt% of bio-oil was prepared to quantify the compounds of interest. A 1 μL-aliquot of the bio-oil/methanol solution was injected into the GC system. Injection temperature was set at 275 °C with a split ratio of 20:1. The GC oven temperature was programmed from 35 °C (3 min hold) to 280 °C at a ramp of 3 °C/min, with a final hold

time of 4 min. In this work, nine carbohydrates derivatives and fifteen lignin derivatives were quantified using GC/FID system after calibrating with commercially available authentic compounds.

Ion chromatograph (DIONEX, ICS-3000) equipped with a conductivity detector and an Anion Micromembrane Suppressor AMMS-ICE 300 was used to quantify organic acids in bio-oil. For sample preparation, 0.1 g of bio-oil was dissolved in 1.5 mL of methanol and 6 mL of deionized water mixture. 25 μL-aliqout of solution was injected into the IC system. The eluent used was 1.0 mM heptafluorobutyric acid with an IonPac ICE-AS1 analytical column with a flow rate of 0.12 mL/min at 19 °C. A commercial calibration external standard (Inorganic Ventures, USA) with a mixture of four compounds (acetate, glycolate, formate and propionate) was used for quantitative analysis.

The amount of hydrolyzable sugar in bio-oil was quantified with a high performance liquid chromatograph (HPLC, Ultimate 3000 series, DIONEX). Only SF1 bio-oil was hydrolyzed since SF2 bio-oil does not contain sugars due to the characteristic feature of the bio-oil collection system used in the present study. SF1 bio-oil sample was hydrolyzed with 400 mM of sulfuric acid solution at 125 °C for 45 min. The HPLC system was equipped with a quaternary analytical pump and a Shodex Refractive Index (RI) detector. The analytical column used was either a HyperRex XP Carbohydrate or a BioRad Aminex 87P. The mobile phase was deionized water with a flow rate of 0.6 mL/min. The column temperature was set at 85 °C. The HPLC system was pre-calibrated for cellobiosan, glucose, xylose, sorbitol and levoglucosan. Pyrolytic lignin, a hydrophobic component mainly from lignin fragments, was extracted from each SF1 bio-oil and quantified using the method described by Scholze and Meier [15].

Statistical analysis

The effect of oxygen concentrations in the sweep gas on product distributions and the total sugar content in the bio-oil were evaluated by analysis of variance (ANOVA) [14]. One-way ANOVA was performed to test the null hypothesis of no difference in average values for different oxygen concentrations in the range tested in this study. SAS Institute's SAS 9.3 statistical software was used to perform ANOVA test. The *F-statistic* and the *p-value* were reported in this study. Parameters with *p*-values less than 0.05 were considered significant with 95 % confidence. Pyrolysis test was conducted twice at each condition and their respective average yields of pyrolysis products are reported in this paper. All analytical results of pyrolysis products reported are the average of triplicate measurements of each test.

Results and discussion

Product distributions

Fig. 1(a) shows the mass yield of bio-oil, char agglomerates, and NCG from control pyrolysis and the oxidative pyrolysis of acid infused red oak. In here, char agglomerate indicates the solid residue that accumulates inside the reactor bed. It was found that no biochar was collected in the cyclone when acid-infused red oak was pyrolyzed. It should also be noted that mass yields are reported on the basis of biomass processed (g/100 g biomass) instead of weight percentages to avoid confusion about some yields exceeding 100 wt% since oxygen molecules in the fluidizing gas also participate in the reactions [14]. The bio-oil yield for the control case (which is pyrolysis of acid infused biomass with pure nitrogen as the sweep gas) was 54.5 g/100 g biomass. This value is lower than the yield from pyrolysis of

untreated red oak (63 g/ 100 g biomass) reported in our previous research [14]. The yield of bio-oil in this study was found to be higher for oxidative pyrolysis of acid infused biomass than for the control case. The yield of bio-oil steadily increased to 62.0 g/100 g biomass for oxidative pyrolysis with oxygen concentration increasing up to 4.2 vol%, but then slightly decreased to 58.2 g/100 g biomass when oxygen content was further increased to 8.4 vol%. However, differences in bio-oil yields among the different oxidative pyrolysis trials were statistically insignificant (*F=1.32, p=0.4115*) over the range of oxygen concentration used in this study. On the other hand, as shown in Fig. 1(a), the yield of NCG dramatically increased from 11.7 to 80.5 g/100 g biomass (*F=40.33, p=0.0063*) while the yield of char agglomerate significantly decreased from 24.3 to 2.7 g/100 g biomass *(F=57.56, p=0.0038)* for oxygen concentration increasing up to 8.4 vol%, which is 88.9% of reduction. In our previous study, the yield of NCG increased from 13.2 to 55.3 g/100 g biomass while the yield of biochar decreased from 13.1 to 9.1 g/100 g biomass when the untreated red oak was pyrolyzed at the same oxygen concentrations [14]. In comparison, the influence of oxygen had a greater effect on the yield of NCG and char agglomerate during oxidative pyrolysis of acid infused red oak compared to untreated red oak.

The distribution of bio-oil fractions (SF1 and SF2) is shown in Fig. 1(b). The yield of SF1 (heavy fraction) increased from 30.6 to 34.1 g/100 g biomass when 2.1 vol% of oxygen was added to the sweep gas. Then, it started to decrease with the increasing oxygen concentrations resulting to 24.4 g/100 g biomass at the pyrolysis with 8.4 vol% of oxygen (*F=2.77, p= 0.2129*). On the other hand, the yield of SF2 (light fraction) monotonically increased from 23.8 to 33.8 g/100 g biomass as the oxygen concentration increased in the range tested (*F=3.23, p=0.1808*). However, the difference in the fractional bio-oil yield was

observed to be statistically insignificant over the tested oxygen concentration range. The ratio of heavy fraction to light fraction (SF1 to SF2) decreased from 1.29 to 0.72 with increasing oxygen concentration in the range used. This indicates that the formation of small molecular weight compounds is preferred as oxygen concentration increases. The same trend was previously observed in the oxidative pyrolysis of untreated red oak [14].

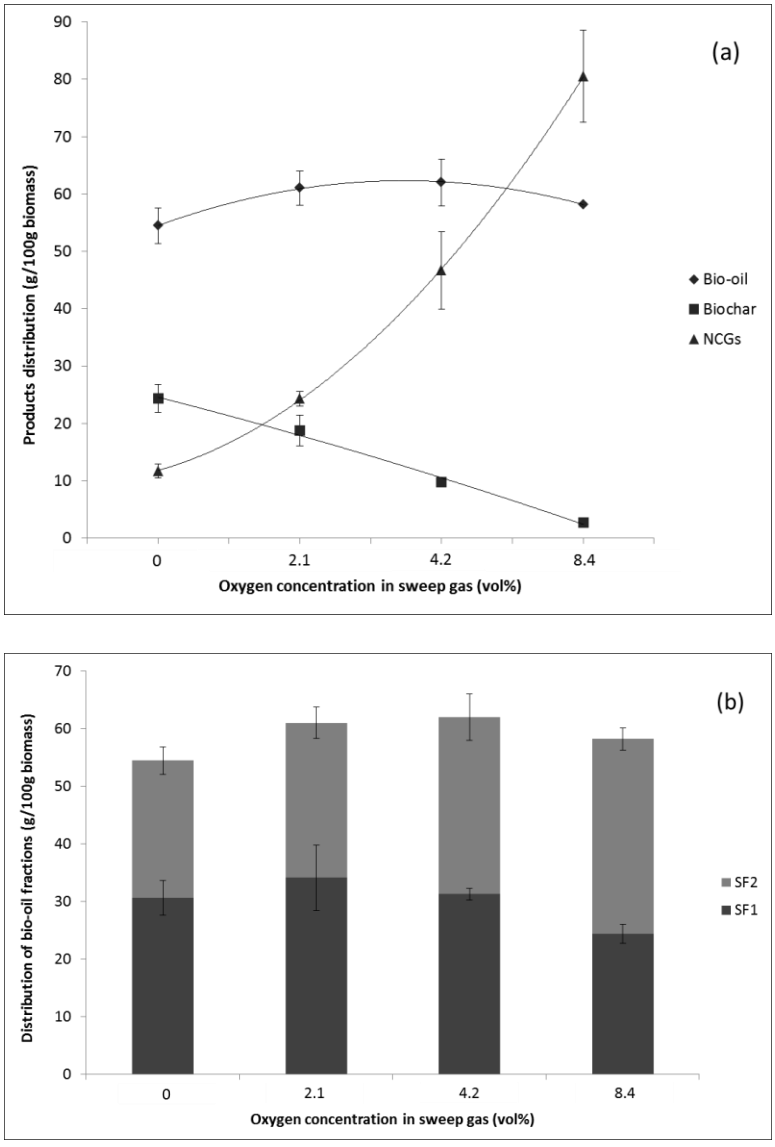

Figure 1. Mass balance for control and oxidative pyrolysis; (a) distribution of pyrolysis products; (b) fractional mass yield of each bio-oil fraction

The agglomerated char chunks found inside the reactor bed after the control case and partial oxidative pyrolysis cases are shown in Fig. 2. The agglomeration of char was previously reported by Zhou et *al*. during pyrolysis of the acid infused biomass [11]. The visual observation of the agglomerates (Fig. 2(a)) clearly indicated that they were once viscous liquid before turning into char. Although the mechanism of char agglomeration requires further investigation, it is likely that the acid-catalyzed condensation and polymerization reactions of the pyrolysis products [16, 17] resulted in the formation of non-volatile liquid with large molecular sizes and eventually dehydrated into char. These agglomerates incorporated sand from the fluidized bed. During the testing for the control case, char agglomerates quickly obstructed effective fluidization and resulting in a continuous buildup of pressure in the reactor over the 2.5 hour run. In the previous run at identical condition, the reactor was forced to shut down only after 35 minutes due to the raising back pressure, proving the difficulty of pyrolyzing acid-infused biomass in a fluidized bed. Not only does such an accumulation of char prevent steady reactor operation, it might catalyze secondary pyrolysis reactions, resulting in decreased levoglucosan yield and the formation of secondary char, water and NCGs [18, 19]. When oxygen was introduced to the fluidized bed reactor, the formation of agglomerated char in the reactor noticeably diminished (Fig. 2(b-d)). The reduced char agglomeration under oxidative pyrolysis conditions allowed the reactor to run at a steady state without a pressure buildup.

Carbon mass balance of the pyrolysis products is given in Fig. 3 as function of the oxygen concentration. The carbon content in char agglomerate considerably decreased from 40.3 to 4.0 % ($F=62.81$, $p=0.0033$) in increasing oxygen concentration from 0 to 8.4 vol% in the sweep gas. The carbon content in bio-oil decreased from 43.4 to 31.8 % at the oxygen

range tested (*F=5.24, p=0.1036*). However, with the oxygen concentrations up to 4.2 vol%, carbons in bio-oil remained at a similar level. The carbon content in NCG, on the other hand, increased from 8.3 to 57.3 % (*F=35.48, p=0.0076*) at the expense of carbon in the bio-oil and char agglomerate. Clearly, the most pronounced effect of oxygen in sweep gas was to promote the conversion of carbon in char agglomerate to light gases. These results agree with our previous findings during pyrolysis of untreated red oak [14].

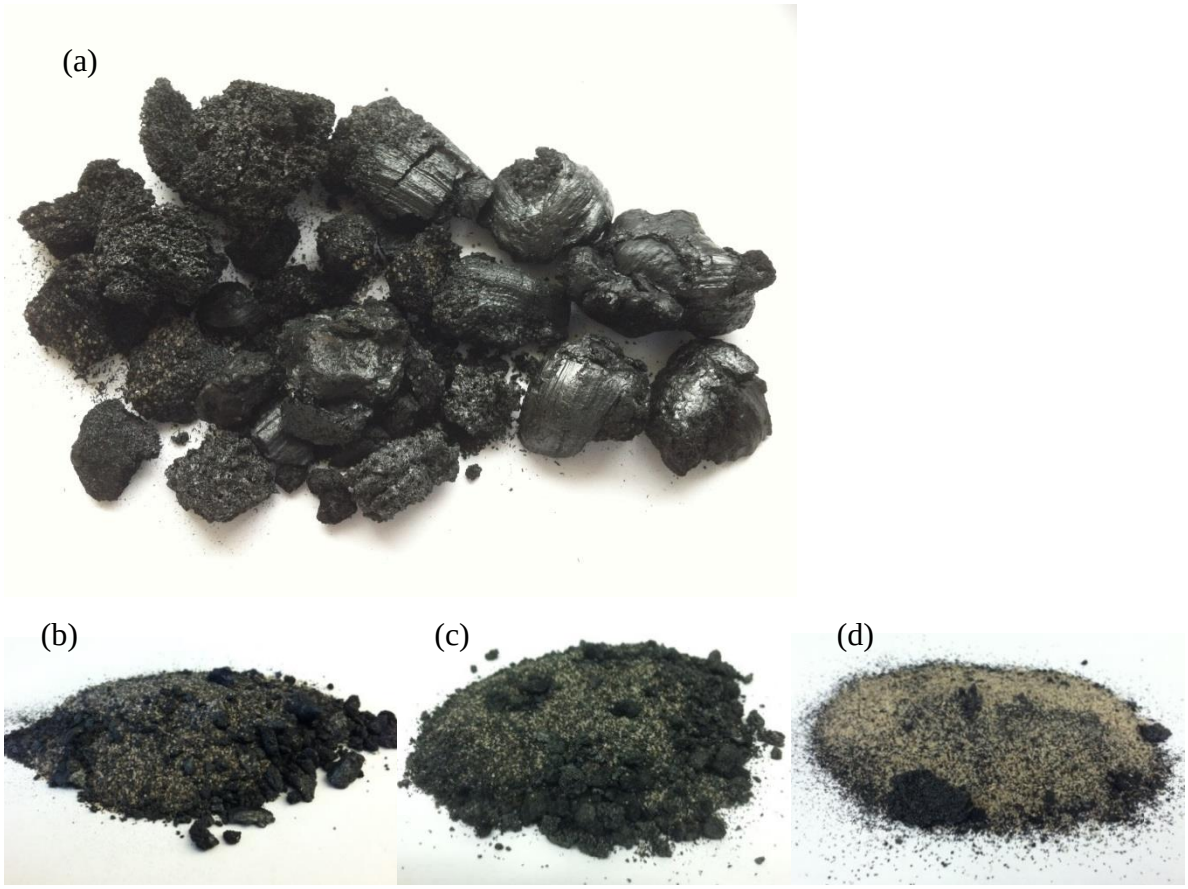

Figure 2. Char agglomerates and the fluidizing sand recovered from the fluidized bed pyrolyzer upon completion of (a) the control test (no oxygen admitted); (b) 2.1 vol% oxygen run; (c) 4.2 vol% oxygen run; (d) 8.4 vol% oxygen run

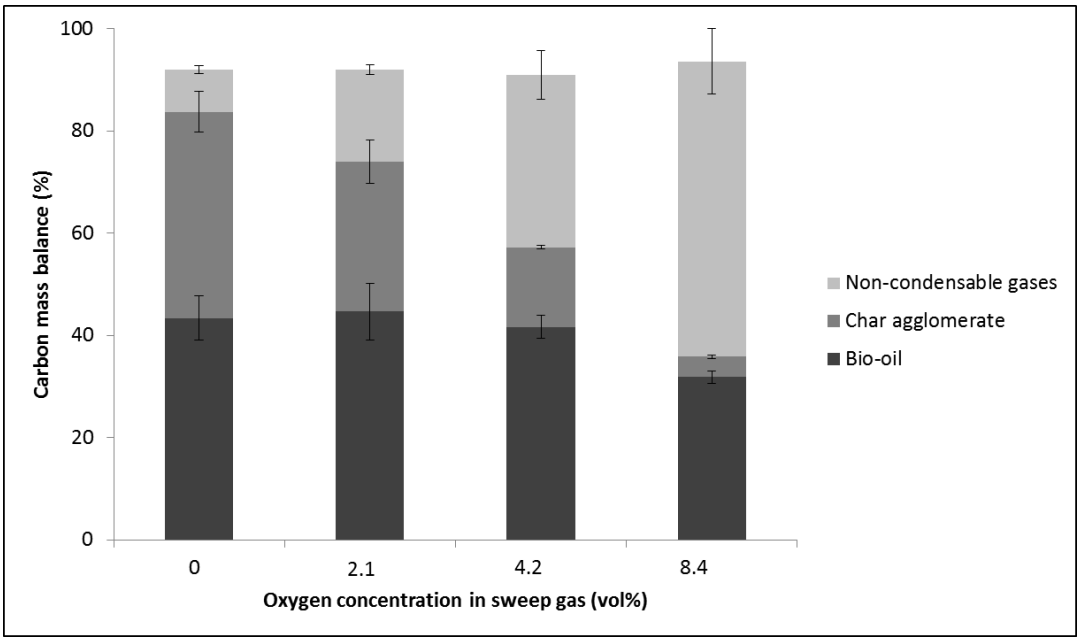

Figure 3. Carbon balance analysis of pyrolysis products

Characterization of bio-oil

Table 2 presents the result of quantitative analysis on bio-oils determined by IC and GC-MS/FID. In this study, 15 lignin derivatives and 13 carbohydrates derivatives were identified and quantified. The total yield of lignin derivatives was 2.24 g/100g biomass for oxidative pyrolysis with 2.1 vol% oxygen, which is higher than the 2.19 g/100g biomass obtained for the control case. However, further increase in oxygen concentration above 2.1 vol% reduced the yield of most of the phenolic monomers to 1.50 g/100g biomass. On the other hand, the yields of aldehydes and ketones, such as vanillin, 4-hydroxy-3-methoxyacetophenone and 4-hydroxy-3,5-dimethoxybenzaldehyde, continuously increased as the concentration of oxygen increased despite the decrease in yield of phenolic monomers overall. For oxidative pyrolysis with 8.4 vol% oxygen, the yield of vanillin and 4-hydroxy-3,5-dimethoxybenzaldehyde increased by 2.4 and 6.9 times, respectively, compared with the

control case. This is because oxygen promoted the formation of phenols with` aldehyde and ketone functional groups through oxidation reactions [14]. As the oxygen concentration increases, the oxidation and cracking effects of oxygen became dominant. Some of the primary phenolic monomers disappeared due to cracking and oxidation reactions.

The total yield of four organic acids (acetic acid, glycolic acid, formic acid and propionic acid) was 3.0 g/100 g biomass for the control case, which monotonically decreased to 2.2 g/100 g biomass with increasing oxygen concentration up to 8.4 vol%. Since the organic acids can be converted into carbon dioxide and water when they react with oxygen molecules [20], the decrease in the acids is likely the result of the secondary reactions with oxygen in the sweep gas. The yields of carbohydrate derivatives including acetol, dimethxoytetrahydrofuran and 2-(5H) furanone in bio-oil produced from the acid infused red oak were lower compared to those from oxidative pyrolysis of untreated red oak [14]. It was also found that the yield of most compounds decreased with increasing oxygen content for the range tested. A similar trend was also found for oxidative pyrolysis of untreated red oak [14].

Table 2. Compositional analysis of bio-oils determined by IC and GC-FID[1)]

	Compounds (g/100 g biomass)	0% O_2	2.1% O_2	4.2% O_2	8.4% O_2
Carbohydrates	**Acetic acid**[2)]	2.328±0.001	2.253±0.021	1.936±0.008	1.646±0.029
	Glycolic acid[2)]	0.214±0.016	0.197±0.015	0.187±0.005	0.116±0.004
	Formic acid[2)]	0.211±0.008	0.201±0.006	0.250±0.002	0.276±0.007
	Propionic acid[2)]	0.200±0.037	0.171±0.018	0.160±0.012	0.147±0.006
	Acetol	0.368±0.023	0.208±0.006	0.196±0.018	0.130±0.011
	Dimethoxytetrahydrofuran	0.131±0.035	0.052±0.004	0.043±0.007	0.041±0.011
	Furfural	1.739±0.078	0.416±0.050	0.329±0.031	0.176±0.006
	2-Furanmethanol	0.002±0.000	0.001±0.000	0.001±0.000	-
	5-methyl furfural	0.166±0.013	0.082±0.004	0.050±0.011	0.031±0.006
	2-(5H)Furanone	0.121±0.004	0.121±0.006	0.109±0.010	0.120±0.021
	Methylcyclopentenolone	0.086±0.002	0.126±0.028	0.071±0.008	0.021±0.003
	5-HMF	0.375±0.064	0.382±0.063	0.278±0.016	0.095±0.007
	Levoglucosan	10.720±0.098	11.923±0.127	11.178±0.079	7.936±0.126
	Sum of carbohydrates derivatives	**16.66±0.20**	**16.13±0.23**	**14.79±0.06**	**10.73±0.18**
Lignin	**Phenol**	0.022±0.001	0.021±0.003	0.022±0.002	0.026±0.008
	2-methoxyphenol	0.093±0.002	0.096±0.006	0.092±0.002	0.053±0.006
	2-methoxy-4-methylphenol	0.087±0.007	0.071±0.003	0.060±0.007	0.036±0.004
	4-ethyl-2-methoxyphenol	0.006±0.001	0.006±0.001	0.007±0.001	-
	2-methoxy-4-vinylphenol	0.885±0.039	0.707±0.011	0.645±0.037	0.509±0.004
	Eugenol	0.005±0.001	0.008±0.004	0.007±0.001	-
	2,6-dimethoxyphenol	0.283±0.006	0.346±0.004	0.276±0.006	0.140±0.011
	Isoeugenol	0.004±0.001	0.008±0.001	0.008±0.001	-
	4-methyl-2,6-dimethoxyphenol	0.357±0.022	0.339±0.004	0.273±0.002	0.128±0.004
	Vanillin	0.042±0.004	0.110±0.007	0.095±0.006	0.104±0.005
	4-hydroxy-3-methoxyacetophenone	0.054±0.011	0.064±0.005	0.051±0.003	0.042±0.004
	2,6-dimethoxy-4-(2-propenyl) phenol	0.080±0.001	0.084±0.002	0.060±0.001	0.024±0.004
	2,6-dimethoxy-4-(1-propenyl) phenol	0.052±0.003	0.066±0.006	0.052±0.004	0.046±0.004
	4-hydroxy-3,5-dimethoxybenzaldehyde	0.050±0.006	0.177±0.008	0.208±0.006	0.314±0.003
	4-hydroxy-3,5-dimethoxyacetophenone	0.178±0.013	0.137±0.007	0.118±0.002	0.080±0.012
	Sum of lignin derivatives	**2.19±0.11**	**2.24±0.05**	**1.97±0.06**	**1.50±0.02**
	Sum of total	***18.85±0.30***	***18.37±0.18***	***16.75±0.12***	***12.23±0.20***

[1)]based on whole bio-oil

[2)]measured by ion chromatography (IC)

The yield of levoglucosan from acid infused red oak (7.94 – 11.92 g/100 g biomass) was higher than that for pyrolysis of untreated red oak (2.36 – 3.43 g/100 g biomass) over the range of oxygen concentrations investigated in this study [14]. This enhanced levoglucosan yield is the result of AAEM passivation by the acid treatment as reported in a previous study [9]. Interestingly, when the acid infused red oak was pyrolyzed under partial oxidation conditions, the yield of levoglucosan showed a statistically significant increase compared to the control case ($F=505.38$, $p=<.0001$). The yields of levoglucosan were 11.8 and 11.2 g/100 g biomass for the 2.1 and 4.2 vol% oxygen cases, respectively. However, further increase in oxygen concentration to 8.4 vol% in the sweep gas reduced the yield of levoglucosan to 8.0 g/100g biomass.

Under the acidic condition, acid catalyzed dehydration reactions of polysaccharides and monomer sugars to furfurals were also facilitated. As can be seen in Table 2, the sum of furfural, 5-methyl furfural and 5-HMF is 2.30 g/100 g biomass in control case, which is four times higher than for non-oxidative pyrolysis of untreated red oak (0.57 g/100 g biomass) [14]. However, the presence of oxygen reduced the yield of furfurals and it is likely that furfurals were oxidized to light molecular weight components.

Since most sugars in bio-oil cannot be detected by GC analysis, SF1 bio-oil was hydrolyzed and the total sugar content determined by HPLC (Table 3). As shown in Table 3, the total amount of hydrolyzable sugars was 16.7 g/100 g biomass for the control case, which was 2.1 times higher than that from non-oxidative pyrolysis of untreated red oak (7.8 g/100 g biomass) [14]. On the other hand, the yields of total sugars increased to 20.6 and 18.3 g/100 g biomass, respectively, when 2.1 and 4.2 vol% of oxygen was added to the sweep gas. Since

sugars were all collected in the first stage condenser, SF1 bio-oil obtained with 2.1 vol% of oxygen consisted of a total 60.76% of hydrolysable sugars, including 44.51% of glucose upon hydrolysis. Further increase in the oxygen concentration to 8.4 vol% reduced the yield of the total sugar to 16.4 g/100g biomass. However, the sugars in SF1 bio-oil were more concentrated, containing over 67% of hydrolysable sugars although the yield of SF1 bio-oil was lower than all other cases conducted with lower oxygen concentrations. The fact that sugars increased in the presence of oxygen is possibly because oxygen attacks the lignin sheath surrounding cellulose fibers, increasing its porosity [21] and allowing melted or vaporized anhydrosugars to diffuse out of the biomass matrix [14]. However, the excessive amount of oxygen molecules could decompose or polymerize the sugars formed and reduces their yield [14].

Table 3. Sugar contents in bio-oil after hydrolysis (SF1 basis and biomass basis)

		0% O_2	2.1% O_2	4.2% O_2	8.4% O_2
g/100g SF1 bio-oil	cellobiosan	0.50±0.00	0.41±0.00	-	0.43±0.00
	glucose	40.45±0.13	44.51±1.17	41.40±0.86	47.88±0.16
	xylose	10.97±0.28	13.20±1.58	14.24±0.30	16.13±0.50
	sorbitol	1.56±0.16	2.17±0.30	2.20±0.38	1.92±0.09
	levoglucosan	1.22±0.64	0.68±0.14	0.83±0.44	0.91±0.18
	Total	54.45±0.86	60.76±2.62	58.68±1.10	67.05±0.73
g/100 g biomass	cellobiosan	0.15±0.00	0.08±0.00	-	0.11±0.00
	glucose	12.39±0.04	15.15±2.14	12.94±0.17	11.68±0.75
	xylose	3.36±0.09	4.46±0.21	4.45±0.06	3.94±0.39
	sorbitol	0.48±0.05	0.73±0.02	0.69±0.10	0.47±0.01
	levoglucosan	0.37±0.20	0.24±0.09	0.22±0.20	0.22±0.06
	Total	16.68±0.26	20.62±2.52	18.31±0.34	16.36±1.28

The yields of pyrolytic lignin are shown in Table 4. Pyrolytic lignin is a water-insoluble fraction of bio-oil and it is mainly a mixture of non-volatile phenolic oligomers [15]. Besides sugars, pyrolytic lignin is the main component of SF1 bio-oil. As shown in the table, the yield of pyrolytic lignin decreased from 4.3 g/ 100g biomass (or 13.9% of SF1 bio-oil) at the control pyrolysis to 3.0 g/100 g biomass (or 12.5% of SF1 bio-oil) at the oxidative pyrolysis with the oxygen concentration of 8.4 vol%. The addition of oxygen to the sweep gas was also able to reduce the yield of pyrolytic lignin at pyrolysis of untreated red oak as we reported previously [14]. Comparing with the results obtained from the pyrolysis of untreated red oak (15.8 – 9.5 g/100 g biomass) at the same oxygen concentrations, the amount of pyrolytic lignin recovered from the acid-infused red oak is significantly low. The acid is known to catalyze repolymerization and condensation of phenolic compounds to phenolic oligomers [22]. On the other hand, compared to that in the control pyrolysis of untreated red oak [14], the yield of NCG did not increase while the yield of char agglomerates increased (compared to biochar) and the yield of bio-oil decreased during the control pyrolysis of the acid-infused red oak. Therefore, the results imply that the pyrolytic lignin is the main source of char agglomerates during pyrolysis of the acid-infused red oak. It is possible that the pyrolytic lignin could form inside the reactor at relatively low temperatures, catalyzed by the acids present in the system [23]. As a result, the viscous pyrolytic lignin could be present on the surface of the incompletely pyrolyzed biomass, as well as the fluidizing sand, and become the main source of char agglomerates inside the reactor. The addition of oxygen could possibly be removing the pyrolytic lignin through combustion therefore reducing its adhesive effect. It is also possible that the addition of

oxygen reduced the formation of pyrolytic lignin by reducing the yield of the organic acids that can catalyze such recombination reactions.

Table 4. Yield of pyrolytic lignin as a function of oxygen concentration during pyrolysis

g/100 g biomass	control	2.1% O_2	4.2% O_2	8.4% O_2
Pyrolytic lignin	4.26 ± 0.26	3.91 ± 0.16	3.61 ± 0.31	3.04 ± 0.07

Water content and MAN of bio-oils were measured and the results are presented in Table 5. Water content in SF1 bio-oil, which was only about 4-5%, was relatively unchanged despite increasing the concentration of oxygen in the fluidizing gas. Water was mostly collected in SF2 bio-oil along with other light molecular weight compounds, which was attributed to the distinct bio-oil collection systems employed in this study. The water content in SF2 bio-oil steadily increased as the concentration of oxygen increased. Its yield was nearly 77% when the oxygen concentration was 8.4 vol%, compared to 61% with the control case. Increased dehydration of red oak and the reaction between oxygen molecules and red oak attributed to the increased amount of water in bio-oil.

Acidity, as determined by MAN, decreased from 30.1 to 19.0 mg KOH/g for SF1 bio-oil and decreased from 93.5 to 58.6 mg KOH/g for SF2 bio-oil as oxygen concentration increased from zero to 8.4 vol%. As described above, quantitative analysis by GC/FID showed that the amount of organic acids in bio-oil decreased with increasing oxygen concentrations in the sweep gas. This result corresponds with the MAN analysis, indicating

the acidity of bio-oils is reduced under partial oxidation conditions. Thermal oxidation of the acids to water and carbon dioxide could be the main cause for the reduction of acids.

Table 5. Characterization of bio-oil properties.

		0% O_2	2.1% O_2	4.2% O_2	8.4% O_2
Water content (wt. %)	**SF1**	4.32	5.40	5.28	4.51
	SF2	60.99	71.94	73.72	76.94
MAN (mg KOH/g)	**SF1**	30.12	28.29	25.99	18.96
	SF2	93.48	89.83	81.98	58.57

Compositional analysis of non-condensable gases

Fig. 4 shows the yield of NCG with varying oxygen concentrations. The total amount of NCG from the control pyrolysis was 11.7 g/100g biomass. CO and CO_2 were the two major NCG and account for more than 99% of total NGCs for all the cases. As shown, the yields of CO and CO_2 statistically significantly increased from 3.9 to 27.2 g/100 g biomass (*F=22.68, p=0.0145)* and from 7.8 to 52.1 g/100 g biomass (*F=55.99, p=0.0039*), respectively.

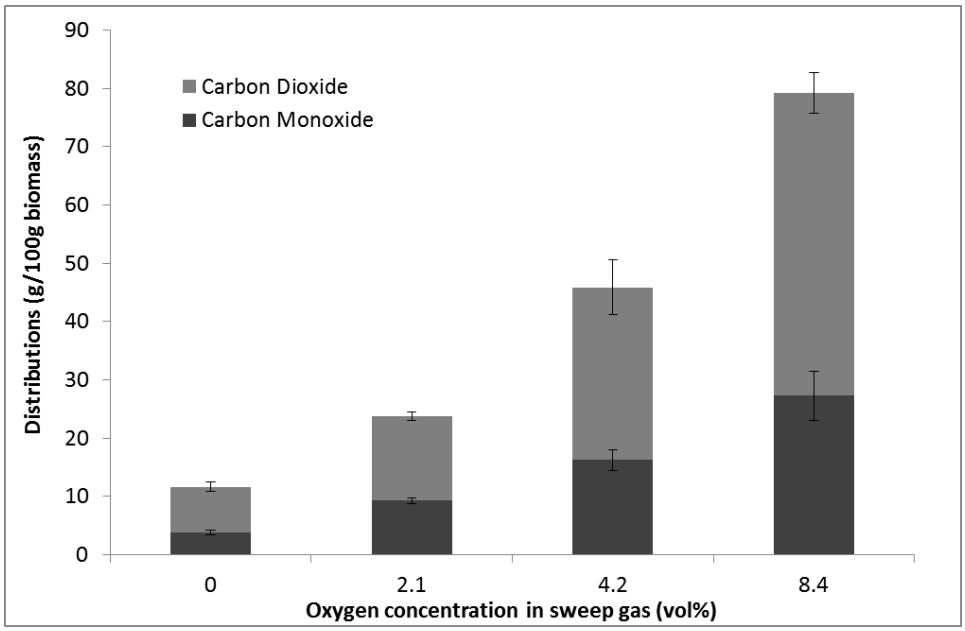

Figure 4. The composition of non-condensable gases (the yield of ethylene, methane and hydrogen was negligible)

Considering the carbon mass balance analysis (Fig. 3), the carbon in bio-oil transferred to NCG in the form of CO and CO_2 with increasing oxygen concentration. In addition to these two gases, the yield of CH_4, C_2H_4 and H_2 also increased with increasing oxygen concentration although the sum of these minor gases was insignificant. The increased NCG yield was accompanied by decreasing char agglomerates during partial oxidative pyrolysis. Pyrolytic lignin was likely the main source. Therefore, these increased light gases, including the hydrocarbons, are mainly the products of oxidative cracking of the lignin-derivatives.

Conclusion

Acid infused red oak was pyrolyzed using a continuous fluidized bed reactor with varying oxygen concentrations in the sweep gas, ranging from 0 to 8.4 vol%. The presence of

oxygen prevented the reactor clogging by reducing the char agglomeration by up to 88.9%. The addition of oxygen up to 4.2 vol% (equivalence ratio up to 0.26) also improved the sugar yield from red oak. The maximum yield of sugar was obtained when 2.1 vol% of oxygen is added, which is 20.62 g/100g biomass. The SF1 bio-oils obtained from oxidative pyrolysis was highly concentrated with hydrolysable sugars, which had a yield as high as 67 %. Carbons in bio-oil remained at a similar level with oxygen concentrations up to 4.2 vol%.

Acknowledgements

The authors would like to acknowledge financial support from the Phillips 66 Company. We would also like to thank Dr. Marjorie Rover, Patrick Johnston and Ryan Smith of Center for Sustainable Environmental Technologies for assistance with many aspects of the work involved in this project. The authors also would like to thank Tannon Daugaard for valuable discussion.

REFERENCES

[1] P. R. Patwardhan, J. A. Satrio, R. C. Brown, B. H. Shanks, Influence of inorganic salts on the primary pyrolysis products of cellulose, Bioresource Technology, 101, (2010) 4646-4655.

[2] R.C. Brown, D. Radlein, J. Piskorz, Pretreatment processes to increase pyrolytic yield of levoglucosan from herbaceous feedstocks, in: Acs Sym Ser, ACS Publications, (2001) 123-132.

[3] D. Mourant, Z.H. Wang, M. He, X.S. Wang, M. Garcia-Perez, K.C. Ling, C.Z. Li, Mallee wood fast pyrolysis: Effects of alkali and alkaline earth metallic species on the yield and composition of bio-oil, Fuel, 90, (2011) 2915-2922.

[4] J. Piskorz, P. Majerski, D. Radlein, D.S. Scott, A.V. Bridgwater, Fast pyrolysis of sweet sorghum and sweet sorghum bagasse, J Anal Appl Pyrol, 46, (1998) 15-29.

[5] D.S. Scott, J. Piskorz, D. Radlein, P. Majerski, Process for the production of anhydrosugars from lignin and cellulose containing biomass by pyrolysis, in, US Patents (5395455 A), (1995).

[6] Q. Li, P.H. Steele, F. Yu, B. Mitchell, E.M. Hassan, Pyrolytic spray increases levoglucosan production during fast pyrolysis, J Anal Appl Pyrol, 100, (2013) 33-40.

[7] C.U. Pittman, D. Mohan, A. Eseyin, Q. Li, L. Ingram, E.B.M. Hassan, B. Mitchell, H. Guo, P.H. Steele, Characterization of bio-oils produced from fast pyrolysis of corn stalks in an auger reactor, Energ Fuel, 26, (2012) 3816-3825.

[8] A. Zhurinsh, G. Dobele, J. Rizhikovs, J. Zandersons, K. Grigus, Effect of pre-treatment conditions on the analytical pyrolysis products from birch wood lignocellulose, J Anal Appl Pyrol, 103, (2013) 227-231.

[9] N. Kuzhiyil, D. Dalluge, X. Bai, K.H. Kim, R.C. Brown, Pyrolytic sugars from cellulosic biomass, ChemSusChem, 5, (2012) 2228-2236.

[10] G. Dobele, T. Dizhbite, G. Rossinskaja, G. Telysheva, D. Mier, S. Radtke, O. Faix, Pre-treatment of biomass with phosphoric acid prior to fast pyrolysis - A promising method for obtaining 1,6-anhydrosaccharides in high yields, J Anal Appl Pyrol, 68, (2003) 197-211.

[11] S. Zhou, D. Mourant, C. Lievens, Y. Wang, C.Z. Li, M. Garcia-Perez, Effect of sulfuric acid concentration on the yield and properties of the bio-oils obtained from the auger and fast pyrolysis of Douglas Fir, Fuel, 104 (2013) 536-46.

[12] D. Butt, Formation of phenols from the low-temperature fast pyrolysis of Radiata Pine (Pinus radiata): Part I. Influence of molecular oxygen, Journal of Analytical and Applied Pyrolysis, 76, (2006) 38-47.

[13] M. Amutio, G. Lopez, R. Aguado, J. Bilbao and M. Olazar, Biomass oxidative flash pyrolysis: autothermal operation, yields and product properties, Energy & Fuels, 26, (2012) 1353.

[14] K.H. Kim, X. Bai, M. Rover, R.C. Brown, Partial oxidative pyrolysis of Red Oak using a fluidized bed reactor, Fuel, 124, (2014) 49-56.

[15] B. Scholze, D. Meier, Characterization of the water-insoluble fraction from pyrolysis oil (pyrolytic lignin). Part I. PY–GC/MS, FTIR, and functional groups, J Anal Appl Pyrol , 60, (2001);60:41-54.

[16] R.E. Wrolstad, Reactions of sugars, Wiley-Blackwell, (2011).

[17] J.B. Li, G. Henriksson, G. Gellerstedt, Lignin depolymerization/repolymerization and its critical role for delignification of aspen wood by steam explosion, Bioresource Technol, 98 (2007) 3061-3068.

[18] F. Ronsse, X.L. Bai, W. Prins, R.C. Brown, Secondary reactions of levoglucosan and char in the fast pyrolysis of cellulose, Environ Prog Sustain, 31 (2012) 256-260.

[19] F. Melligan, R. Auccaise, E.H. Novotny, J.J. Leahy, M.H.B. Hayes, W. Kwapinski, Pressurised pyrolysis of Miscanthus using a fixed bed reactor, Bioresource Technol, 102, (2011) 3466-3470.

[20] J.C. Meyer, P.A. Marrone, J.W. Tester, Acetic-Acid Oxidation and Hydrolysis in Supercritical Water, Aiche J, 41, (1995) 2108-2121.

[21] O. Senneca, Kinetics of pyrolysis, combustion and gasification of three biomass fuels, Fuel Process Technol, 88, (2007) 87-97.

[22] K. Lundquist, Low-molecular weight lignin hydrolysis products, in: Applied Polymer Symposium, (1976) 1393-1407.

[23] P.R. Patwardhan, R.C. Brown, B.H. Shanks, Understanding the Fast Pyrolysis of Lignin, ChemSusChem, 4 (2011) 1629-1636.

CHAPTER 4

HYDROGEN-DONOR-ASSISTED SOLVENT LIQUEFACTION OF LIGNIN TO SHORT-CHAIN ALKYLPHENOLS USING A MICRO REACTOR/GAS CHROMATOGRAPHY SYSTEM

A paper published in *Energy & fuels*

Kwang Ho Kim, Robert Brown, Matt Kieffer, Xianglan Bai

Abstract

The benefit of using hydrogen donor solvents in lignin solvolytic conversion was studied using a micro reactor coupled to an online GC/MS-FID. This system is able to achieve very high heating rates of reactants and capable of analyzing the reaction products immediately after the reaction is completed, thus allows probing "semi" time-resolved reactions occurring during lignin conversion. These features have been impossible for the batch reactors typically employed in previous solvent liquefaction studies. The study showed that the hydrogen donor solvents tetralin and isopropanol were effective in converting lignin into short chain alkyl phenols (SCAP) at high yield. The yield of SCAP increased with increasing reaction temperature over the range of 300 – 400 °C and reaction time over the range of 5 – 15 min, which is attributed to stabilization of lignin-derived products by hydrogen abstraction from the hydrogen donor solvents. The molecular weight distributions of solvolysis products revealed that molecular weight significantly decreased with increasing reaction times in the presence of a hydrogen donor solvent. In contrast, in the absence of a hydrogen donor solvent the molecular weight of products increased with increasing reaction times. Also, the peak assigned to oligomers increased and shifted to higher molecular weights at the same reaction conditions. Overall, the solvolytic conversion of lignin involves

thermal cleavage of lignin macromolecules followed by secondary reactions, including cracking and repolymerization, among the primary products. The presence of a hydrogen donor was found to suppress repolymerization reactions by stabilizing the primary products to alkyl-substituted phenols and promoting demethoxylation.

Introduction

Lignin, the second most abundant natural polymer in the biosphere, is produced in large quantities by the pulp and paper industry and is expected to become increasingly available with the commercial development of cellulosic ethanol [1]. Lignin differs chemically from carbohydrates in that it has a complex aromatic substructure. Unlike cellulose, which consists of a linear chain of repeating glucose units, lignin is a three dimensional polymer of phenolic monomers with a variety of functional groups and chemical bonds, the structure of which varies with biomass source. This complicates chemical or biological modification and recovery of products [2].

Lignin is commonly used as low value boiler fuels with less than 5% of the world's supply used for other purposes [3]. Because of its availability and low cost, lignin has been intensely studied as a renewable feedstock for production of biofuels and biobased chemicals. Lignin macro molecules can be depolymerized into value-added monomeric phenols via thermochemical processing, including pyrolysis and solvolysis [4].

Solvolysis of lignin has several advantages over lignin pyrolysis. Depending on the choice of solvent, it is possible to selectively depolymerize lignin because the solvent can strongly influence the decomposition of lignin [4]. Whereas pyrolysis of lignin produces up to 40 wt% of char as product [5, 6], solvolysis in appropriate solvents yields only small

amounts of char [7]. Several solvents and solvent combinations with and without catalysts have been tested for their ability to depolymerize lignin [8-10]. Previous studies suggest that phenolic compounds produced during solvolysis are reactive, with a strong tendency to repolymerize [7, 11]. Addition of hydrogen gas or hydrogen donor agent is expected to reduce repolymerization by stabilizing reactive phenols. The main advantages of using hydrogen donor solvents instead of hydrogen gas for solvolysis is that lower operating pressures can be employed [12]. Hydrogen donor solvent (HDS), such as tetralin and isopropanol, were first employed in coal liquefaction to stabilize free radicals that otherwise recombine to form char [12]. Several HDS have been tested in biomass solvolysis [12-19]. Vasilakos and Austgen [12] converted cellulose in tetralin solvent, and reported that tetralin promoted bio-oil yield while reducing oxygen content in the bio-oil. They also used isopropanol as a hydrogen donor solvent to obtain 75 wt% yield of bio-oil from cellulose. Rinaldi et *al*.[20, 21] recently investigated lignin valorization in the presence of catalyst using isopropanol. They tested to decompose lignin using isopropanol as a hydrogen-transfer initiator and found that molecular weight of bio-oil decreased and did not undergo repolymerization [20]. Davoudzadeh et *al*. [14] investigated depolymerization of lignin at low pressure using catalyst and tetralin. They found that increasing reaction temperature to 400 °C increased lignin liquefaction in tetralin in the presence of hydrogen gas. Dorrestijn et *al*. [15] tested lignin solvolysis using 9, 10-dihydroanthracene and 7*H*-benz[*de*]anthracene as the hydrogen-donor solvent, and reported that the yield of phenolic compounds increased with hydrogen donor addition. Kleinert et *al*. [16] optimized solvolysis conditions for depolymerization of lignin to produce liquid biofuel using a mixture of formic acid and alcohol solvent as hydrogen donors.

In the previous studies using lab-scale batch reactors, it took relatively long time (up to an hour) before the samples reach preset temperatures. After reactions, the reactors had to be completely cooled down to room temperature before the post-reaction products were taken out from the reactors for subsequence analysis. Thus, it has been difficult to investigate time-resolved reactions occurring during solvolysis at a given experimental condition in these studies. The present study overcomes these limitations by conducting solvolysis experiments in a micro reactor with online GC/MS-FID, which is able to rapidly heat reactants to the preset temperature and immediately analyze the vapor phase products before secondary reactions occur. Since very small amount of samples are used in the system, heat and mass transfer limitations are also greatly suppressed. By employing this system, the benefit of using hydrogen donor solvents over non-hydrogen donor solvent is investigated using two hydrogen donor solvents and a non-hydrogen donor solvent.

Experimental

Materials

Cornstover-derived organosolv lignin used in this study was obtained from Archer Daniels Midland (ADM) Company. To remove any catalytic effects of inorganic impurities, the lignin was purified by washing in 0.1 N hydrochloric acid, followed by repeated washing with deionized water until a neutral pH was obtained. The proximate and ultimate analyses of organosolv lignin were conducted using thermogravimetric analysis (TGA) (Mettler Toledo, USA) and a Vario Micro Cube elemental analyzer (Elementar, Germany), respectively. The results of proximate and ultimate analyses are shown in Table 1. Tetralin, isopropanol and naphthalene were purchased from Sigma-Aldrich and used without further purification.

Table 1. Ultimate and proximate analysis of organosolv lignin

Proximate analysis (wt%)	
Moisture	4.92
Volatiles	59.64
Fixed carbon	34.48
Ashes	0.97
Ultimate analysis (wt%)	
C	62.80
H	5.75
O[1)]	29.81
N	1.64

[1)] By difference

Solvolysis using an online micro reactor

Solvolysis of lignin was conducted in a sealed glass capsule (id: 1.6 mm, od: 2.24 mm, height: 26 mm) and heated in a micro-reactor (PY1-1050, Frontier Laboratories, Japan) attached to a micro-furnace pyrolyzer (PY-3030D, Frontier Laboratories, Japan) with online product analysis, illustrated in in Fig 1. Tetralin and isopropanol were used as hydrogen donor solvents and naphthalene was used as a non-hydrogen donor solvent for comparison. Prior to actual test, blank run test was performed. From this blank test, it was confirmed that isopropanol and tetralin act as hydrogen donating agents in the given experimental conditions. For example, it was found that isopropanol converted to acetone upon donation of hydrogen and tetralin converted to naphthalene in the same manner. Approximately 500 μg of lignin samples and 5μL of solvent (except for naphthalene, for which 5.7 mg was added)

were placed in a glass capsule. After the capsule was inserted in a heat sink, the open end was purged with nitrogen and sealed using a micro torch.

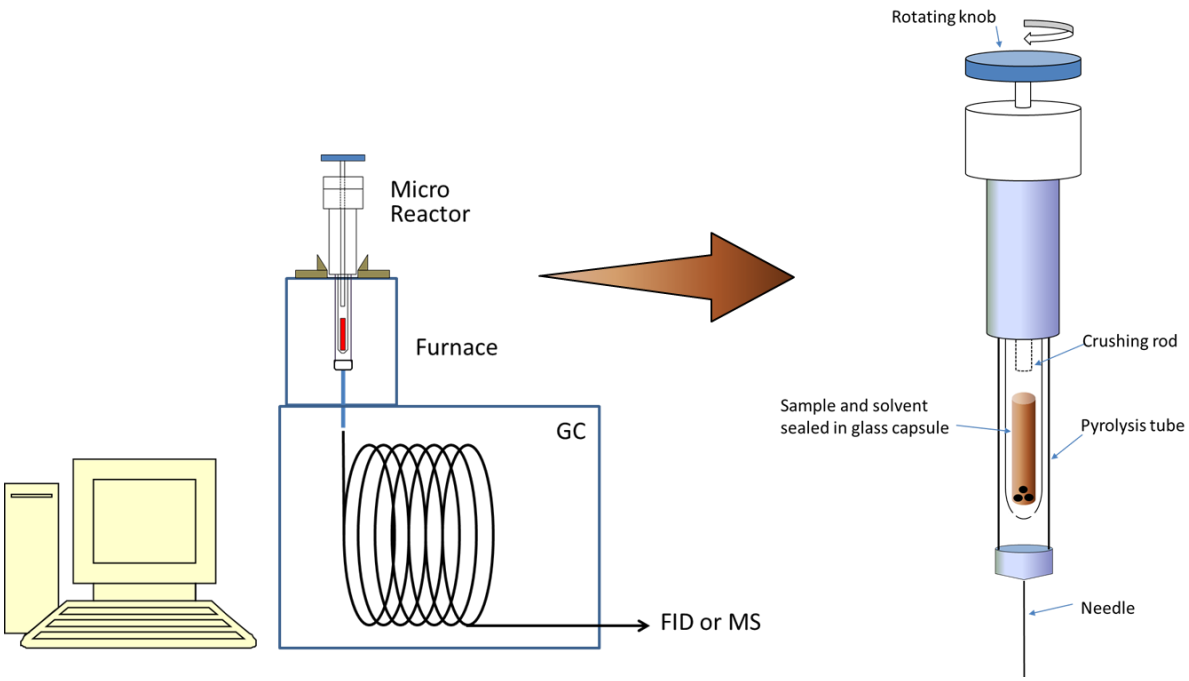

Figure 1. Schematic diagram of online micro reactor system.

The sealed glass capsule was inserted into the micro-reactor, and the micro-reactor placed in the furnace of the Frontier micropyrolyzer. Although the actual heating rate of the sample is difficult to directly measure, a CFD simulation of the system indicated an approximate heating rate of 6 °C/s (compared to only less than 0.5°C /s for autoclave experiments). Experiments were conducted at 300, 350 and 400 °C for 5, 10 or 15min. Pressure within the glass capsule was calculated for each reaction temperature using the Van der Waals Equation of State. The calculated pressure ranged from 1.5 to 1.9 MPa for tetralin and from 3.1 to 3.8 MPa for isopropanol in the temperature range of 300 – 400 °C. After the desired reaction time was reached, the screw on the top of the micro-reactor was turned,

which crushed the glass capsule, releasing volatiles to the gas stream, which were directly swept to a GC system for analysis. Identification and quantification of solvolysis products of lignin were performed using a GC (Varian CP-3800, USA) equipped with mass spectrometry (Saturn 2200 MS, USA) and flame ionization detector (FID). The capillary column used was a Phenomenex ZB-1701 (60m × 0.25 mm × 0.25μm). Injection temperature was 275 °C and the split ratio used was 1:100. The GC oven temperature was programmed to hold at 35 °C for 3 min, ramp up to 280 °C with 3 °C / min and then hold for additional 4 min. In this work, 21 lignin derived monomeric phenols were identified and quantified using a GC-MS/FID system after calibrating with authentic compounds purchased from Sigma-Aldrich.

Separate solvolysis experiments were conducted to investigate molecular weight distribution of products, including non-volatile products that cannot be detected by GC. Instead of crushing the glass capsule after the desired reaction time, it was removed from furnace chamber and immediately cooled in an ice bath to prevent further reaction. The glass capsule was cracked open and the liquid products dissolved in 1mL of tetrahydrofuran (THF). All samples were filtered with a Whatman 0.45μ Glass Microfiber (GMF) syringe filter before analysis. Gel permeation chromatography (GPC) analysis was performed using a high performance liquid chromatography system (Ultimate 3000, Dionex, USA) equipped with a Shodex Refractive Index (RI) and Diode Array Detector (DAD). GPC standards which contained polystyrene ranging from 162 – 38,640 g/mol were purchased from Agilent and used for calibration.

Results and discussion

Lignin solvolysis with tetralin

Table 2 lists the compounds identified and quantified by GC analysis. Among the 21 phenolic compounds investigated in this study, alkylated (methyl, ethyl and propyl) phenolic monomers as well as phenol, guaiacol and syringol are referred to as short chain alkyl phenols (SCAP). Similarly, 4-vinylphenol, 2-methoxy-4-vinylphenol and 2,6-dimethoxy-4-vinylphenol are categorized as vinylphenols (VP). Since the peaks of 4-vinylphenol and 2-methoxy-4-vinylphenol on the chromatogram slightly overlapped each other, the peaks were treated as one and quantified using the response factor of 4-vinylphenol.

Table 2. List of monomeric phenols identified and quantified.

Compounds	Molecular formula	Carbon distribution[3)]
Phenol[1)]	C_6H_6O	C6
2-methoxyphenol[1)]	$C_7H_8O_2$	C6
2-methoxy-4-methylphenol[1)]	$C_8H_{10}O_2$	C1C6
4-ethylphenol[1)]	$C_8H_{10}O$	C2C6
4-ethyl-2-methoxyphenol[1)]	$C_9H_{12}O_2$	C2C6
4-vinylphenol[2)]	C_8H_8O	-
2-methoxy-4-vinylphenol[2)]	$C_9H_{10}O_2$	-
2-methoxy-4-propylphenol[1)]	$C_{10}H_{14}O_2$	C3C6
2,6-dimethoxyphenol[1)]	$C_8H_{10}O_3$	C6
isoeugenol (trans)	$C_{10}H_{12}O_2$	-
2,6-dimethoxy-4-methylphenol[1)]	$C_9H_{12}O_3$	C1C6
Vanillin	$C_8H_8O_3$	-
2,6-dimethoxy-4-ethylphenol[1)]	$C_{10}H_{14}O_3$	C2C6
1-(4-hydroxy-3-methoxyphenyl)-ethanone	$C_9H_{10}O_3$	-
2,6-dimethoxy-4-vinylphenol[2)]	$C_{10}H_{12}O_3$	-
1-(4-hydroxy-3-methoxyphenyl)-2-propanone	$C_{10}H_{12}O_3$	-
2,6-dimethoxy-4-propylphenol[1)]	$C_{11}H_{16}O_3$	C3C6
4-hydroxybenzenepropanoic acid, methyl ester	$C_{10}H_{12}O_3$	-
2,6-dimethoxy-4-(1-propenyl)-phenol (trans)	$C_{11}H_{14}O_3$	-
1-(4-hydroxy-3,5-dimethoxyphenyl)-ethanone	$C_{10}H_{12}O_4$	-
1-(4-hydroxy-3,5-dimethoxyphenyl)-2-propanone	$C_{11}H_{14}O_4$	-

[1)] short chain alkylphenols
[2)] vinylphenols
[3)] carbon distribution was determined by the number of carbons in the side chain for the alkylphenols

The yields of monomeric phenols from the solvolysis of lignin with tetralin are presented in Fig 2. It should be noted that the GC retention times of 2-methoxyphenol and 4-methylphenol coincided with the tetralin, precluding their quantitative analysis. As shown in this figure, the yield of total monomeric phenols (TMP) slightly increased with increasing reaction time over the range investigated. However, the influence of reaction time was relatively small in the overall range tested. Increasing reaction times from 5 to 15 min at 300 °C increased the yield of TMP from 5.5 to 5.9 wt%, SCAP from 1.9 to 2.8 wt%, and decreased VP from 2.8 to 2.3 wt%. Although the same trend was observed at higher temperatures (350 and 400 °C), the effect was small.

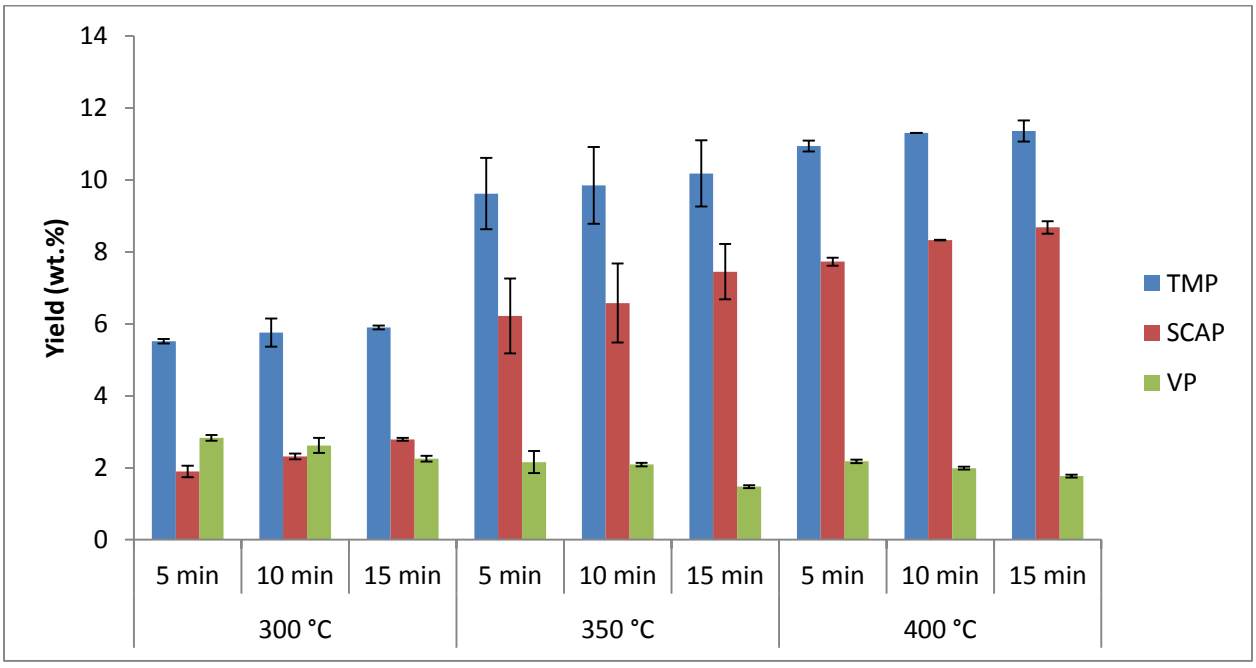

Figure 2. Products distribution obtained from lignin/tetralin system at various reaction conditions (TMP: total monomeric phenols, SCAP: short-chain alkylphenols and VP: vinylphenols).

Reaction temperature, different from the influence of reaction time, had a larger influence on products yields for lignin decomposition in tetralin. For the shortest reaction time tested (5 min), as reaction temperature increased from 300 to 400 °C, the yield of TMP increased from 5.5 to 10.9 wt%, SCAP increased from 1.9 to 7.7 wt%, and VP decreased from 2.8 to 2.2 wt%. The highest yields of TMP and SCAP were observed at 400 °C. For the longest reaction time (15 min), the yield of TMP increased from 5.9 to 11.4 wt%, and SCAP increased from 2.8 to 8.7 wt% as reaction temperature increased from 300 to 400 °C. Using a hydrogen donor solvent resulted in a decrease in the yield of vinyl (styrene derivatives) group containing phenols with increasing time and temperature, possibly due to further hydrogenation [15]. The increase in the yield of SCAP and decrease in the yield of VP in the overall reaction conditions investigated resulted in increasing selectivity toward SCAP. As shown in Table S1 (see supplemental data), the selectivity of SCAP increased from 34.4 (300 °C and 5 min) to 76.4 % (400 °C and 15 min) over the entire reaction temperature and time tested.

Distribution into the different product groups (C6, C1C6, C2C6 and C3C6; see Table 2 for descriptions) was determined by the number of carbons in the side chain of the products (see Table S1). For tetralin, the yield of each group increased with both increasing reaction temperature and time. After 15 min at 400 °C, the yield of C6 units was 3.5 wt%, followed by C2C6 (3.2 wt%), C1C6 (1.7 wt%) and C3C6 (0.3 wt%) units. This suggests that the high yield of C6 units is attributed to enhanced cracking of side chains with increasing reaction time [22]. Furthermore, the increase in the yield of C2C6 units can be explained by hydrogen donor solvent-induced stabilization. In previous work with the same lignin phenol (C6), syringol (C6), 4-vinylphenol (C2C6) and 2-methoxy-4-vinylphenol (C2C6) were found

to be the major products from lignin pyrolysis [6]. Generally, VPs are the major phenolic compounds in the pyrolysates of lignocellulosic materials, resulting from the cleavage of β-O-4 linkages [23]. Since tetralin is capable of capping the highly reactive allyl and vinyl substituted phenols [24], VPs are thought to have stabilized via hydrogenation to alkyl substituted phenols (SCAPs), predominantly to 4-ethylphenol (C2C6) and 4-ethyl-2-methoxyphenol (C2C6) found in this study (see Fig 3).

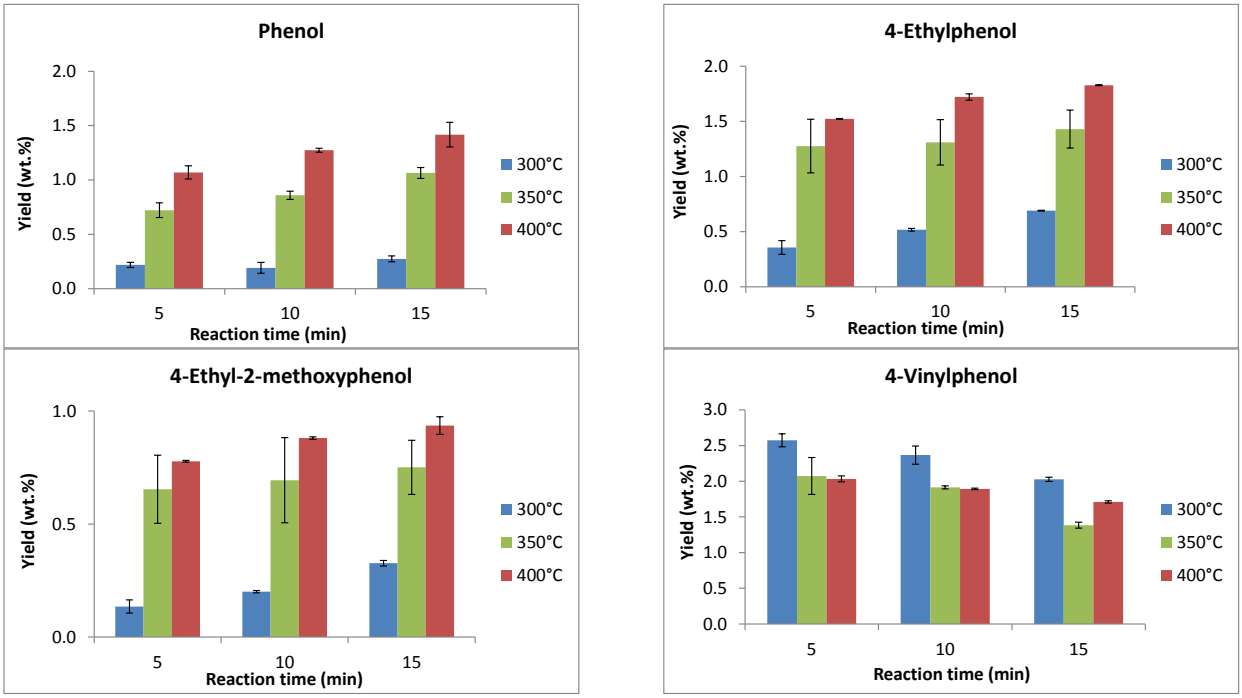

Figure 3. Products from solvent liquefaction of lignin in tetralin.

At higher reaction temperatures and longer reaction times decreases were observed in guaiacyl/*p*-hydroxyphenyl (G/H) ratios and syringyl /*p*-hydroxyphenyl (S/H) ratios, which demonstrates that demethoxylation reactions were promoted in the presence of tetralin [15]. At 400 °C, the G/H ratio and S/H ratio decreased 13 and 15 % when reaction time increased

from 5 to 15 min. The conversion of G- or S- unit phenols to H- unit phenols due to demethoxylation is expected.

Lignin solvolysis with isopropanol

The influences of reaction temperature and time on product yields for lignin decomposition in isopropanol solvent are shown in Fig 4. In general, the influence of reaction time was relatively small in the range investigated. At the lowest temperature tested (300 °C), as reaction time was increased from 5 to 15 min, the yield of TMP increased from 3.9 to 4.3 wt%, SCAP increased from 1.6 to 2.4 wt%, and VP showed a relatively modest decrease from 1.7 to 1.2 wt%. Similarly small effects of reaction time were also observed at higher reaction temperatures.

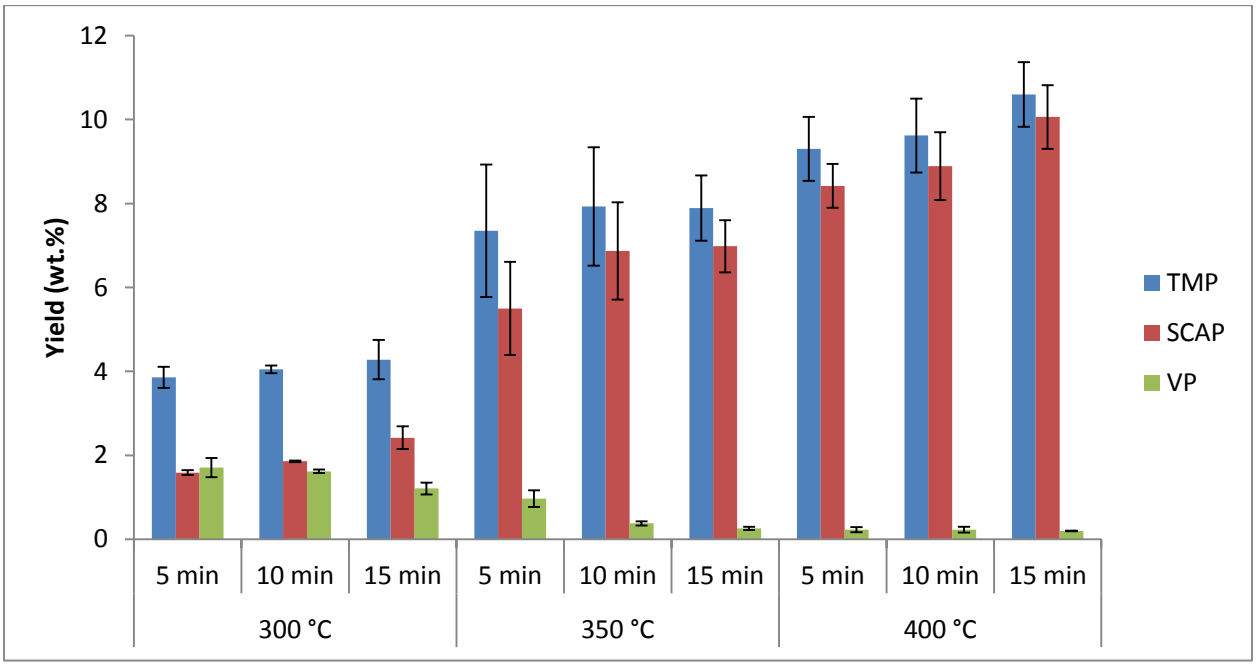

Figure 4. Product distribution obtained from lignin/isopropanol system at various reaction conditions (TMP: total monomeric phenols, SCAP: short-chain alkylphenols and VP: vinylphenols).

Temperature had a much larger influence on product composition. For the shortest reaction time tested (5 min), as reaction temperature increased from 300 to 400 ºC, the yield of TMP increased from 3.9 to 9.3 wt%, SCAP increased from 1.6 to 8.4 wt%, while VP decreased from 1.7 to 0.2 wt%. Similarly large changes with temperature were observed for longer reaction times.

Selectivity toward SCAP was strongly influenced by both reaction time and temperature (see Table S2). The selectivity toward SCAP increased from 41.2% (at 300 °C and 5 min run) to 94.9% (at 400 °C and 15 min run) over the entire reaction temperature and reaction time tested. Examination of the product distribution compared with the lignin/tetralin system (34.4 – 76.4%) showed higher selectivity of SCAP. This might be attributed to the high hydrogen-donor capability of isopropanol because the yield of VP from lignin/isopropanol was significantly lower than that from lignin/tetralin at all reaction conditions.

Table S2 shows the distribution of products into the different groups. The yield of each group increased as reaction time increased at all temperatures tested. At 400 °C, the highest yield was observed from C6 units (4.9 wt%), followed by C2C6 (3.3 wt%), C1C6 (1.5 wt%) and C3C6 (0.3 wt%), which are in the same order as found from lignin/tetralin system. Fig 5 shows the yield of major products from lignin decomposition in isopropanol solvent at each reaction condition. As discussed, the yield of phenol (C6), 4-ethylphenol (C2C6) and 4-ethyl-2-methoxyphenol (C2C6) increased with a prolonged reaction time, while the yield of 4-vinylphenol (include 2-methoxy-4-vinylphenol) decreased at the same reaction conditions. Other vinylphenols showed similar trends at this condition. This result

supports the hypothesis that secondary reactions, including side chain cleavage and stabilization of reactive functional groups through hydrogenation, take place in the presence of a hydrogen donor solvent.

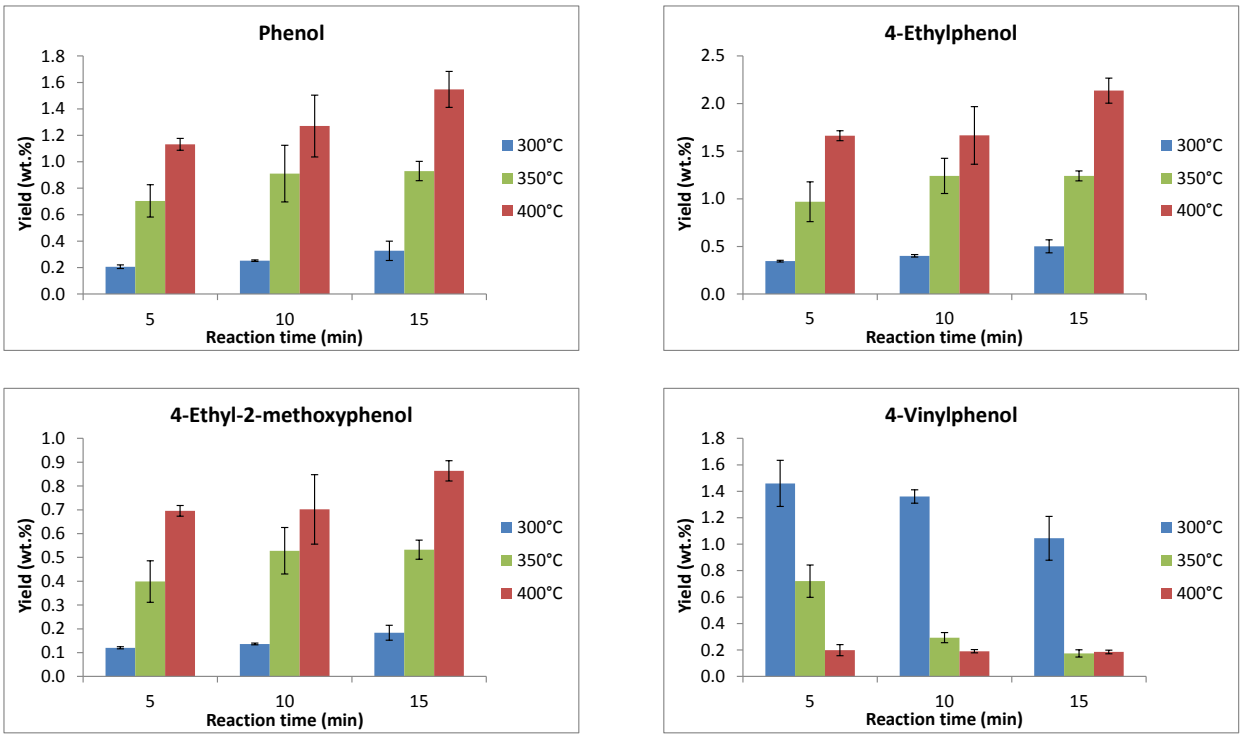

Figure 5. Products from solvent liquefaction of lignin in isopropanol.

Also, a conversion from S and G unit to H unit was observed at higher reaction temperature and longer reaction time. As found in lignin/tetralin system, a demethoxylation was promoted in the presence of hydrogen donor solvent. G/H and S/H ratio decreased 5.2 and 26.4%, respectively, after 15 min at 400 °C compared to the ratios after reacting 5 min at the same temperature.

Lignin solvolysis with naphthalene

Lignin was reacted in naphthalene, which is not a hydrogen donor, to further test the hypothesis that the hydrogen donor solvents increase selectivity toward SCAP [25, 26]. The results of these tests are presented in Fig 6. The solvolytic conversion of lignin in naphthalene at 400 °C for 5 min resulted in TMP yields of 7.8 wt%. The yield of SCAP in this reaction condition was 6.4 wt%, which was lower than that for tetralin (7.7 wt%) and isopropanol (8.4 wt%) . In contrast to the cases with tetralin and isopropanol, increasing reaction time to 15 minute increased the yield of TMP to 7.5 wt% and decreased the yield of SCAP to 6.3 wt%. While the yield of SCAP increased with time when the solvent was tetralin or isopropanol, the yield decreased with time when naphthalene was the solvent. The decrease in yields of TMP and SCAP with reaction time when naphthalene was the solvent is likely to the result of secondary reactions, with primary products likely converted into higher molecular weight substances. This suggests that prolonged reaction time in the absence of hydrogen is deleterious to yields of TMP and SCAP [26]. Although the selectivity toward SCAP slightly increased from 81.9 to 84.4 % with increasing reaction time from 5 to 15 min at 400 °C, this is because the yield of TMP (which includes both reactive phenols and SCAP) was reduced more significantly compared to the yield of SCAP. Table S3 shows the distribution of SCAP into the different product groups. As shown, the yield of C6 compounds increased while the yield of other groups decreased or remained the constant with increasing reaction time. The increase in the yield of C6 units can be explained by secondary reactions that crack side chains of phenolic compounds [22, 27], which occurred regardless of the solvent type. The yields of phenol and 2-methoxyphenol as shown in Fig 7 support this explanation. As the reaction time was prolonged to 15 min, the yield of C2C6 units,

including 4-ethylphenol, decreased from 3.1 to 2.8 wt%. In the absence of a hydrogen donor, the primary products are able to repolymerize to high molecular weight compounds or char [24].

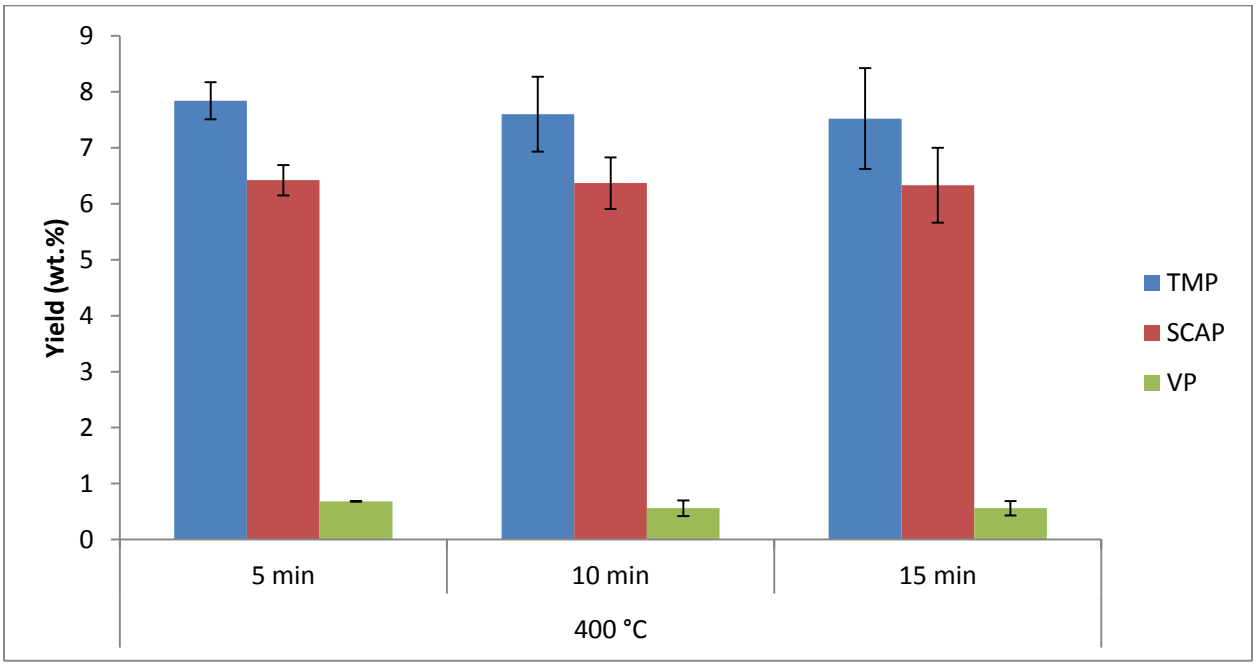

Figure 6. Product distribution obtained from lignin/naphthalene system at various reaction conditions (TMP: total monomeric phenols, SCAP: short-chain alkylphenols and VP: vinylphenols).

Demethoxylation reaction observed from lignin/hydrogen donor solvent system was not occurred in the absence of hydrogen donor. At 400 °C, the yield of H unit decreased 11 % with increasing reaction time from 5 to 15 min and the yield of G and S unit was marginally affected over this reaction condition, which led to increase in G/H and S/H ratio (Table S3).

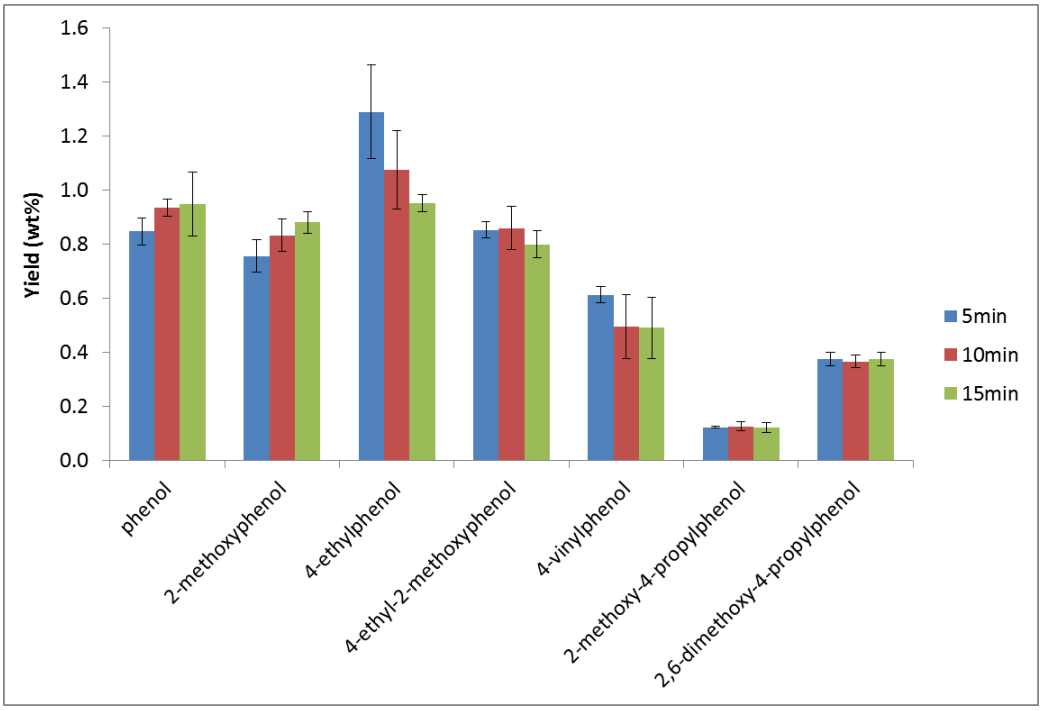

Figure 7. Products from solvent liquefaction of lignin in naphthalene at 400 ºC

Molecular weight distributions by GPC

The molecular weight distributions of the reaction products of lignin in tetralin, isopropanol or naphthalene, determined by GPC analysis, are shown in Fig 8. As described in our previous work, the unreacted lignin had Mw of 1640 Da and PD of 1.9 [28]. At 300 °C and 10 min (Fig 8a), the molecular weight (Mw) of reaction products obtained for tetralin as solvent ranged from 78 and 4000 Da. The average Mw and polydispersity (PD) at this reaction condition were 773 Da and 2.0, respectively. As shown in Fig 8a and Fig 8b, the broad peak at 400 – 4000 Da decreased or shifted to a lower molecular weight region with elevated reaction temperature (300 – 400 °C) and increased reaction time (5 – 15 min). The peak around 100 Da slightly increased over the entire reaction conditions tested. The average Mw of reaction products considerably decreased to 259 Da at 400 °C and 15 min with

reduced PD value of 1.3. These results indicate that thermal decomposition of lignin in the presence of a hydrogen donor solvent encouraged the production of low molecular weight bio-oil with relatively uniform molecular size distribution.

Lignin depolymerization in isopropanol showed a similar trend in molecular weight distributions, as shown in Fig 8c and Fig 8d. When the lignin was thermally decomposed in isopropanol, the average Mw of the reaction products significantly decreased from 1065 to 326 Da and the PD value decreased from 2.4 to 1.8 with increasing reaction temperatures (300 – 400 °C) at fixed reaction time (Fig 8c). Also, it was found that the broad peak which appeared around 200 – 1000 Da decreased with increasing reaction times (5 – 15 min), as shown in Fig 8d. In this figure, a shoulder below 100 Da increased with prolonged reaction times, corresponding with the GC results of increased C6 phenolic units.

The molecular weight distributions of solvolysis products obtained for naphthalene as solvent are shown in Fig 8e and Fig 8f. Compared with the reaction at 300 °C, a shoulder in the spectra above 1000 Da decreased and the peak below 200 Da increased when reaction temperature was increased to 400 °C (Fig 8e). Because of the incomplete lignin conversion at low temperature, the decrease in the molecular weight of products with increasing reaction temperature can be explained by thermally induced bond rupture, regardless of solvent type. It has been observed that the cleavage of the OH functional group linked to aliphatic side chain as well as the breaking of alkyl side chain and aryl ethers occurs when temperature increases [4]. However, it appeared that hydrogen donor solvents were more effective in reducing the formation of oligomers with Mw around 1000 Da than when naphthalene was the solvent.

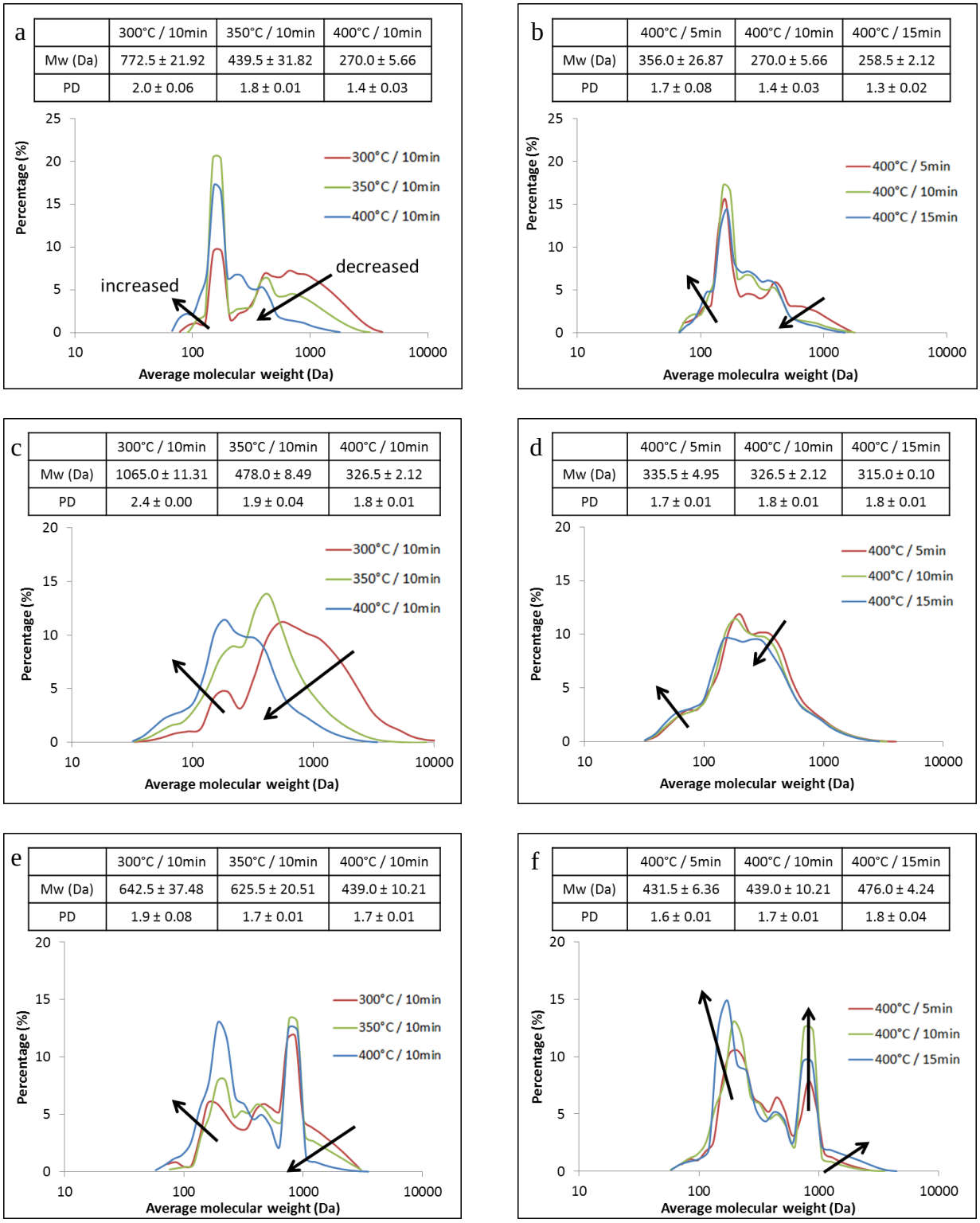

Figure 8. Average molecular weight and molecular weight distribution of solvolysis products from each solvent system; a) and b) lignin/tetralin, c) and d) lignin/isopropanol and e) and f) lignin/naphthalene.

Fig 8f shows that the molecular weight of products from the thermal conversion of lignin in naphthalene increased with increasing reaction times (5 – 15 min). The peaks below 130 Da shifted to a lower molecular weight region possibly due to cracking reactions. The overall molecular weight of the reaction products, however, increased as the reaction further progresses in the absence of a hydrogen donor. This could be attributed to the increase in oligomers with molecular weight 1000 Da or higher, as shown in Fig 8f, as a result of primary products repolymerizing. Inspection of this figure confirms that secondary cracking and secondary repolymerization reactions take place simultaneously during thermal decomposition of lignin. In the presence of a hydrogen donor solvent, however, the secondary repolymerization reactions are mitigated. The low volatility and high viscosity of high molecular weight phenolic oligomers are undesirable constituents in bio-oil whether the bio-oil is directly used for fuel or upgraded to gasoline and diesel. Preventing the formation of phenolic oligomers in favor of low molecular weight compounds would improve the utilization of bio-oil.

Repolymerization is likely caused by the high reactivity of lower molecular weight phenolic products. While the solvolytic conversion of lignin produced a significant amount of VP as primary products, they are known to be very reactive toward repolymerization due to the highly reactive unsaturated C=C group on the side chain [22, 28]. It was observed that SCAP increased at the expense of VPs when hydrogen-donors were used as solvents. Therefore, this repolymerization could potentially be suppressed through the reaction of hydrogen donors with vinyl functionalities to form saturated alkyl groups. In the case of naphthalene, VPs cannot be stabilized against repolymerization due to absence of hydrogen donors. To test this hypothesis, 2-methoxy-4-vinylphenol was reacted with both hydrogen

donor and non-hydrogen donor solvents. The products obtained from each solvent system were analyzed by GPC to determine molecular weight distributions (Fig 9). As shown, two peaks appeared around 150 and 700 Da from the thermal reaction of 2-methoxy-4-vinylphenol with naphthalene (non-HDS), which could be assigned to monomers and oligomers, respectively. When reacted with hydrogen donor solvent, however, the peak around 150 Da significantly increased while the broad peak of the oligomeric region noticeably decreased. This result indicates that secondary repolymerization reactions involving vinyl functionalities can be suppressed with the assistance of hydrogen-donor solvents.

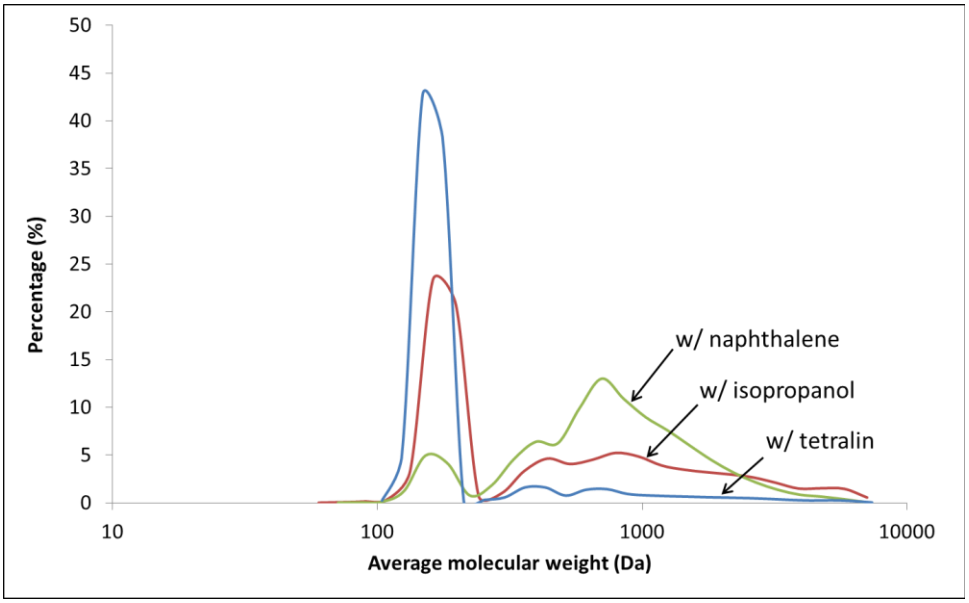

Figure 9. Molecular weight distribution of products obtained from 2-methoxy-4-vinylphenol with each solvent.

It was previously reported that methoxy groups promote repolymerization which could cause char formation [29]. Thus demethoxylation of lignin products occurred by the

reaction with hydrogen-donor solvents could also contributed this suppression of repolymerization.

It should be noted that due to the amounts of samples (500 µg) and solvents (~5µl) used for the present study, unreacted solvents were not able to be separated from the reaction products at post-reactions. Thus, the GPC chromatograms reported above may also include the solvent peaks. However, this does not affect usefulness of the discussion above since only the differences in decreasing or increasing trends of the compounds at varied MW ranges with different reaction conditions are important in the present study.

Conclusion

The benefit of using hydrogen-donor solvents for lignin solvolysis over non-hydrogen donor solvent was explored using a micro-reactor system coupled with online GC/MS-FID. It was found that hydrogen donor solvents were effective in converting lignin to SCAP. The yield of SCAP was over 10wt% of lignin, although no any catalysts were used. When a hydrogen donating solvent was employed, hydrogen abstraction from the solvents stabilized the primary products of lignin decomposition and resulted in the formation of increasing amount of alkyl-substituted phenols. In comparison, lignin does not only yield relatively smaller amounts of TMP and SCAP but the yield of SCAP also decreased with increasing reaction time when non-hydrogen donor solvent was employed. This is because highly reactive phenols, including VPs and possibly free radicals, produced as primary products of lignin decomposition repolymerized to high molecular weight compounds. The conversion of G- or S- unit to H- unit phenolic monomers was also observed with hydrogen-donor solvents, suggesting hydrogen-donor solvents also facilitate demethoxylation.

Analysis of molecular weight distributions of the reaction products indicated that the solvolytic conversion of lignin involved thermally induced decomposition of lignin macromolecules followed by secondary reactions, including side chain cracking and repolymerization reactions among the primary products. It was found that the presence of a hydrogen donor significantly reduced oligomer formation and stabilized products to alkyl-substituted phenols. Further, the present results will help to provide a basis for developing solvolysis models that can predict specific chemical compounds.

Acknowledgement

This work was supported by the National Advanced Biofuel Consortium through a subcontract with the National Renewable Energy Laboratory. The authors would like to thank Juan Proano for performing a CFD simulation of the system.

Supplemental data

Table S1. List of monomeric phenols identified and quantified (tetralin).

	300 °C			350 °C			400 °C		
	5 min	10 min	15 min	5 min	10 min	15 min	5 min	10 min	15 min
Total phenols (wt.%)	5.52±0.06	5.76±0.39	5.90±0.05	9.62±0.99	9.85±1.17	10.18±0.92	10.94±0.15	11.31±0.00	11.36±0.29
Alkylphenols (wt.%)	1.90±0.16	2.32±0.08	2.79±0.04	6.22±1.04	6.58±1.10	7.45±0.77	7.73±0.11	8.33±0.01	8.68±0.17
C6	*0.67±0.05*	*0.70±0.13*	*0.94±0.00*	*2.48±0.28*	*2.68±0.25*	*3.20±0.22*	*3.10±0.06*	*3.45±0.04*	*3.52±0.20*
C1C6	*0.63±0.00*	*0.79±0.04*	*0.67±0.00*	*1.26±0.27*	*1.30±0.31*	*1.42±0.17*	*1.66±0.01*	*1.59±0.02*	*1.69±0.00*
C2C6	*0.54±0.10*	*0.77±0.01*	*1.11±0.03*	*2.29±0.48*	*2.38±0.48*	*2.59±0.34*	*2.69±0.02*	*3.02±0.05*	*3.19±0.03*
C3C6	*0.05±0.01*	*0.06±0.00*	*0.07±0.01*	*0.19±0.03*	*0.21±0.06*	*0.24±0.03*	*0.27±0.01*	*0.27±0.02*	*0.29±0.01*
G/H ratio[1)]	*0.34*	*0.47*	*0.34*	*0.48*	*0.47*	*0.46*	*0.53*	*0.48*	*0.46*
S/H ratio[1)]	*0.56*	*0.57*	*0.63*	*1.12*	*1.08*	*1.08*	*1.05*	*0.99*	*0.89*
Vinylphenols (wt.%)	2.83±0.08	2.62±0.21	2.25±0.08	2.16±0.31	2.09±0.05	1.48±0.04	2.18±0.05	1.99±0.04	1.77±0.04
Selectivity (%)	34.4±2.46	40.3±1.22	47.4±1.06	64.5±5.07	66.6±3.24	73.1±0.95	70.6±0.01	73.7±0.08	76.4±0.49

[1)] H: *p*-hydroxyphenyl unit; G: guaiacyl unit; S: syringyl unit.

Table S2. List of monomeric phenols identified and quantified (isopropanol).

	300 °C			350 °C			400 °C		
	5 min	10 min	15 min	5 min	10 min	15 min	5 min	10 min	15 min
Total phenols (wt.%)	3.86±0.25	4.05±0.09	4.28±0.47	7.35±1.58	7.93±1.41	7.89±0.78	9.30±0.76	9.62±0.88	10.60±0.77
Alkylphenols (wt.%)	1.59±0.06	1.86±0.02	2.42±0.27	5.50±1.11	6.87±1.16	6.98±0.62	8.42±0.52	8.89±0.81	10.06±0.76
C6	*0.93±0.04*	*1.11±0.01*	*1.46±0.15*	*3.22±0.61*	*3.95±0.64*	*3.95±0.36*	*4.25±0.32*	*4.56±0.56*	*4.89±0.45*
C1C6	*0.10±0.00*	*0.11±0.01*	*0.15±0.02*	*0.59±0.10*	*0.72±0.15*	*0.78±0.11*	*1.23±0.07*	*1.33±0.10*	*1.50±0.08*
C2C6	*0.52±0.02*	*0.60±0.01*	*0.78±0.10*	*1.61±0.38*	*2.06±0.33*	*2.07±0.12*	*2.72±0.12*	*2.71±0.15*	*3.34±0.20*
C3C6	*0.03±0.00*	*0.03±0.00*	*0.04±0.01*	*0.09±0.02*	*0.15±0.03*	*0.18±0.02*	*0.23±0.02*	*0.29±0.00*	*0.32±0.03*
G/H ratio	*0.64*	*0.65*	*0.71*	*0.82*	*0.84*	*0.85*	*0.77*	*0.80*	*0.73*
S/H ratio	*1.13*	*1.11*	*1.13*	*1.25*	*1.15*	*1.12*	*0.91*	*0.87*	*0.67*
Vinylphenols (wt.%)	1.71±0.23	1.62±0.04	1.21±0.14	0.97±0.20	0.38±0.05	0.26±0.04	0.23±0.06	0.23±0.07	0.20±0.01
Selectivity (%)	41.2±4.13	45.9±0.66	56.6±0.15	75.0±0.97	86.7±0.79	88.5±0.97	90.6±1.80	92.5±0.09	94.9±0.30

Table S3. List of monomeric phenols identified and quantified (naphthalene).

	400 °C		
	5 min	10 min	15 min
Total phenols (wt.%)	7.84±0.33	7.60±0.67	7.52±0.90
Alkylphenols (wt.%)	6.42±0.27	6.37±0.46	6.33±0.67
C6	*2.35±0.34*	*2.55±0.15*	*2.58±0.28*
C1C6	*0.46±0.01*	*0.44±0.04*	*0.46±0.07*
C2C6	*3.12±0.06*	*2.89±0.28*	*2.80±0.29*
C3C6	*0.50±0.03*	*0.49±0.04*	*0.49±0.04*
G/H ratio	*0.81*	*0.91*	*0.99*
S/H ratio	*1.19*	*1.25*	*1.34*
Vinylphenols (wt.%)	0.68±0.00	0.56±0.14	0.56±0.13
Selectivity (%)	81.86±0.02	83.94±2.12	84.35±1.52

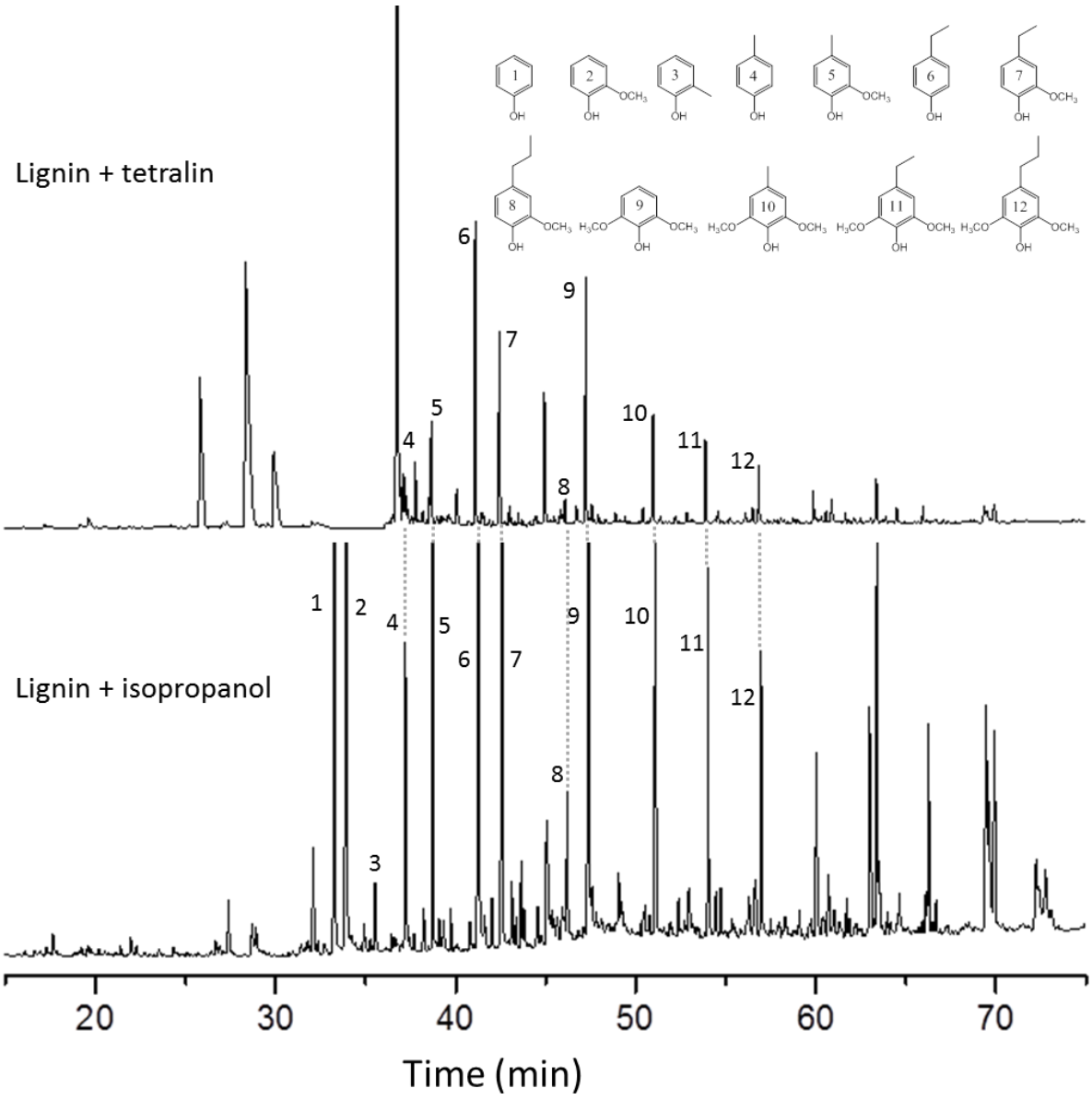

Figure S1. Gas chromatogram of lignin solvolysis with tetralin (top) and isopropanol (bottom).

REFERENCES

[1] G.Z. Jiang, D.J. Nowakowski, A.V. Bridgwater, Effect of the Temperature on the Composition of Lignin Pyrolysis Products, Energ Fuel 2010;24:4470-75.

[2] J. Holladay, J. Bozell, J. White, D. Johnson, Top value-added chemicals from biomass, Volume II: Results of screening for potential candidates from biorefinery lignin, in: DOE Report PNNL-16983, Pacific Northwest National Laboratory, Richland, WA, 2007.

[3] M. Kleinert, T. Barth, Phenols from lignin, Chem Eng Technol 2008;31:736-45.

[4] M.P. Pandey, C.S. Kim, Lignin Depolymerization and Conversion: A Review of Thermochemical Methods, Chem Eng Technol 2011;34:29-41.

[5] B. Holmelid, M. Kleinert, T. Barth, Reactivity and reaction pathways in thermochemical treatment of selected lignin-like model compounds under hydrogen rich conditions, J Anal Appl Pyrol 2012;98:37-44.

[6] P.R. Patwardhan, R.C. Brown, B.H. Shanks, Understanding the Fast Pyrolysis of Lignin, ChemSusChem 2011;4:1629-36.

[7] M. Saisu, T. Sato, M. Watanabe, T. Adschiri, K. Arai, Conversion of lignin with supercritical water-phenol mixtures, Energ Fuel 2003;17:922-28.

[8] A.L. Jongerius, P.C.A. Bruijnincx, B.M. Weckhuysen, Liquid-phase reforming and hydrodeoxygenation as a two-step route to aromatics from lignin, Green Chem 2013;15:3049-56.

[9] Q. Song, F. Wang, J.Y. Cai, Y.H. Wang, J.J. Zhang, W.Q. Yu, J. Xu, Lignin depolymerization (LDP) in alcohol over nickel-based catalysts via a fragmentation-hydrogenolysis process, Energ Environ Sci 2013;6:994-1007.

[10] H. Wang, M. Tucker, Y. Ji, Recent Development in Chemical Depolymerization of Lignin: A Review, Journal of Applied Chemistry 2013;2013.

[11] V.M. Roberts, V. Stein, T. Reiner, A. Lemonidou, X.B. Li, J.A. Lercher, Towards Quantitative Catalytic Lignin Depolymerization, Chem-Eur J 2011;17:5939-48.

[12] N.P. Vasilakos, D.M. Austgen, Hydrogen-Donor Solvents in Biomass Liquefaction, Ind Eng Chem Proc Dd 1985;24:304-11.

[13] T. Barth, M. Kleinert, Motor fuels from biomass pyrolysis, Chem Eng Technol 2008;31:773-81.

[14] F. Davoudzadeh, B. Smith, E. Avni, R.W. Coughlin, Depolymerization of Lignin at Low-Pressure Using Lewis Acid Catalysts and under High-Pressure Using Hydrogen Donor Solvents, Holzforschung 1985;39:159-66.

[15] E. Dorrestijn, M. Kranenburg, D. Poinsot, P. Mulder, Lignin depolymerization in hydrogen-donor solvents, Holzforschung 1999;53:611-16.

[16] M. Kleinert, J.R. Gasson, T. Barth, Optimizing solvolysis conditions for integrated depolymerisation and hydrodeoxygenation of lignin to produce liquid biofuel, J Anal Appl Pyrol 2009;85:108-17.

[17] M. Kleinert, J.R. Gasson, I. Eide, A.M. Hilmen, T. Barth, Developing solvolytic Conversion of Lignin-To-Liquid (LtL) Fuel Components: Optimization of Quality and Process Factors, Cell Chem Technol 2011;45:3-12.

[18] R.W. Thring, J. Breau, Hydrocracking of solvolysis lignin in a batch reactor, Fuel 1996;75:795-800.

[19] R.W. Thring, E. Chornet, R.P. Overend, Thermolysis of Glycol Lignin in the Presence of Tetralin, Can J Chem Eng 1993;71:107-15.

[20] P. Ferrini, R. Rinaldi, Catalytic Biorefining of Plant Biomass to Non-Pyrolytic Lignin Bio-Oil and Carbohydrates through Hydrogen Transfer Reactions, Angewandte Chemie International Edition 2014;53:1-7.

[21] X.Y. Wang, R. Rinaldi, A Route for Lignin and Bio-Oil Conversion: Dehydroxylation of Phenols into Arenes by Catalytic Tandem Reactions, Angew Chem Int Edit 2013;52:11499-503.

[22] T. Hosoya, H. Kawamoto, S. Saka, Secondary reactions of lignin-derived primary tar components, J Anal Appl Pyrol 2008;83:78-87.

[23] C. Saizjimenez, J.W. Deleeuw, Lignin Pyrolysis Products - Their Structures and Their Significance as Biomarkers, Org Geochem 1986;10:869-76.

[24] H.E. Jegers, M.T. Klein, Primary and Secondary Lignin Pyrolysis Reaction Pathways, Ind Eng Chem Proc Dd 1985;24:173-83.

[25] H. Marsh, R.C. Neavel, Carbonization and Liquid-Crystal (Mesophase) Development .15. A Common Stage in Mechanisms of Coal-Liquefaction and of Coal Blends for Coke Making, Fuel 1980;59:511-13.

[26] R.C. Neavel, Liquefaction of Coal in Hydrogen-Donor and Non-Donor Vehicles, Fuel 1976;55:237-42.

[27] D.K. Shen, S. Gu, K.H. Luo, S.R. Wang, M.X. Fang, The pyrolytic degradation of wood-derived lignin from pulping process, Bioresource Technol 2010;101:6136-46.

[28] X. Bai, K.H. Kim, R.C. Brown, E. Dalluge, C. Hutchinson, Y.J. Lee, D. Dalluge, Formation of phenolic oligomers during fast pyrolysis of lignin, Fuel 2014;128:170-79.

[29] T. Hosoya, H. Kawamoto, S. Saka, Role of methoxyl group in char formation from lignin-related compounds, J Anal Appl Pyrol 2009;84:79-83.

CHAPTER 5

PYROLYSIS MECHANISMS OF METHOXY SUBSTITUTED α-O-4 LIGNIN DIMERIC MODEL COMPOUNDS AND DETECTION OF FREE RADICALS USING ELECTRON PARAMAGNETIC RESONANCE ANALYSIS

A paper published in *Journal of analytical and applied pyrolysis*

Kwang Ho Kim, Robert Brown, Xianglan Bai

Abstract

We report on the pyrolysis of methoxy substituted α-O-4 dimeric phenolic compounds at 500 °C using a Frontier Lab micro pyrolyzer to provide mechanistic insight into lignin pyrolysis. The model compounds were benzyl phenyl ether (BPE), 1-(benzyloxy)-2-methoxybenzene (MBPE) and 1-(benzyloxy)-2,6-dimethoxybenzene (DMBPE). Pyrolysis of model dimers primarily involved homolytic cleavage of the C-O linkage in the α-O-4 group. In addition, cleavage of the C-O linkage in the methoxy group dominated at 500 °C. It was found that the methoxy group substitution on the aromatic ring increases the reactivity toward C-O homolysis. Also, methoxy substituted structures can produce many different radical species that can participate in a variety of reaction mechanisms, resulting in complex reaction pathways and pyrolysis products. In addition, free radicals in the condensed phase of the pyrolysis products were detected by electron paramagnetic resonance (EPR) spectroscopy, providing information on the presence of oxygen-centered phenoxy and carbon-centered benzyl radicals. The radical concentrations derived from pyrolysis of the methoxy-substituted dimers, MBPE and DMBPE, were respectively 55 and 30 times higher than the radical concentration derived from BPE. Lastly, it was found that the methoxy group

substitution on the aromatic ring significantly promoted oligomerization reactions to form large molecular weight compounds.

Introduction

Lignin is the second most plentiful renewable organic compound next to cellulose. It constitutes up to 30 % of dry weight and 40 % of the heating value of biomass [1]. Extracted lignin is the major by-product of second-generation bioethanol production. Lignin is a large but underutilized renewable source of aromatic chemicals and liquid fuels [2].

Among the several conversion technologies of biomass into fuel and chemicals, fast pyrolysis is receiving attention for its ability to directly convert biomass into a liquid known as bio-oil, which has potential to be upgraded to hydrocarbon fuels. Despite extensive research on pyrolysis of lignin, the efforts have only been moderately successful due to its chemical diversity and thermal reactivity [3, 4].

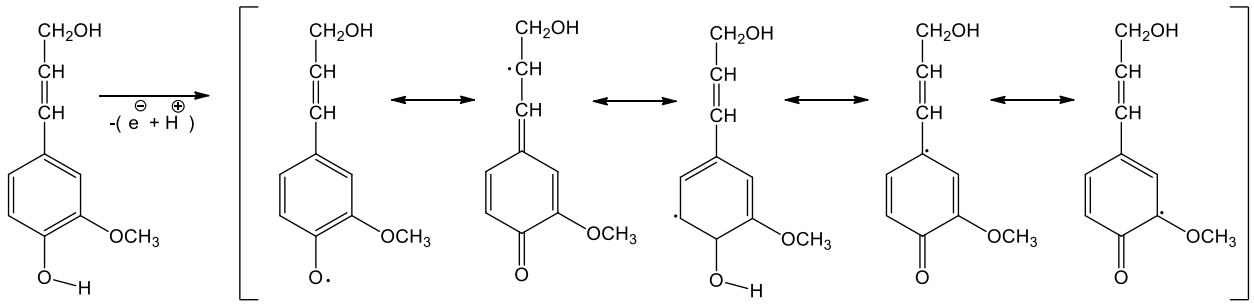

Scheme 1. Resonance-stabilized phenoxy radical formed by enzymatic dehydrogenation of coniferyl alcohol [6].

Lignin is a polymer of phenylpropanes linked through ether and C – C bonds. Biosynthesis of lignin occurs through polymerization of *p*-coumarly alcohol, coniferyl alcohol, and sinapyl alcohol [5]. Enzymatic dehydrogenation responsible for polymerization

of these cinnamyl alcohols is initiated by an electron transfer, which results in the formation of resonance-stabilized phenoxy radicals as shown in Scheme 1. Combination of the monomeric radicals to the phenolic end groups through β-O-4 and β-5 coupling leads to a linear polymer while α-O-4 coupling leads to branching of the polymer [6].

Several researchers have studied the fundamental mechanisms of lignin pyrolysis through the use of model compounds. Britt et *al*. [2, 3, 7-9] used β-O-4 dimeric phenolic compounds for this purpose. They proposed a complex reaction pathway dominated by free radical reactions. Nakamura et *al*.[10] used various dimeric model compounds in their studies and found C – O (β-O-4) cleavage is one of the major pyrolytic pathways in lignin decomposition. Kawamoto et *al*.[11] employed dimers with α-O-4, β-O-4, and β-1linkages and biphenyl. They found that the reactivity of α-O-4 and β-O-4 structures is higher than that of β-1 and biphenyl structures. Hosoya et *al*.[12] used lignin-related compounds to investigate the effect of methoxy groups in lignin on char formation. They proposed that *o*-quinone methide derived from methoxy groups in lignin is a key intermediate in char formation during pyrolysis. Kawamoto et *al*.[13] studied the effect of hydroxyl groups on pyrolytic β-ether cleavage using lignin model dimers. They found that hydroxyl groups increased the reactivity toward β-ether cleavage.

Despite these studies, it is still unclear whether pyrolytic depolymerization of lignin follows a concerted or homolytic unimolecular decomposition pathway. Jarvis et *al*.[14] investigated the pyrolysis of phenyl ethers (β-O-4) using a microtubular reactor with a residence time of less than 100 microseconds and claimed that concerted reactions dominate at temperatures below 1000 °C, whereas homolytic bond scission dominate at higher temperatures. On the other hand, Britt et *al*.[2] reported that they found no evidence for

significant contribution of concerted retro-ene reactions to the pyrolysis of model compounds. Complicating these studies is the difficulty of directly observing reaction intermediates [14]. Some progress in this respect has been made by Kibet et *al*.[15] who used *in*-situ electron paramagnetic resonance (EPR) to detect free radicals during lignin pyrolysis. EPR is a spectroscopic technique used to detect species having one or unpaired electrons exclusively. They suggested the presence of methoxyl, phenoxy, and substituted phenoxy radicals as precursors for formation of phenolic compounds.

In this study, we investigated the pyrolysis of α-O-4 lignin model dimers with a focus on methoxy group substitution. This interunit linkage is the second most abundant linkage in lignin after β-O-4. Methoxy groups are also an important structural feature of lignin. We also report the detection of free radicals in the fast pyrolysis products of these model compounds using EPR.

Materials and methods

Model compounds

Figure 1 shows the structures of the α-O-4 dimeric model compounds tested in this study. Benzyl phenyl ether (BPE) was purchased from Tokyo Chemical Industry Co. 1-(benzyloxy)-2-methoxybenzene (MBPE) and 1-(benzyloxy)-2,6-dimethoxybenzene (DMBPE) were synthesized and provided from The Chemistry Research Solution LLC. The purity of each compound was 98 % for BPE, 98 % (by HPLC) for MBPE and 96 % (by HPLC) for DMBPE. ^{1}H NMR spectra of MBPE and DMBPE were measured at 300 MHz with the following results:

1-(benzyloxy)-2-methoxybenzene: ^{1}H NMR δ 7.5-7.3 (5H), 7.1-6.8 (4H), 5.1(2H), 3.8 (3H); 1-(benzyloxy)-2,6-dimethoxybenzene: ^{1}H NMR δ 7.5-7.3 (5H), 7.0 (1H), 6.7 (2H), 4.9(2H), 3.8 (6H).

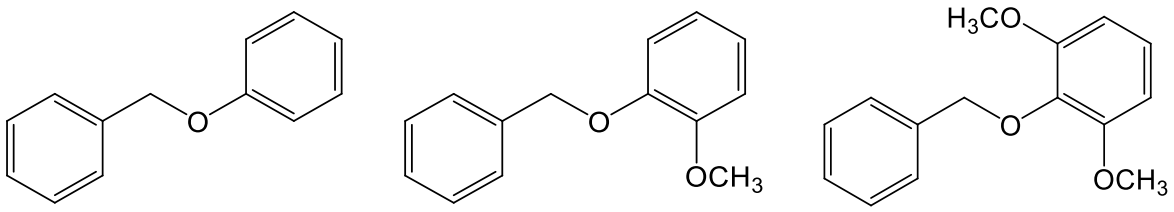

Figure 1. The structure of α-O-4 lignin model compounds; benzylphenylether, 1-(benzyloxy)-2-methoxybenzene and 1-(benzyloxy)-2,6-dimethoxybenzene (from left to right)

Procedure for pyrolysis test of dimeric model compounds

Fast pyrolysis of model compounds was performed using a micro-furnace pyrolyzer (PY-2020iS, Frontier Laboratories, Japan) equipped with auto-shot sampler (AS-1020E, Frontier Laboratories, Japan). Approximately 0.5 mg sample was placed in a deactivated stainless steel cup and automatically dropped into the preheated furnace. All pyrolysis tests were conducted at 500 °C and atmospheric pressure. Helium was used as sweep gas at flow rate of 100 mL/min. Pyrolysis vapors were swept directly to a gas chromatography (GC) column. Identification and quantification of volatile chemical compounds in the pyrolysis products were performed using a Varian CP-3800 GC equipped with Saturn 2200 mass spectrometry (MS) and flame ionization detector (FID). The 60 m × 0.25 mm × 0.25μm capillary column was a Phenomenex ZB-1701. Injection temperature was 275 °C with the oven programmed to hold at 35 °C for 3 minutes, ramped to 280 °C at 3 °C/min and then held for an additional 4 minutes. Non-condensable gases (NCG) were measured by substituting a Porous Layer Open Tubular (PLOT) column (60 m × 0.32 mm, GS-GasPro,

Agilent, USA) in the GC. MS was used to both identify and quantify volatile chemical compounds. A standard gas mixture consisting of CO, CO_2, CH_4, C_2H_4, C_2H_6, C_3H_6, C_3H_8 and C_4H_8 in helium (Praxair, USA) was used to calibrate the yield of NCG [16]. In this study, the conversion of each dimer was calculated based on the amount of GC detectable compounds.

Determination of molecular weight distributions

Separate experiments were performed to investigate molecular weight distribution of the pyrolysis products for each dimeric model compound. The micro pyrolyzer was separated from the GC and the gas needle from the pyrolyzer was directly inserted into a glass vial containing 2 mL of tetrahydrofuran (THF). Approximately 1 mg samples were placed in each of five pyrolysis cups and consecutively pyrolyzed. The pyrolysis vapor was condensed directly in the THF solvent after which the solution was filtered with a Whatman 0.45μ Glass Microfiber syringe filter before analysis. Gel permeation chromatography (GPC) analysis was conducted using a high performance liquid chromatography (HPLC) system (Ultimate 3000, Dionex, USA) equipped with a Shodex Refractive Index (RI) and Diode Array Detector (DAD). Polystyrene standards ranging from 162 – 38,640 g/mol were used for calibration.

Procedure for electron paramagnetic resonance analysis

Electron paramagnetic resonance (EPR) was used to test for the existence of radicals in the condensed phase products from the pyrolysis of α-O-4 dimeric model compounds. EPR measures energy absorption due to the transition of an electron between different energy

levels [17]. This energy transition is caused by the interaction of the unpaired electron (i.e. free radicals) with the magnetic component of microwave radiation while an external magnetic field is applied to the sample. The pyrolysis experiments were similar to those conducted to measure molecular weight distributions. The needle from the pyrolyzer was inserted into a U-shaped quartz tube immersed in liquid nitrogen, which assured rapid quenching of pyrolysis vapors. Approximately 1 mg samples were placed in each of five pyrolysis cups and consecutively pyrolyzed. After pyrolysis, the U-shaped tube was rinsed with 2 mL of 1,4-dioxane and resulting solution transferred to an EPR quartz tube for analysis. EPR spectra were recorded on a Buker ELEXYS E580 FT-EPR spectrometer. EPR was performed at room temperature with X-band (9.5 GHz) and with a magnetic field modulation of 100 kHz. 2,2-diphenyl-1-picrylhydrazyl (DPPH) was used as a free radical standard. Typical parameters were: center field of 3340 Gauss (G), sweep width of 200 G, sweep time of 83 sec, receiver gain of 60 dB and modulation amplitude of 2 G. For relative quantification of radicals the number of electron spins was calculated using Xepr software (Bruker, USA). Double integration across the defined spectral region of 3310 – 3370 G gave the number of electron spins in a sample.

Results and discussion

The GC chromatograms from the pyrolysis of the three model dimers at 500 °C are shown in Figure 2. The interpretation of these results is discussed separately for each model compound in the paragraphs that follow.

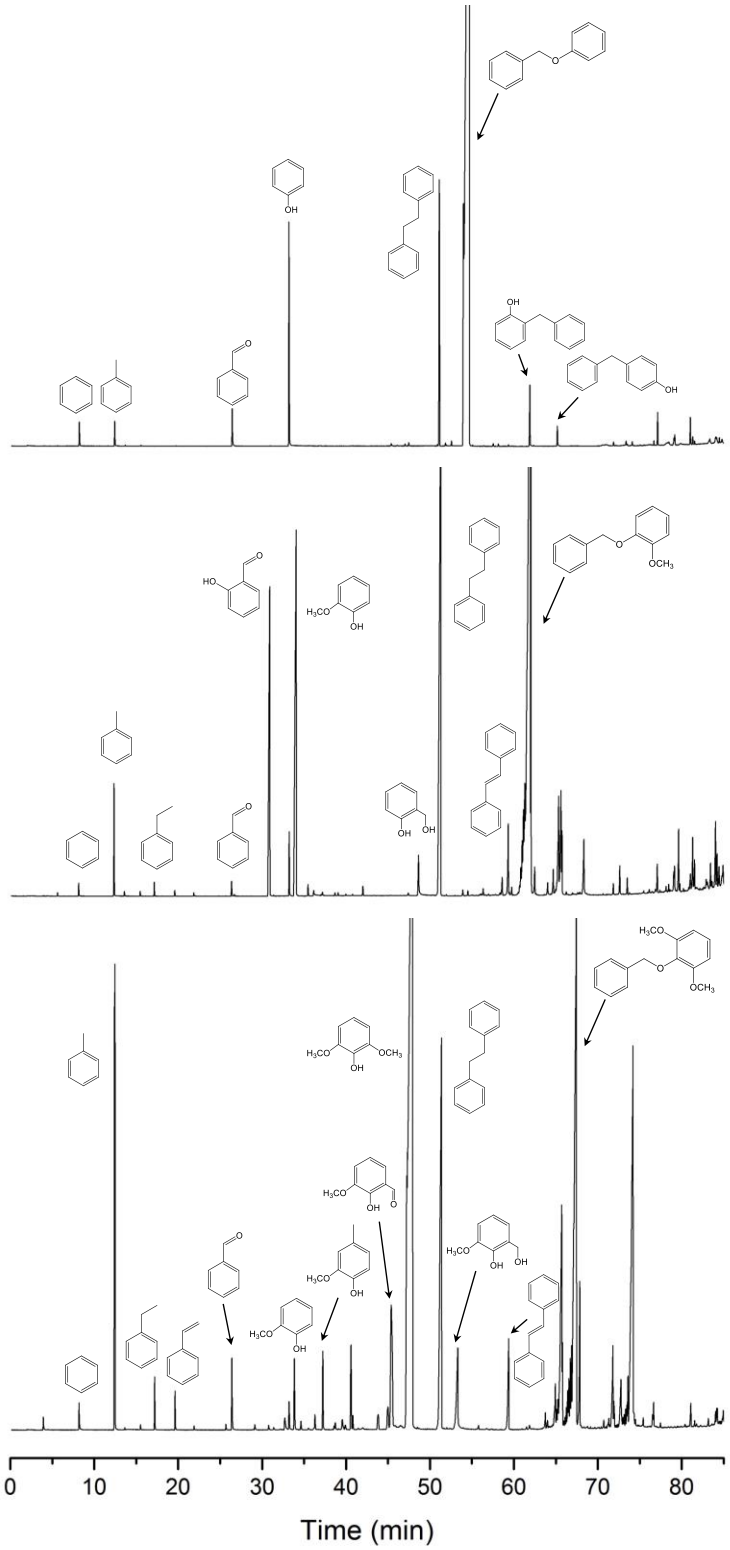

Figure 2. GC chromatograms of the products of pyrolysis at 500 °C for the model compounds BPE, MBPE and DMBPE (from top to bottom).

Pyrolysis of BPE

The products of pyrolysis at 500 °C for BPE, which has the simplest α-O-4 dimeric structure of the three model compounds, are quantified in Table 1. Total GC detectable products were 14.6 wt%. Phenol, bibenzyl, 2-benzylphenol and 4-benzylphenol were major pyrolysis products of BPE. Pyrolysis products were formed mainly by ether bond cleavage, the weakest bond in the molecule with a bond dissociation energy (BDE) of 56.4 kcal/mol [5]. Homolytic bond cleavage of C – O forms the benzyl radical **2**, and the phenoxy radical **3** illustrated in scheme 2.

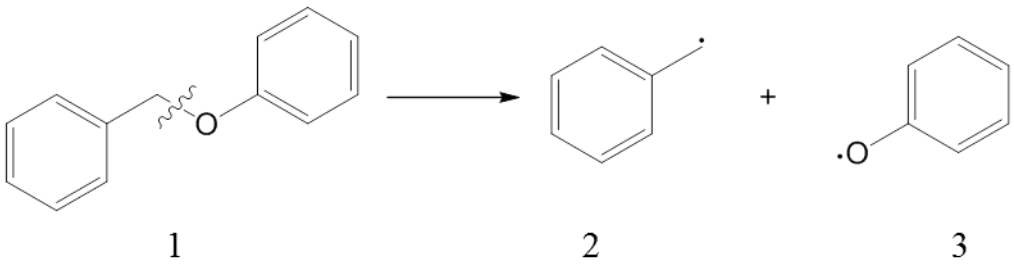

Scheme 2. The homolytic C – O cleavage of BPE.

The benzyl and phenoxy radicals can abstract hydrogen at the benzylic position of BPE or bibenzyl (from termination reaction of two benzyl radicals) to form toluene and phenol, respectively [18]. As shown in Table 1, the phenoxy radical **3** is more active in hydrogen abstraction reactions to form phenol than is benzyl radical **2** to form toluene (Scheme 3). Because the BDE of phenol (PhO – H, 370 kJ/mol) is higher than that of toluene ($PhCH_2$ – H, 360 kJ/mol), the benzyl radical is more stable than the phenoxy radical, which could explain the higher reactivity of phenoxy radical toward hydrogen abstraction. From a

structural standpoint, the formation of phenol is also favored due to the polar effects in the transition state [2, 18, 19].

Table 1. Product distribution for pyrolysis of BPE at 500 °C.

Compounds	Yield (wt %)	mol selectivity (%)
Benzene	0.22 ± 0.06	2.32
Toluene	0.19 ± 0.05	1.74
Benzaldehyde	0.57 ± 0.10	4.50
Phenol	6.66 ± 0.76	59.42
Bibenzyl	3.59 ± 0.46	16.52
Stilbene	0.08 ± 0.03	0.35
2-benzylphenol	2.40 ± 0.16	10.96
4-benzylphenol	0.92 ± 0.16	4.20
Sum	**14.62 ± 1.18**	**100.0**
Char	**n.d.**	

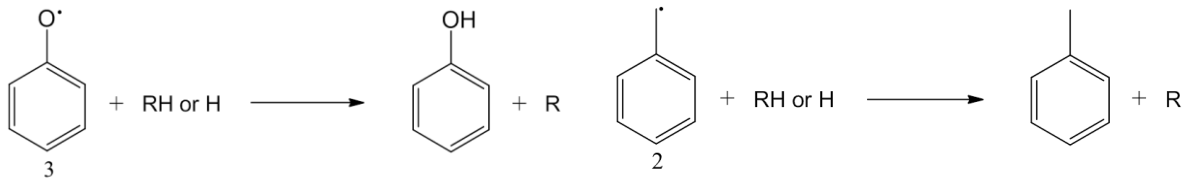

Scheme 3. Hydrogen abstraction of phenoxy radical **3** to phenol and benzyl radical **2** to toluene (RH = BPE or bibenzyl).

Benzyl radicals, on the other hand, favor termination reactions compared to phenoxy radicals. For example, two benzyl radicals can form bibenzyl. 2-benzylphenol and 4-benzylphenol can form from the termination reaction between benzyl radical **2**and phenoxy radical **3** (Scheme 4). Because the phenoxy radical has significant unpaired-electron density delocalized into the aromatic ring, ring-substituted products are expected to form from pyrolysis of BPE [18]. This property of phenoxy radical results in it being delocalized into *ortho* and *para* positions on the aromatic ring. However, the *meta* position is not favored as it

produces ring strain [20]. 2-benzylphenol and 4-benzylphenol are the identified products of BPE pyrolysis, which suggests Scheme 4 for the reaction pathway. The selectivity of 2-benzylphenol was 2.6 times higher than for 4-benzylphenol because there are two reaction sites in the *ortho* position whereas there is only one in the *para* position.

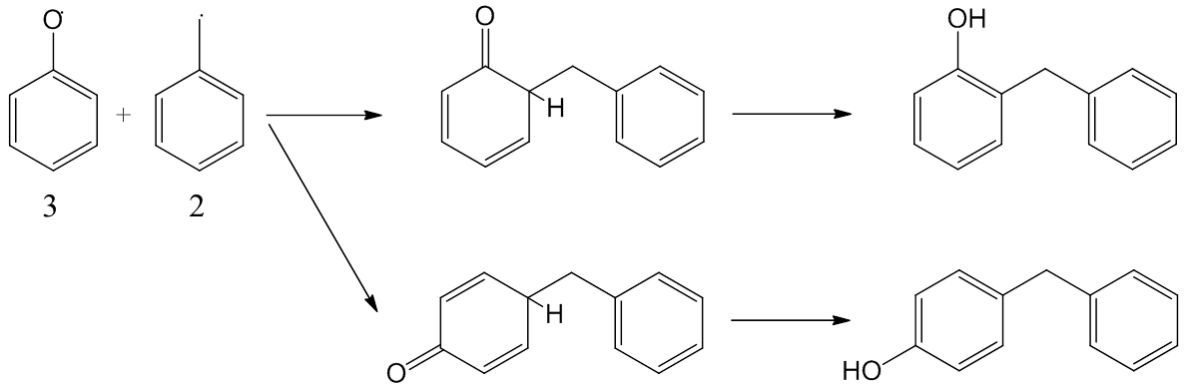

Scheme 4. Formation of 2-benzylphenol and 4-benzylphenol from the reaction of phenoxy and benzyl radicals.

In addition to the above products, benzene, benzaldehyde and stilbene were also observed for the pyrolysis of BPE (Scheme 5). The formation of these compounds is explained by β-scission of BPE radical **4** and bibenzyl radical **5** produced from hydrogen abstraction. The BPE radical **4** could produce benzaldehyde by β-scission of the phenyl radical and the bibenzyl radical **5** could produce stilbene by β-scission of the hydrogen atom, respectively. Considering that phenol is mainly produced by hydrogen abstraction from BPE or bibenzyl as shown in Scheme 3, a large amount of BPE or bibenzyl radicals are expected to form. However, the amounts of benzaldehyde and stilbene formed from BPE and bibenzyl radicals were relatively small. Thus, BPE and bibenzyl radicals are likely involved in different reaction pathways rather than β-scission reaction to form benzaldehyde or stilbene. Inspection of the GC/MS chromatogram of BPE pyrolysis products reveals several peaks

with molecular weight of 274. Comparing these peaks with mass fragmentation spectra from MS, these peaks were assigned to trimers whose structure is likely a benzyl group attached to α-carbon or benzene ring on BPE (Scheme 6). This observation indicates that BPE or bibenzyl radicals are involved in termination reactions to form large molecular weight compounds, which could account for the large amount of phenol.

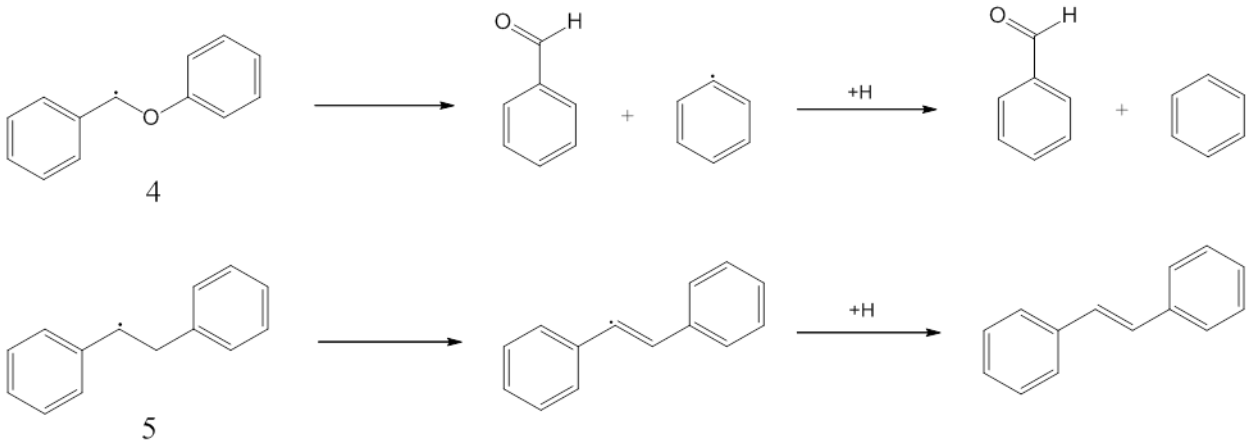

Scheme 5. β-scission reactions between BPE radical **4** and bibenzyl radical **5**.

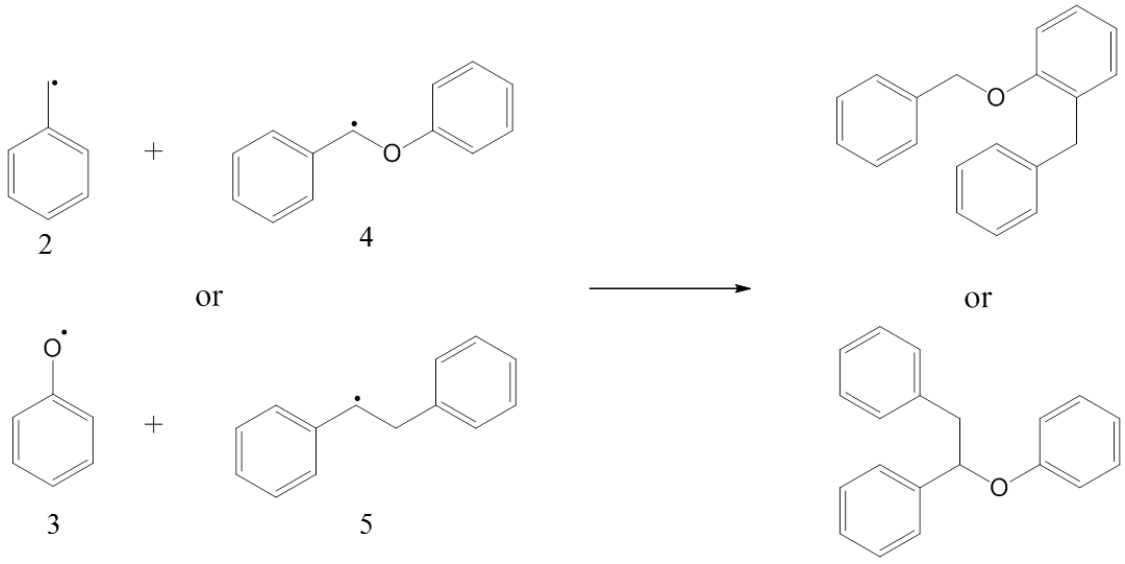

Scheme 6. Reactions of benzyl **2**, phenoxy **3**, BPE **4** and bibenzyl radical **5** to form trimers.

Pyrolysis of MBPE

The major products from the pyrolysis of MBPE at 500 °C are shown in Table 2. The yield of GC detectable compounds from MBPE was approximately 61.6 %, which was significantly higher than for BPE. As shown, guaiacol, bibenzyl, 2-hydroxybenzaldehyde, 2-benzylphenol and 4-benzylphenol are the major products of MBPE pyrolysis. Single methoxy substitution at *ortho* positions lowered BDE for the C – O linkage (50.6 kcal/mol) [5]. The weakening of the ether linkage in the methoxy substituted α-O-4 dimer can be attributed to steric hindrance induced by the *ortho*-methoxy groups [5, 21]. It has been found that methoxy substituent enhances C – O homolysis [3].

Table 2. Product distribution for pyrolysis of MBPE at 500 °C.

	Yield (wt %)	mol selectivity (%)
Methanol	tr	-
Formaldehyde	tr	-
Benzene	0.13 ± 0.01	0.36
Toluene	1.50 ± 0.19	3.63
Ethylbenzene	0.11 ± 0.00	0.23
Styrene	0.04 ± 0.01	0.09
Anisole	0.05 ± 0.02	0.10
Benzaldehyde	0.30 ± 0.02	0.63
2-hydroxybenzaldehyde	11.43 ± 0.02	20.84
Phenol	0.93 ± 0.04	2.21
Guaiacol	24.71 ± 2.38	44.34
o-Cresol	0.26 ± 0.01	0.54
Bibenzyl	15.69 ± 0.35	19.17
Stilbene	0.58 ± 0.06	0.71
2-benzylphenol	2.56 ± 0.01	3.09
4-benzylphenol	3.34 ± 0.02	4.04
Sum	**61.63 ± 3.07**	**100.0**
Char	**0.28 ± 0.02**	

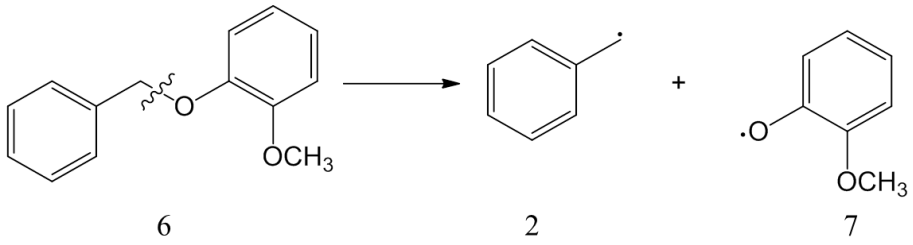

6 2 7

Scheme 7. Homolytic cleavage of C – O in MBPE.

The homolytic cleavage of the C – O bond forms benzyl radical **2** and 2-methoxyphenoxy radical **7** (Scheme 7). Similar to the hydrogen abstraction reaction of phenoxy radical shown in BPE pyrolysis, the 2-methoxyphenoxy radical **7** is involved in internal hydrogen abstraction to form guaiacol, which is a major product of the pyrolysis of MBPE. In addition to guaiacol, 2-hydroxybenzaldehyde (salicylaldehyde), an ether rearrangement product, was the second most prevalent product of MBPE pyrolysis. As shown in Scheme 8, the phenoxy moiety participates in intramolecular abstraction of hydrogen at the methoxy group adjacent to oxygen. And 2-hydroxybenzaldehyde is formed by ether-rearrangement of radical via 1,2-aryl migration [12, 22]. The loss of formaldehyde via β-scission of intermediate **8** to form phenol is a possible competing reaction. The formation of *o*-cresol from the intermediate **9** via *o*-quinone methide has also been proposed as a competing reaction [12, 22, 23].

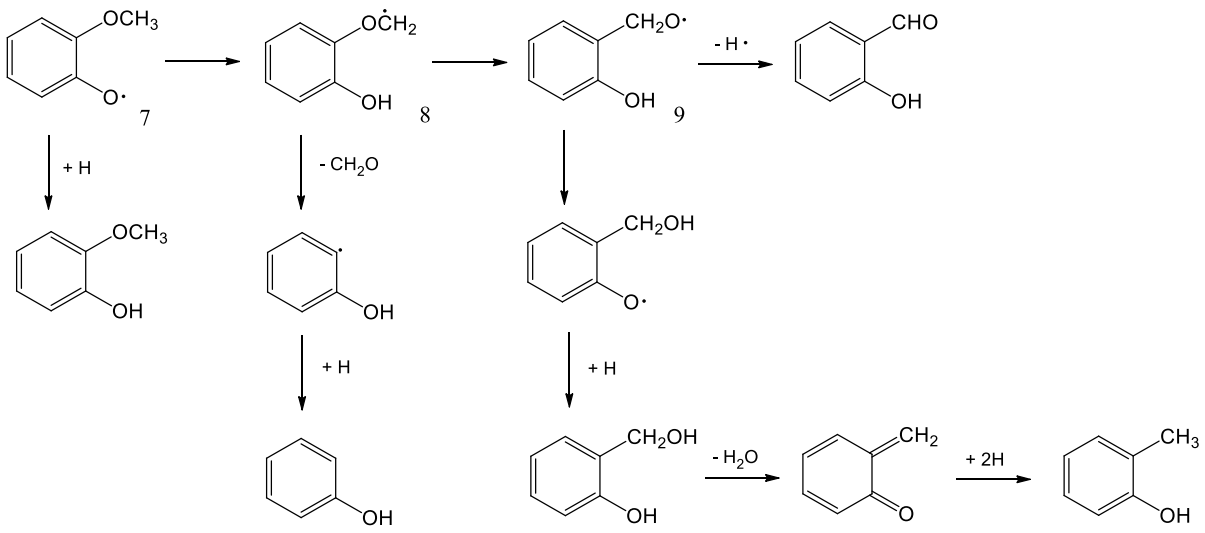

Scheme 8. Reaction mechanism for the formation of guaiacol, phenol, *o*-cresol and 2-hydroxylbenzaldehyde from the 2-methoxyphenoxy radical **7**.

In addition to C – O aryl ether cleavage, the C – O bond of the methoxy group can also break, although at less frequency [3]. The estimated BDE of C – O bond in methoxy group is 58.3 kcal/mol [24], which is higher than that for C – O aryl ether bond. The homolysis of C – O bond of the methoxy group in MBPE can produce 2-(benzyloxy) phenoxy radical **10**. This radical can undergo intramolecular hydrogen abstraction reaction (1,5-hydrogen shift) to form the intermediate **11**, which is followed by β-scission to form benzaldehyde and phenol (Scheme 9). Anisole was produced from the pyrolysis of MBPE although the yield was not significant. As shown in Scheme 10, MBPE radical **12** produced from hydrogen abstraction at α-carbon could undergo β-scission reaction to form benzaldehyde and anisole.

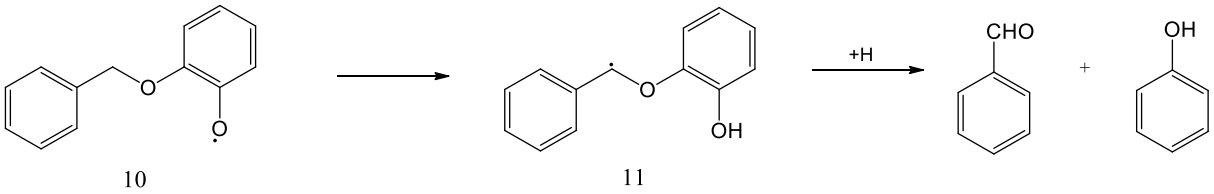

Scheme 9. Reaction of 2-(benzyloxy)phenoxy radical **11** to form benzaldehyde and phenol.

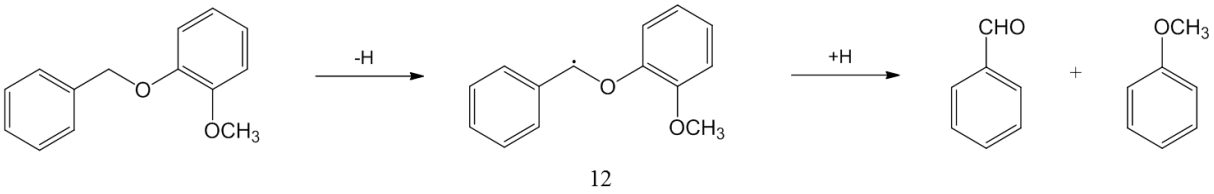

Scheme 10. Reaction of MBPE radical **12** to form benzylaldehyde and anisole.

In addition, ethylbenezene and styrene appeared during MBPE pyrolysis. Because both ethylbenzene and styrene have two carbons in their side chains, β-carbon might arise from the homolysis of the methoxy group in MBPE. Scheme 11 shows the possible reaction pathway to form ethylbenzene and styrene. Benzyl radicals produced from radical channels formed bibenzyl and stilbene. Benzyl radicals also reacted with phenoxy radicals to form 2-benzylphenol and 4-benzylphenol, which are the same reaction pathways described for BPE pyrolysis. Pyrolysis of MBPE produced 0.3 wt% char but no detectable NCG.

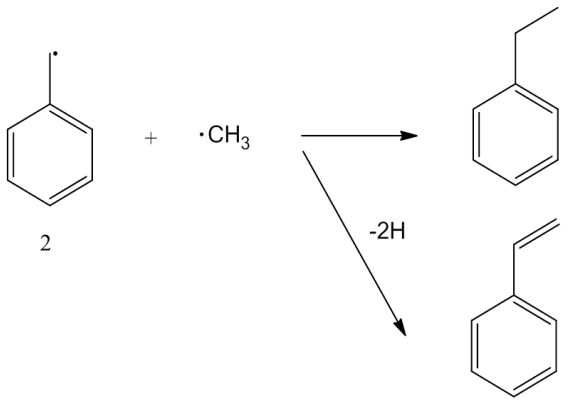

Scheme 11. Reaction of benzyl radical and methyl radical to form ethylbenzene and styrene.

Pyrolysis of DMBPE

The product distribution for the pyrolysis of DMBPE at 500 °C is shown in Table 3. The major pyrolysis products were syringol, bibenzyl, 2-hydroxy-3-methoxybenzylalcohol, toluene and 2-hydroxy-3-methoxybenzaldehyde. The pyrolysis of dimethoxylated dimers cleaves α-O-4 linkages to form benzyl radical and 2,6-dimethoxyphenoxy radical **14** (Scheme 12). Methoxy group substitutions at the di-*ortho* position in the aromatic ring adjacent to the ether bond have the lowest BDE, estimated to be 48.5 kcal/mol [5], thus increasing the reactivity toward α-O-4 ether cleavage.

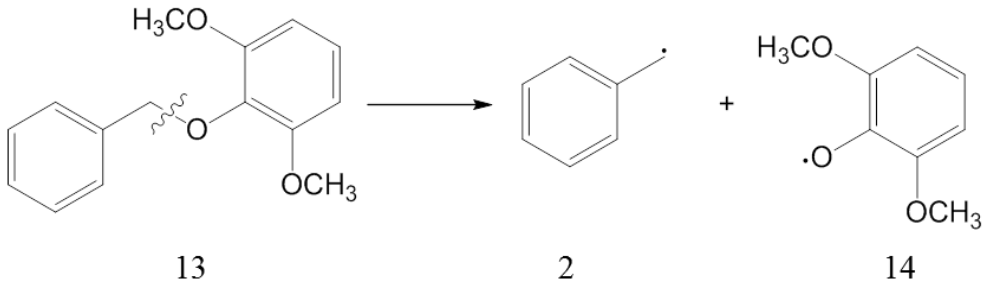

Scheme 12. Homolytic C – O cleavage of DMBPE.

Table 3. Product distribution for pyrolysis of DMBPE at 500 °C.

	Yield (wt %)	mol selectivity (%)
CO	0.42 ± 0.01	3.06
Methanol	0.14 ± 0.01	0.89
Formaldehyde	0.62 ± 0.03	4.22
Benzene	0.06 ± 0.00	0.16
Toluene	2.88 ± 0.22	6.38
Ethylbenzene	0.18 ± 0.00	0.34
Styrene	0.08 ± 0.01	0.15
Anisole	0.01 ± 0.00	0.03
Benzyl methylether	0.01 ± 0.00	0.02
Benzaldehyde	0.24 ± 0.02	0.46
2-hydroxybenzaldehyde	0.02 ±0.01	0.04
Benzylalcohol	0.03 ±0.00	0.06
Phenol	0.10 ±0.01	0.21
Guaiacol	0.53 ± 0.00	0.86
o-Cresol	0.01 ± 0.00	0.02
1,3-Dimethoxybenzene	0.03 ± 0.03	0.05
2-Hydroxy-3-methylbenzaldehyde	0.04 ±0.01	0.06
2-Methoxy-6-methylphenol	0.33 ± 0.01	0.48
4-Ethyl-2-methoxyphenol	0.08 ± 0.00	0.10
2-Hydroxy-6-methoxybenzaldehyde	0.11 ± 0.00	0.15
2-Hydroxy-3-methoxybenzaldehyde	2.86 ± 0.18	3.85
Syringol	39.61 ± 1.35	52.48
Bibenzyl	17.46 ± 0.78	19.57
2-Hydroxy-3-methoxybenzylalcohol	3.31 ± 0.20	4.38
Stilbene	1.09 ± 0.08	1.24
2-Benzylphenol	0.12 ± 0.02	0.13
4-Benzylphenol	0.54 ± 0.02	0.60
Sum	**70.90 ± 0.91**	**100.0**
Char	**1.01 ± 0.22**	

Intermolecular hydrogen abstraction converted 2,6-dimethoxyphenoxy radical into syringol, the major product of DMBPE pyrolysis. Hydrogen abstraction of benzyl radical formed toluene. However, as discussed previously, the benzyl radical more readily

participated in termination reactions to form bibenzyl, the second most abundant product. Surprisingly, the yield of 2-hydroxy-3-methoxybenzaldehyde and 2-hydroxy-3-methoxybenzylalcohol were relatively high. The reaction pathway for 2-hydroxy-3-methoxybenzaldehyde and 2-hydroxy-3-methoxybenzylalcohol is given in Scheme 13. Intramolecular hydrogen abstraction from the methoxy group of 2,6-dimethoxyphenoxy radical **14** forms the intermediate **15**. This intermediate can either rearrange to form intermediate **16** by 1,2-aryl migration or lose formaldehyde to form intermediate **17**, which can abstract hydrogen to form guaiacol. Hydrogen abstraction from the intermediate radical **16** can produce 2-hydroxy-3-methoxybenzalcohol while 2-hydroxy-3-methoxybenzaldehyde is formed by β-scission of a hydrogen atom.

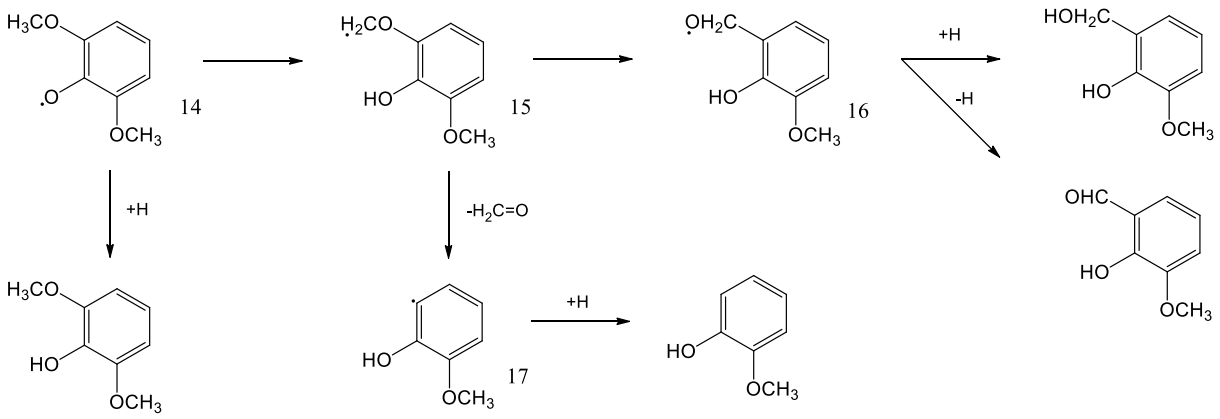

Scheme 13. Reaction pathways for 2,6-methoxyphenoxy radical **14**.

In addition to α-O-4 cleavage, homolysis of the methoxy group can occur to form methyl and phenoxy radicals, as shown in Scheme 14. Intramolecular hydrogen abstraction from the α-carbon of the phenoxy radical **18** forms intermediate **19**, which is followed by 1,2-aryl migration to form **20** and β-scission to give benzene and 2-hydroxy-6-

methoxybenzaldehyde. 1,3-dimethoxybenzene can be produced via β-scission from DMBPE radical **21** as shown in Scheme 15.

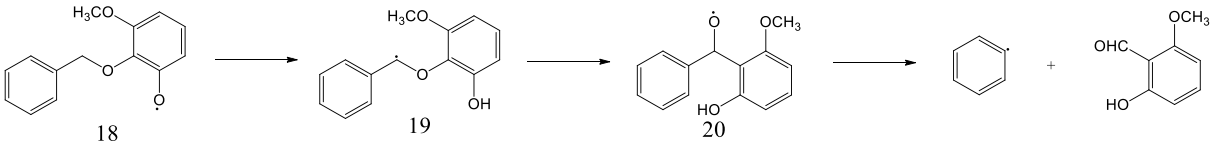

Scheme 14. Formation of benzene and 2-hydroxy-6-methoxybenzaldehyde from DMBPE radical **18**.

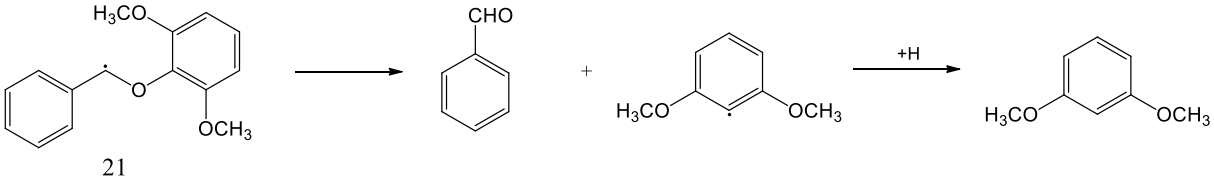

Scheme 15. Formation of 1,3-dimethoxybenzene from BMBE radical **21**.

As discussed above, 2-hydroxy-3-methoxybenzalcohol can be formed from 2,6-dimethoxyphenol radical **14** (Scheme 13). This product can be involved in further reactions, as shown in Scheme 16 [3]. 2-hydroxy-3-methoxybenzalcohol forms *o*-benzoquinone methide **22** releasing water, and further reacts to form 2-methoxy-6-methyl phenoxy radical **23**. This radical forms 2-methoxy-6-methylphenol, *o*-cresol and 2-hydroxy-3-methyl benzylalcohol.

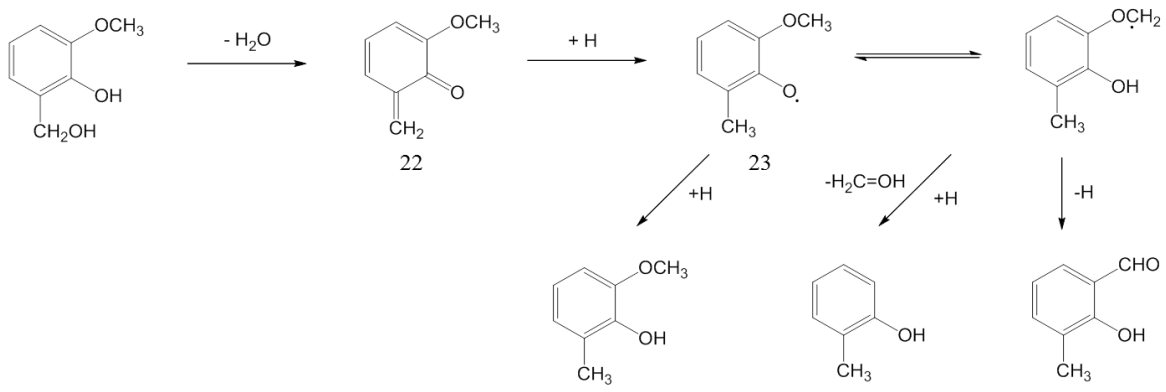

Scheme 16. Reaction of 2-hydroxy-3-methoxybenzalcohol [3].

Pyrolysis of DMBPE produces approximately 0.4 wt% of CO whereas BPE and MBPE produced no detectable CO. Carbon monoxide can be a product of the decomposition of methoxy group or formaldehyde. Interestingly, char yield from the pyrolysis of DMBPE was approximately 1.0 wt%, which was higher than for MBPE. Since the methoxy group plays an important role in charring of lignin [12, 25], this increase in char yield was not surprising. As discussed above, a methoxy substitution in the *ortho*-position in the aromatic ring of the α-O-4 dimeric model compounds increased the reactivity towards ether cleavage. Also, methyl radical formed from the cleavage of C – O bond in the methoxy group can be involved in a variety of radical coupling reactions to form large molecular weight compounds [26]. This hypothesis is further investigated below.

Molecular weight distribution

GPC analysis of condensed products from the pyrolysis of the dimeric model compounds was investigated to see how the presence of methoxy groups affected the molecular weight of the products. Figure 3 shows that the distribution of molecular weights

of products from pyrolysis of BPE ranged from 44 to 439 Da. The large peak around 150 Da is unconverted BPE while the smaller peaks at 70 and 205 Da correspond to monomers and trimers, respectively, formed from the reaction of BPE. MPBE shows a similar distribution of unreacted dimer surrounded by peaks for monomeric and trimeric products and a small tail of oligomers. The condensed products from pyrolysis of DMBPE show little of the original dimer or monomeric products, being mostly larger molecular weight products. The shift towards higher molecular weight products with increasing methoxy substitution of the model dimer compounds gives strong evidence that the methoxy group plays an important role in the oligomerization of the products of lignin pyrolysis.

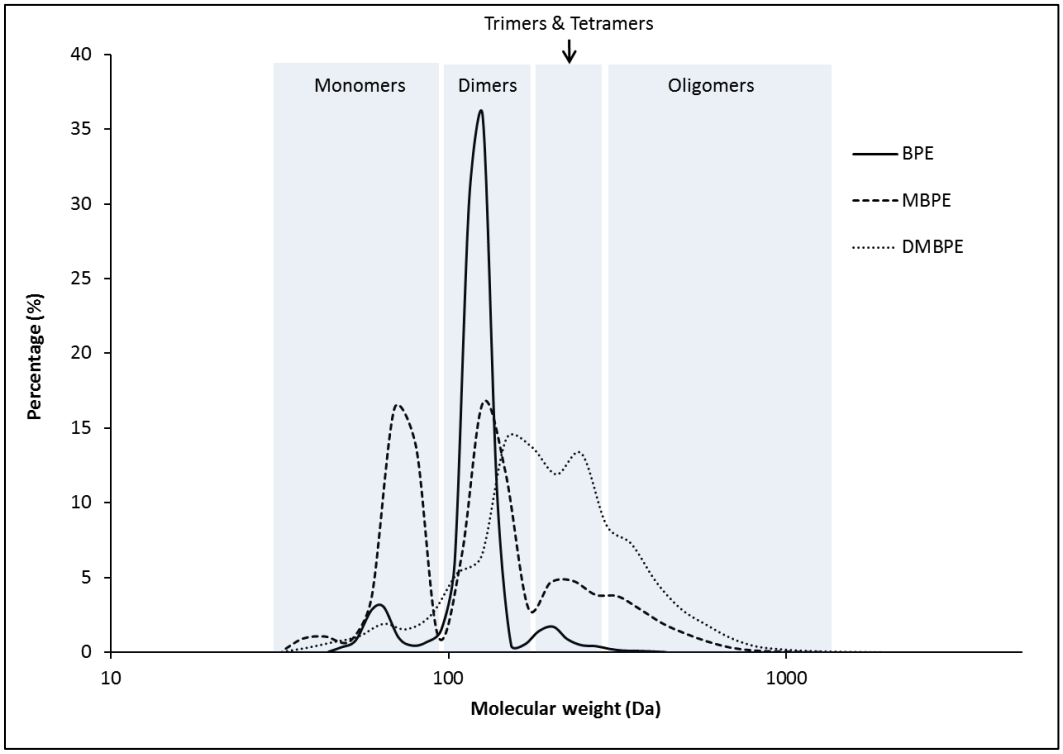

Figure 3. GPC analysis of condensed products from the pyrolysis dimeric model compounds.

Detection of free radicals

The EPR spectra of the condensed phase products of pyrolysis of the three dimeric model compounds are shown in Figure 4. All three dimeric compounds produced free radicals of similar anisotropy. The g-values obtained from the spectra were 2.0035 for BPE, 2.0035 for MBPE and 2.0036 for DMBPE (see Table 4). Considering the structure and reaction pathway of α-O-4 dimeric model compounds, the peaks in the spectra are thought mainly to arise from carbon-centered benzyl radical and oxygen-centered phenoxy radical. It has been reported that the g-value of phenoxy radical ranges from 2.0040 to 2.0053 [27-29] and benzyl radical is 2.0030 [30]. In general, the g-values of EPR spectra can be used to determine whether a radical is carbon-centered or oxygen-centered [29]. However, these values can be shifted by the chemical neighborhood of the unpaired electron [28]. Also, if the free radicals are not exclusively centered on a single atom, the EPR spectrum is broadened. The complex mixtures of pyrolysis products and the broad character of the EPR spectra, make it difficult to determine the types of radicals.

The concentration of free radicals derived from pyrolysis of the three kinds of dimers is presented in Table 4. Radical concentrations in methoxy substituted dimers were more than one order of magnitude higher than radical concentration from pyrolysis of BPE. Radical concentration for MBPE pyrolysis products was highest, followed by DMBPE and BPE. The free radical concentration of MBPE pyrolysis products was 6.6×10^{17} spins/g, which was 1.8 and 56 times higher than for DMBPE and BPE, respectively. The rate of C – O homolysis for DMBPE has been measured to be approximately 4 times faster than for MBPE [3] . Thus, higher radical concentration for DMBPE pyrolysis products was expected since it has two methoxy groups in the *ortho* positions, which can generate free radicals. The enhanced free

radical production from di-methoxy substituted dimers r results in enhanced production of large molecular weight compounds, as previously described. Therefore, more reactive sites and faster reaction rate of di-methoxy substituted model compound can explain the decreased radical concentration in the condensed pyrolysis products than MBPE. However, its radical concentration is still significantly higher than BPE pyrolysis, which does not have methoxy group.

It should be noted that highly reactive or short-lived free radicals, typically with half-lives less than 10^{-3} s [19], cannot be detected by our technique, which is a limitation in this study. Since these types of radicals can involve in various radical processes during pyrolysis of biomass, new approach is necessary to identify or characterize them. For example, in-situ EPR studies can observe short-lived radicals and may provide insights to understand the point at which radicals are formed during biomass pyrolysis and the rate of radical formation.

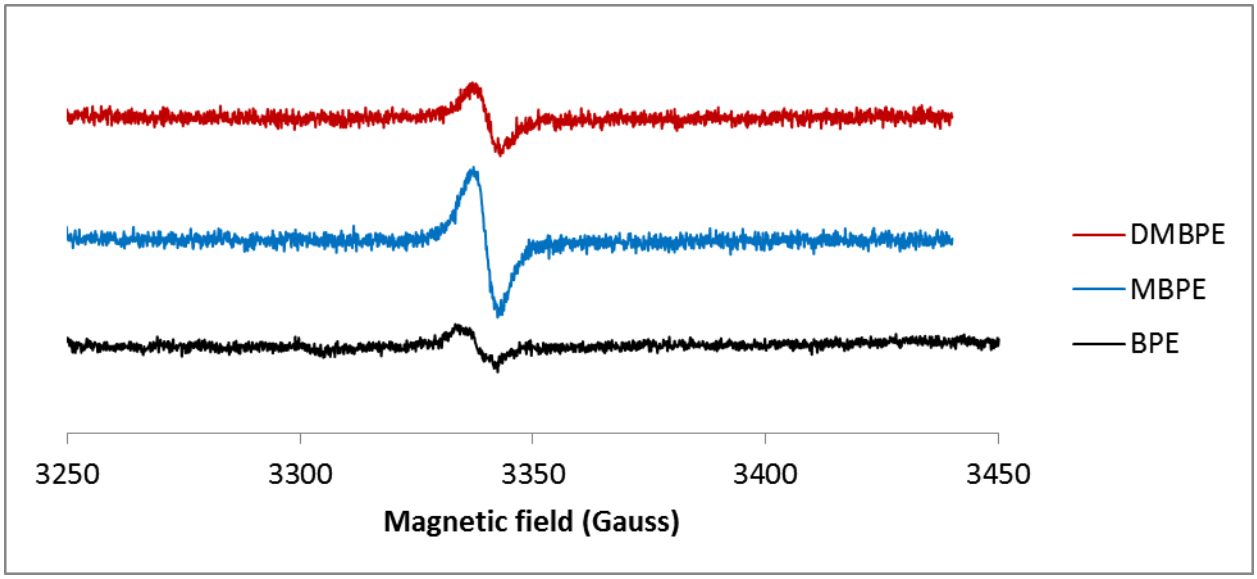

Figure 4. The EPR spectra of condensed phase products from the pyrolysis of dimeric model compounds(each spectra is the average of four scans).

Table 4. The EPR parameters of radicals produced from the pyrolysis of model dimers at 500 °C.

	BPE	MBPE	DMBPE
g-value	2.0035	2.0035	2.0036
ΔHp-p (G)	8.77	6.60	6.23
spins (spins/g sample)	1.19×10^{16}	6.63×10^{17}	3.68×10^{17}

Conclusion

We investigated pyrolysis of methoxy substituted α-O-4 dimeric compounds at 500 °C. A methoxy substitution in the *ortho*-position in the aromatic ring of the α-O-4 dimeric model compounds increased the reactivity towards ether cleavage. By analyzing pyrolysis products of each model dimer, it was found that the reaction pathways of methoxy substituted α-O-4 dimers (MBPE and DMBPE) were significantly more complex than BPE. Because methoxy substituted structures have higher reactivity toward C-O homolysis than BPE and they produce more complex radical species, various types of pyrolysis products were formed. Also, the presence of free radicals as intermediates of pyrolysis reactions has been demonstrated by using EPR technique and their relative concentrations were determined. This revealed that methoxy substituted α-O-4 model dimer produces a relatively large amount of radicals not only from aryl ether C-O bond but also from methoxy C-O bond cleavages. GPC analysis of condensed products from the pyrolysis of the dimeric model compounds showed that the presence of methoxy groups affected the molecular weight of the products. Clearly, methoxy substitution promoted the formation of large molecular weight products, possibly by radical coupling reaction.

Acknowledgement

This work was supported by the National Advanced Biofuel Consortium through a subcontract with the National Renewable Energy Laboratory. The authors would like to thank Patrick Johnston, Marjorie Rover and Ryan Smith of the Center for Sustainable Environmental Technologies for their support. The authors would also like to thank Stephanie Villano and Anthony Dean at Colorado School of Mines for valuable discussion.

REFERENCES

[1] J.E. Holladay, J.J. Bozell, J.F. White, D. Johnson, Top Value-Added Chemicals from Biomass - volume 2 - Results of Screening for Potential Candidates from Biorefinery Lignin, in, Pacific Northwest National Laboratory, Richland, 2007.

[2] P.F. Britt, A.C. Buchanan, E.A. Malcolm, Thermolysis of Phenethyl Phenyl Ether - a Model for Ether Linkages in Lignin and Low-Rank Coal, J Org Chem 1995;60:6523-36.

[3] P.F. Britt, A.C. Buchanan, M.J. Cooney, D.R. Martineau, Flash vacuum pyrolysis of methoxy-substituted lignin model compounds, J Org Chem 2000;65:1376-89.

[4] E.R.E. Vanderhage, M.M. Mulder, J.J. Boon, Structural Characterization of Lignin Polymers by Temperature-Resolved in-Source Pyrolysis Mass-Spectrometry and Curie-Point Pyrolysis-Gas Chromatography Mass-Spectrometry, J Anal Appl Pyrol 1993;25:149-83.

[5] R. Parthasarathi, R.A. Romero, A. Redondo, S. Gnanakaran, Theoretical Study of the Remarkably Diverse Linkages in Lignin, J Phys Chem Lett 2011;2:2660-66.

[6] E. Sjöström, Wood chemistry: fundamentals and applications, 2nd ed., Academic Press, Inc., San Diego, 1993.

[7] A.C. Buchanan, P.F. Britt, J.T. Skeen, J.A. Struss, C.L. Elam, Pyrolysis of silica-immobilized benzyl phenyl ether: Competing radical rearrangement pathways under restricted diffusion, J Org Chem 1998;63:9895-903.

[8] P.F. Britt, M.K. Kidder, A.C. Buchanan, Oxygen substituent effects in the pyrolysis of phenethyl phenyl ethers, Energ Fuel 2007;21:3102-08.

[9] A. Beste, A.C. Buchanan, P.F. Britt, B.C. Hathorn, R.J. Harrison, Kinetic analysis of the pyrolysis of phenethyl phenyl ether: Computational prediction of alpha/beta-selectivities, J Phys Chem A 2007;111:12118-26.

[10] T. Nakamura, H. Kawamoto, S. Saka, Pyrolysis behavior of Japanese cedar wood lignin studied with various model dimers, J Anal Appl Pyrol 2008;81:173-82.

[11] H. Kawamoto, S. Horigoshi, S. Saka, Pyrolysis reactions of various lignin model dimers, J Wood Sci 2007;53:168-74.

[12] T. Hosoya, H. Kawamoto, S. Saka, Role of methoxyl group in char formation from lignin-related compounds, J Anal Appl Pyrol 2009;84:79-83.

[13] H. Kawamoto, S. Horigoshi, S. Saka, Effects of side-chain hydroxyl groups on pyrolytic beta-ether cleavage of phenolic lignin model dimer, J Wood Sci 2007;53:268-71.

[14] M.W. Jarvis, J.W. Daily, H.H. Carstensen, A.M. Dean, S. Sharma, D.C. Dayton, D.J. Robichaud, M.R. Nimlos, Direct Detection of Products from the Pyrolysis of 2-Phenethyl Phenyl Ether, J Phys Chem A 2011;115:428-38.

[15] J. Kibet, L. Khachatryan, B. Dellinger, Molecular Products and Radicals from Pyrolysis of Lignin, Environ Sci Technol 2012;46:12994-3001.

[16] K. Wang, K.H. Kim, R.C. Brown, Catalytic pyrolysis of individual components of lignocellulosic biomass, Green Chem 2014.

[17] G.R. Eaton, S. Eaton, S, D.P. Barr, R.T. Weber, Quantitative EPR, 1st ed., Springer, New York, 2010.

[18] R.H. Schlosberg, W.H. Davis, T.R. Ashe, Pyrolysis Studies of Organic Oxygenates .2. Benzyl Phenyl Ether Pyrolysis under Batch Autoclave Conditions, Fuel 1981;60:201-04.

[19] J. Fossey, D. Lefort, J. Sorba, Free radicals in organic chemistry, Wiley, Paris, 1995.

[20] S. Gopalan, P.E. Savage, Reaction-Mechanism for Phenol Oxidation in Supercritical Water, J Phys Chem-Us 1994;98:12646-52.

[21] E. Dorrestijn, L.J.J. Laarhoven, I.W.C.E. Arends, P. Mulder, The occurrence and reactivity of phenoxyl linkages in lignin and low rank coal, J Anal Appl Pyrol 2000;54:153-92.

[22] E. Dorrestijn, P. Mulder, The radical-induced decomposition of 2-methoxyphenol, J Chem Soc Perk T 2 1999:777-80.

[23] E. Dorrestijn, R. Pugin, M.V.C. Nogales, P. Mulder, Thermal decomposition of chroman. Reactivity of o-quinone methide, J Org Chem 1997;62:4804-10.

[24] A. Demirbas, Mechanisms of liquefaction and pyrolysis reactions of biomass, Energ Convers Manage 2000;41:633-46.

[25] T. Hosoya, H. Kawamoto, S. Saka, Pyrolysis gasification reactivities of primary tar and char fractions from cellulose and lignin as studied with a closed ampoule reactor, J Anal Appl Pyrol 2008;83:71-77.

[26] A. Demirbas, Effects of temperature and particle size on bio-char yield from pyrolysis of agricultural residues, J Anal Appl Pyrol 2004;72:243-48.

[27] F. Graf, K. Loth, H.H. Gunthard, Chlorine Hyperfine Splittings and Spin-Density Distributions of Phenoxy Radicals - Esr and Quantum Chemical Study, Helv Chim Acta 1977;60:710-21.

[28] C.L.B. Guedes, E. Di Mauro, V. Antunes, A.S. Mangrich, Photochemical weathering study of Brazilian petroleum by EPR spectroscopy, Mar Chem 2003;84:105-12.

[29] E. Vejerano, S. Lomnicki, B. Dellinger, Formation and Stabilization of Combustion-Generated Environmentally Persistent Free Radicals on an Fe(III)(2)O-3/Silica Surface, Environ Sci Technol 2011;45:589-94.

[30] N.J. Turro, V. Ramamurthy, J. Scaiano, Modern molecular photochemistry of organic molecules, 1st ed., University Science Books, Sausalito, 2010.

CHAPTER 6

A QUANTITATIVE INVESTIGATION OF FREE RADICALS IN BIO-OIL AND THEIR POTENTIAL ROLE IN CONDENSED PHASE POLYMERIZATION OF CELLULOSE- AND LIGNIN-DERIVED PYROLYSATES

A paper published in *Chemsuschem*

Kwang Ho Kim, Xianglan Bai, Sarah Cady, Preston Gable, Robert Brown

Abstract

We report quantitative analysis of free radicals in bio-oils produced from pyrolysis of cellulose, organosolv lignin and corn stover using an electron paramagnetic resonance (EPR) spectroscopy. Also we investigated their potential role in condensed phase polymerization. Bio-oil produced from lignin and cellulose show clear evidence of homolytic cleavage reactions during pyrolysis that produce free radicals. The concentration of free radicals in lignin bio-oil was 7.5×10^{20} spins g^{-1}, which was 375 and 138 times higher than the free radical concentrations in bio-oil from cellulose and corn stover, respectively. Pyrolytic lignin contained the most free radicals, which could be a combination of carbon-centered (benzyl radical) and oxygen-centered (phenoxy radical) organic species as they are delocalized in a π system. Free radical concentrations did not change during accelerated aging tests despite increases in molecular weight of bio-oils, suggesting that the free radical in condense bio-oil are stable.

Keywords: EPR spectroscopy • fast pyrolysis • homolytic cleavage • radicals

Introduction

Lignocellulosic biomass is a promising renewable resource that is relatively inexpensive and abundant [1, 2]. Fast pyrolysis is a promising way to utilize lignocellulosic biomass since it utilizes both the carbohydrate and lignin components. Bio-oil from fast pyrolysis can be used in the production of either biofuels or green chemicals, serving as a replacement for petroleum-based products. However, pyrolysis of lignocellulosic biomass is very complex due to the diversity, heterogeneity and limited thermal stability of the components [3], which results in complex nature of bio-oil.

Although bio-oil represents a potential source of renewable fuel or chemicals, its complex nature and low thermal stability limit the use of bio-oil as a commercial resource. Bio-oil contains reactive oxygenates such as acids, ethers, esters and aldehydes, all of which can form higher molecular weight species [4]. Also, bio-oil tends to be unstable when they are stored for extended periods at ambient or elevated temperature [5]. Thermal instability of bio-oil causes the quality reduction during transport and storage, thus an in-depth study on bio-oil stability is necessary.

The pyrolysis of biomass and its components has been extensively studied using a variety of reactor systems and computational methods [6-10]. These previous studies provide evidence of homolytic cleavage reactions giving rise to free radicals, particularly from aryl-ether bonds in lignin [11]. The resulting radicals likely play an important role in subsequent reactions. Recently, Kibet et *al*.[12] observed volatile radicals evolved during lignin pyrolysis using electron paramagnetic resonance (EPR) spectroscopy to detect the labile reaction intermediates. Also, Bährle et *al*.[13] detected free radicals generated from lignin pyrolysis using in-situ high-temperature EPR spectroscopy. The radicals produced from the

initial stage of pyrolysis have been observed in the condensed bio-oil [14] and biochar [15]. Free radicals in the gas phase are likely to contribute to secondary pyrolysis reactions including polymerization of phenolic compounds. Polymerization is also observed in bio-oil, suggesting that free radicals might contribute to this condensed-phase process unless they are stable free radicals.

Although previous research has extensively analyzed the chemical composition of bio-oil, few studies have focused on the free radicals, from its formation to thermal reactivity in bio-oil. Meng et *al*.[16] recently investigated free radicals in bio-oil and their impact on bio-oil stability. They measured the relative amounts of free radicals after aging test and claimed that radicals in bio-oil are stable. However, no previous studies have quantified the concentration of free radicals in bio-oil nor investigated whether free radical concentration was dependent on the component of biomass pyrolyzed. And the thermal behavior of radicals which could be present in bio-oil toward secondary reactions in condensed phase is not clear yet.

In this work, EPR spectroscopy was used to investigate the role of radicals in bio-oils produced in a free fall pyrolyzer. EPR spectroscopy has been widely used to identify and characterize free radicals in chemical systems. EPR measures energy absorption which is attributed to the transition of a sub atomic particle between different energy levels. This energy transition is caused by the interaction of the free radicals with the magnetic component of microwave radiation while an external magnetic field if applied to the sample [17]. EPR has been used extensively to study free radicals in coal pyrolysis [18-22]. It also has been used to study free radicals in airborne particulate matter [23] and petroleum [24].

Corn stover (selected as representative of lignocellulosic biomass), corn stover-derived organosolv lignin and cellulose were separately pyrolyzed and the resultant bio-oils were analyzed for free radicals. Also, pyrolytic lignin was extracted from corn stover bio-oil and analyzed for free radicals. Accelerated aging test was performed to investigate the relationship between free radicals and secondary repolymerization of bio-oil.

Results and discussion

Quantitative analysis of free radicals in pyrolysis products

The EPR spectra of three bio-oils obtained from the pyrolysis of corn stover, cellulose and lignin using a free fall reactor are given in Figure 1. As shown, the EPR spectrum of lignin bio-oil had a strong singlet peak around 3340 G. The EPR spectra of corn stover bio-oil and cellulose bio-oil were similar to lignin bio-oil and exhibited similar anisotropy although their peak heights were significantly smaller. The EPR spectra of three bio-oils and pyrolytic lignin were broad, featureless and did not have hyperfine splitting. This may indicate that multiple radicals are present or strong matrix interactions occur between the products [25]. It can also arise from inhomogeneity of the samples or if the free radical is not exclusively centered on a single atom [23, 25]. It should be noted that unresolved hyperfine interaction can contribute to inhomogeneous broadening. The unresolved hyperfine interaction with surrounding nuclei affects EPR line shape and broadening of the line width.

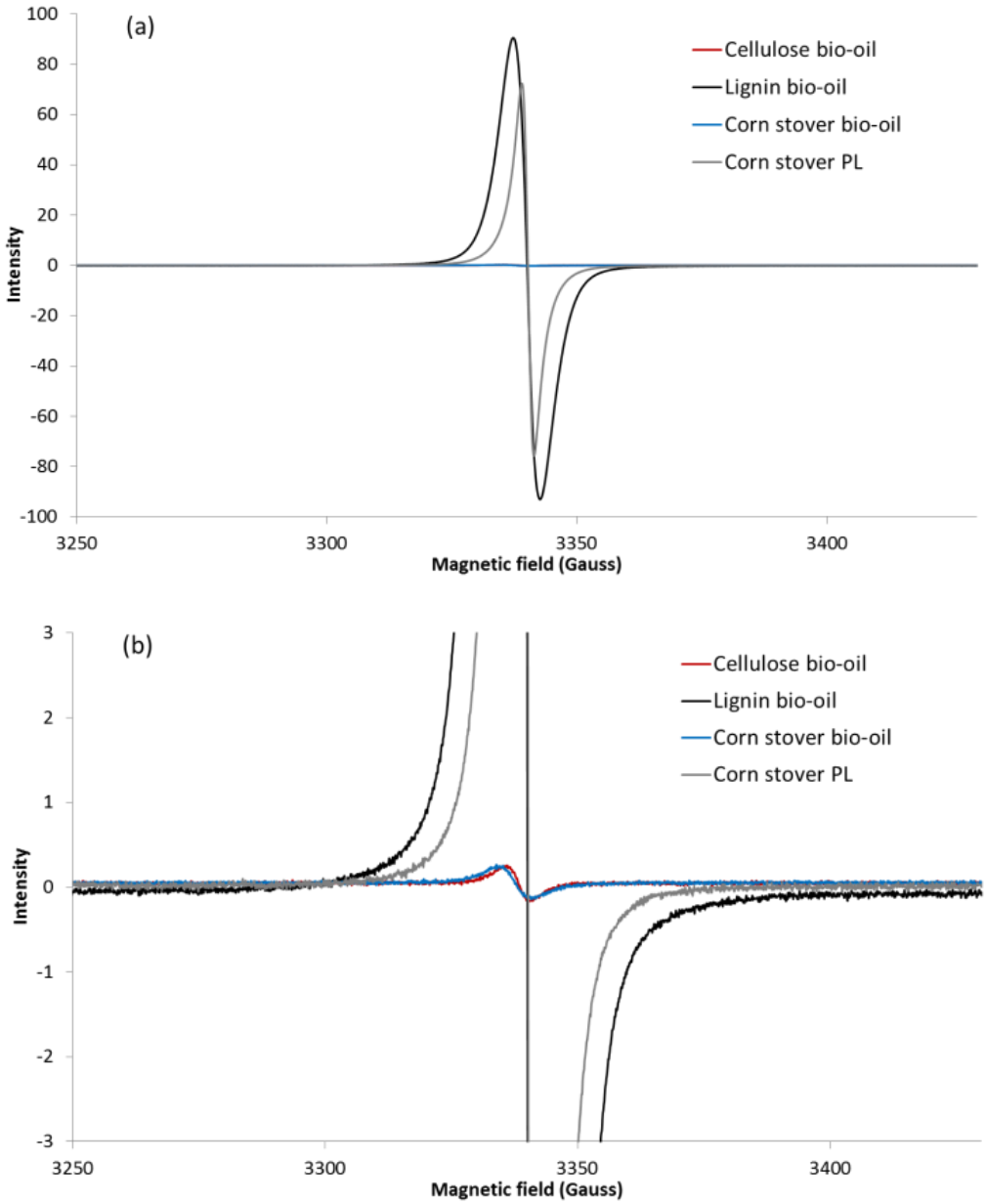

Figure 1. (a) EPR spectra of bio-oils produced from pyrolysis cellulose, lignin and corn stover and pyrolytic lignin (PL) extracted from corn stover bio-oil. EPR parameters: 100 kHz, X-band; microwave frequency, 9.5 GHz; modulation amplitude, 2 G; sweep time, 83.9 seconds; number of scans, 4; sweep width, 200 G; receiver gain 50 for cellulose bio-oil and corn stover bio-oil, and 30 for lignin bio-oil and corn stover PL. (b) Zoomed in EPR spectra with the magnetic field of 3250 – 3430 G and intensity of -3 – +3.

EPR parameters for the bio-oils and pyrolytic lignin are given in Table 1. In general, the g-value of EPR spectra can be used to determine the location at which radical exists [25].

The single broad unstructured peak in each EPR spectrum had g-value in the range of 2.0028 – 2.0031, which corresponds to organic free radicals [26]. In comparison, the g-values for the free radicals of asphaltenes reported in the literature ranged from 2.0028 to 2.0034[24] while free radicals observed from coal pyrolysis ranged from 2.0026 to 2.0035 [27]. Benzyl radicals are one of kind of carbon-centered free radicals that can be expected based on the structure of lignin., Benzyl radicals have a g-value on the order of 2.0021 [28], which increases to 2.0040 when it is adjacent to an oxygen atom [25]. Coal has g-values in the range of 2.0035 to 2.0037 [19], which is typical of methoxy benzene radicals and similar radicals. The oxygen-centered phenoxy radical, thought to be a major radical species in lignin pyrolysis, typically has higher g-value ranging from 2.0040 to 2.0053 [24, 29-31]. However, these g-values are very sensitive to interactions between products and neighboring atomic structure [24]. The broad and unstructured peak on EPR spectra suggests contributions from several radical species that have slightly different g-values. Previously, we found that the free radicals produced from the pyrolysis of benzylphenyl ether (BPE), a simple dimeric molecule serving as a model compound to study pyrolysis of aryl-ether linkages, have a g-value of 2.0035 [32]. Because BPE could produce both benzyl radical (carbon-centered) and phenoxy radical (oxygen-centered), we concluded that the radicals produced from the BPE pyrolysis are a combination of carbon-centered or oxygen-centered radicals. The spectral linewidth ($\Delta H_{P\text{-}P}$) of all samples was measured and the values were slightly different, with ranges from 2.35 to 5.48 gauss. Narrowing of EPR lines was observed for the corn stover pyrolytic lignin compared to corn stover bio-oil. This could be caused by electron-electron exchange narrowing due to the high density of free radicals in pyrolytic lignin.

Table 1. EPR parameters of radicals in bio-oils produced from the pyrolysis of cellulose, lignin and corn stover and pyrolytic lignin (PL) extracted from corn stover bio-oil.

	Cellulose bio-oil	Lignin bio-oil	Corn stover bio-oil	Corn stover PL
ΔHp-p, G	5.01	4.92	5.48	2.35
g-value	2.0031	2.0030	2.0028	2.0028

The concentration of free radicals in the different kinds of bio-oils was determined by EPR, as shown in Figure 2. The concentrations of radicals varied by two orders of magnitude among the bio-oil samples. The lignin bio-oil had 7.5×10^{20} spins g^{-1}, which was the highest value among the bio-oil samples. The concentrations of radicals in corn stover bio-oil and cellulose bio-oil were 5.5×10^{18} and 2.0×10^{18} spins g^{-1}, respectively. For comparison, a crystalline 2,2-diphenyl-1-picrylhydrazyl (DPPH, $C_{18}H_{12}N_5O_6$), a stable and low molecular weight free radical standard, contains 1.5×10^{21} spins g^{-1} (1 spin/41 atoms). Coal pyrolysis typically produces samples with radical concentrations in the concentration range of $3 - 9 \times 10^{20}$ spins g^{-1}, although it depends on the types of coal and reaction conditions [27]. This comparison shows that lignin bio-oil contains a significant concentration of free radicals. Thermally induced homolytic cleavage of aryl-ether linkage in lignin could be a major source of these radicals [33, 34].

Most of these radicals would be expected to have half-lives of less than 10^{-3} sec [35]. The presence of radicals in condensed bio-oil indicates that some radicals formed during pyrolysis are transformed into stable forms. Radicals generated from the primary pyrolysis reactions can be trapped in the aromatics originating from the lignin [26]. The highly delocalized unpaired electrons make the radical species stable in the matrix [26, 36, 37], which is called mesomeric effect or resonance effect. This is the principal reason for the

existence of stable radicals in lignin bio-oil [35]. An example of benzylic conjugation, which could be responsible for radicals in lignin bio-oil, is shown in Scheme 1. This benzylic stabilization is also explained by an orbital interaction diagram analogous to that for hyperconjugation. If there are several π orbitals energetically close to the orbital containing the unpaired electron, the effects are bigger [35]. Conjugation with the lone pair of a heteroatom (O in this case) can also occur.

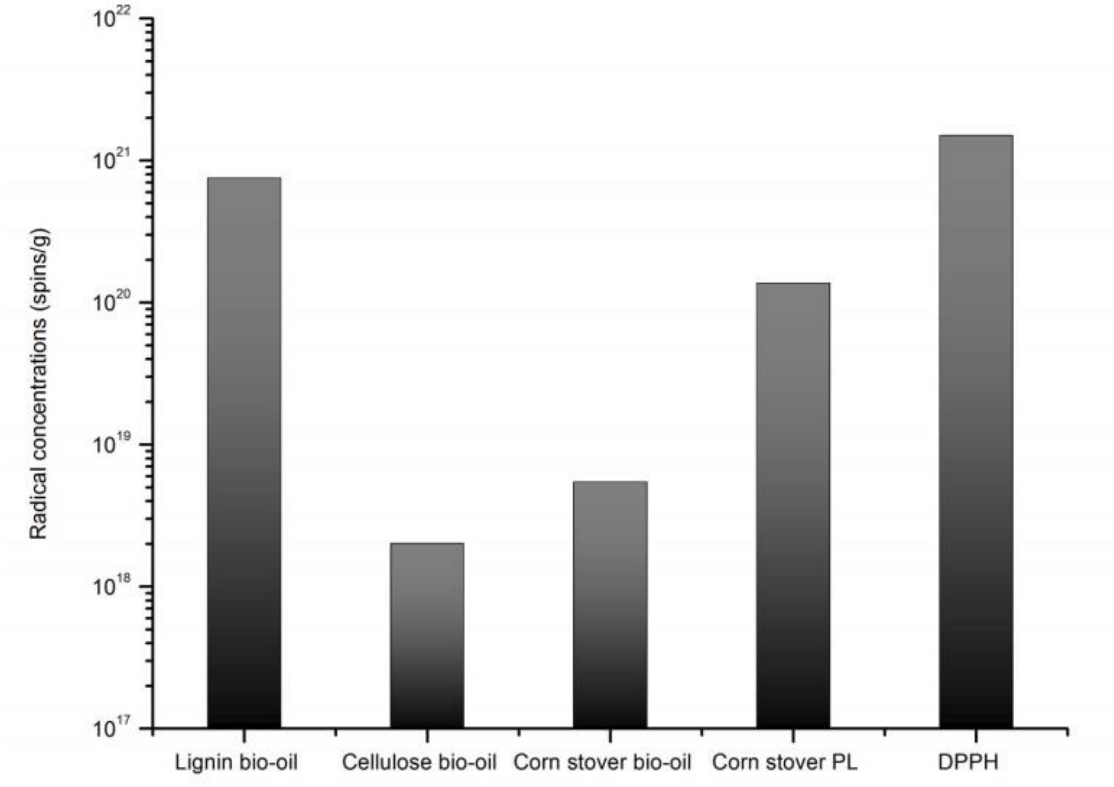

Figure 2. The radical concentrations in each bio-oil and pyrolytic lignin extracted from corn stover bio-oil (PL: pyrolytic lignin and DPPH: 2,2-diphenyl-1-picrylhydrazyl).

Another possible explanation for the radical stabilization is a kinetic effect. The kinetic stability of a radical is generally due to steric factors [35]. When a central radical is encompassed by a great level of molecules, its reactivity with a substrate decreases

considerably becoming persistent radicals. Triphenylmethyl radical and 2,4,6-tri-*tert*-butylphenyl radical are examples of kinetic stability (Figure 3). Considering lignin structure, the explanation of kinetic stability could also be plausible. The steric hindrance of the bulky substituent adjacent to the phenolics which have radicals could make these radical species stable.

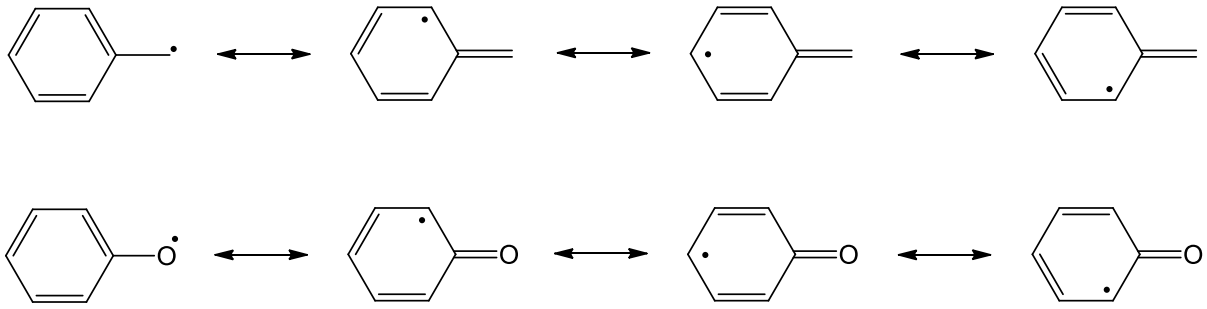

Scheme 1. Benzylic conjugation [35].

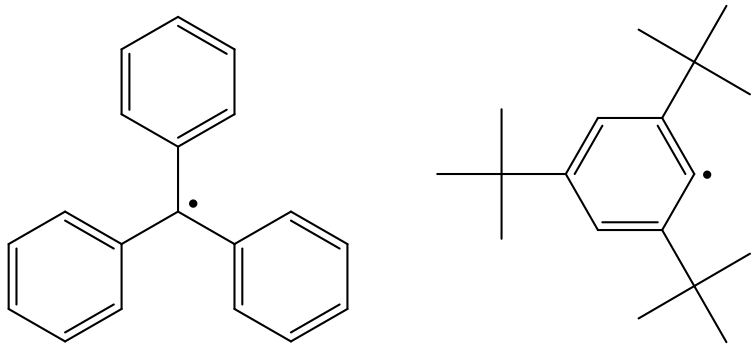

Figure 3. Triphenylmethyl radical (left) and 2,4,6-tri-tert-butylphenyl radical (right).

It should be noted that methoxyl groups in lignin structure could also be a major source of radicals from pyrolysis. Homolytic cleavage of C – O in methoxyl group can generate methyl radicals and anisyl type radicals. While the anisyl type radicals are expected

to be stabilized by mesomeric effect, short-lived methyl radicals might participate in secondary reactions to be consumed by termination reactions. Since the methyl radical is planar, the unpaired electron in a 2p orbital, is not delocalized [35].

To elucidate the origin of radicals in corn stover bio-oil, pyrolytic lignin was precipitated from it using a precipitation method [38], and then subjected to EPR analysis. As seen in Figure 2, the concentration of radicals in pyrolytic lignin was 2.0×10^{20} spins g^{-1}, which was the same order of magnitude as observed for lignin bio-oil. Considering the amount of pyrolytic lignin in corn stover bio-oil (approximately 15 wt%), it appears that free radicals in corn stover bio-oil are highly concentrated in the lignin fraction. From elemental analysis and gel permeation chromatography (supporting information, Table S1), we assumed pyrolytic lignin has a homogeneous structure with molecular formula of $C_{27}H_{31}O_9$ and molecular weight of 408 g mol^{-1}. Thus, the pyrolytic lignin is determined to have approximately 1 unpaired spin per 570 atoms, which is approximately a tenth of radical concentration of DPPH.

Although the radical concentration is significantly lower in cellulose bio-oil, some free radicals were detected by EPR analysis. During the pyrolysis of cellulose, thermal decarbonylation can result in the evolution of CO most likely through a free radical pathway [39]. Also, the cleavage of the glycosidic bond could proceed through homolytic process [40]. Mettler et *al*.[6] reported on the chemistry of cellulose pyrolysis, claiming that both furan and glycolaldehyde formation is initiated by homolytic cleavage of glycosidic bonds. Shafizad claimed that free radicals from cellulose pyrolysis are associated with the formation of char produced by dehydration and degradation of the sugar unit [40, 41]. Figure 4 shows the plausible chemical structure of radical species in cellulose bio-oil. Because levoglucosan

and other light oxygenates, major pyrolysis products from cellulose, do not have unpaired electrons, the stable radical species in cellulose bio-oil could be located in the oligosaccharide moiety. The radical at the C(5) position in glucose unit is comparably stable because of the nearby oxygen and alkyl group at the C(6) position [42].

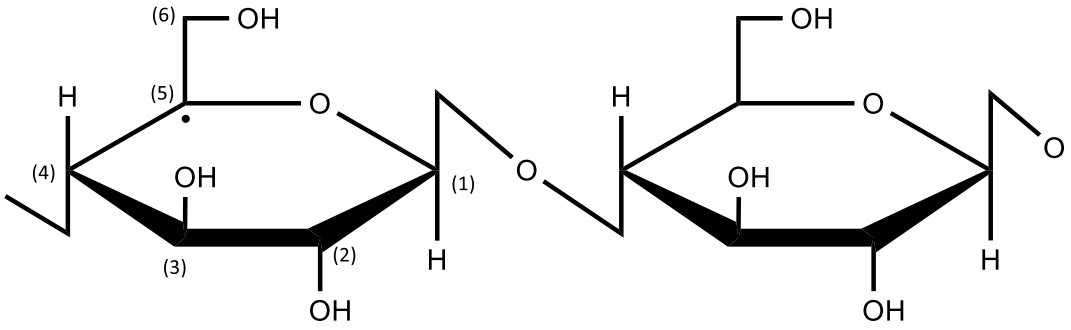

Figure 4. The plausible chemical structure of the radical species in cellulose bio-oil.

It should be noted that the pathway of cellulose pyrolysis is still debated. Hosoya et *al*.[43] and Mayes et *al*.[10] investigated thermal decomposition of glycosidic bond and concluded that a concerted ionic mechanism is more favorable than the direct homolysis of the glycosidic bond because it has a much lower energy barrier. Zhang et *al*.[44] reported that levoglucosan, the main product of cellulose pyrolysis, is unlikely to form via free-radical mechanisms because it has the highest energy barrier. Discussions on heterolytic scission of the glycosidic linkage can be found elsewhere [9, 45, 46]. Despite the uncertainty about the mechanism of cellulose pyrolysis, it is clear from our observation of free radicals in cellulose bio-oil that homolytic cleavage is involved in cellulose pyrolysis. Also, the radicals in cellulose bio-oil are in a stable form, which might be attributed to structural steric hindrance as discussed above.

Investigation of the relationship between bio-oil aging and radical concentrations

Although we confirmed the existence of radicals in bio-oil samples, this result provided limited information because analysis of pyrolysis products (bio-oils and pyrolytic lignin) does not provide the information regarding primary radical reactions because of their short half-lives. Thus, uncertainties about the initial state of pyrolysis still remain, implying that a different approach is required to elucidate the pyrolytic behavior of reactive radicals.

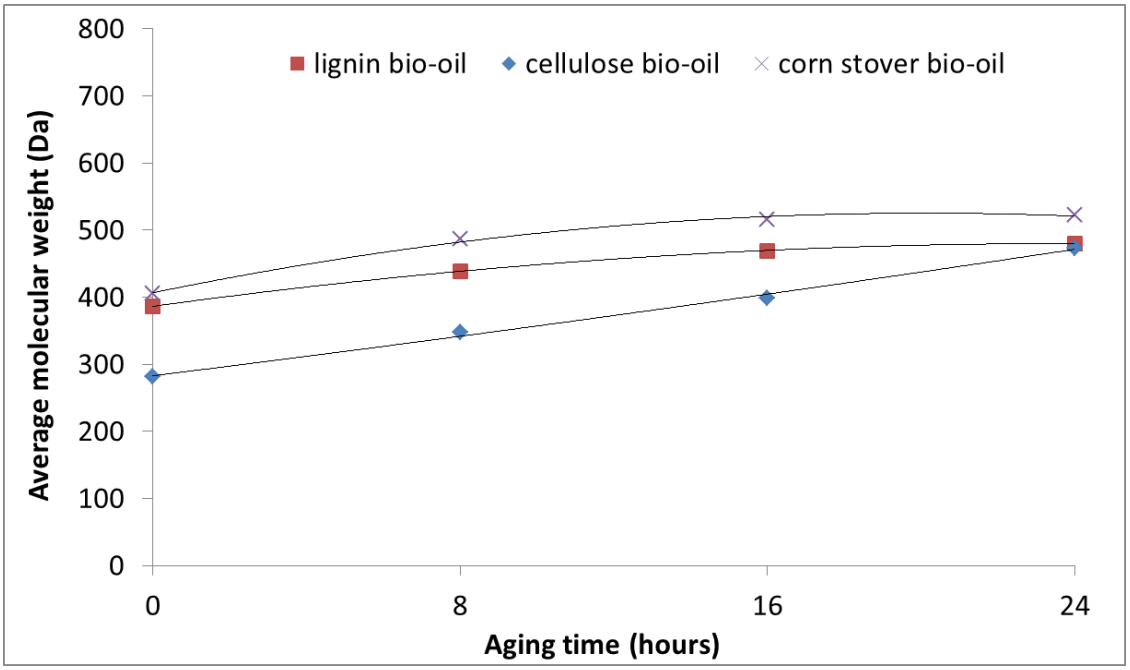

Figure 5. Weight average molecular weight (Mw) of three kinds of bio-oil as a function of aging time.

It is suspected that the free radicals we have detected in condensed bio-oils are stable toward further reactions. Meng et *al.*[16] also revealed that radicals were not responsible for aging by analyzing bio-oils derived from whole biomass. As we described above, free radicals generated from both cellulose and lignin fractions. To investigate if the free radical derived from different components of biomass contributes the instability of bio-oil during

storage, accelerated aging tests were conducted at 80 °C for 24 hours for each bio-oil. The resulting bio-oils were subjected to several analysis including GPC, EPR and GC/MS-FID to determine changes in molecular weight, radical concentrations and chemical composition, respectively, with time. Figure 5 displays the gel permeation chromatograms obtained from three bio-oils as a function of aging time. The weight average molecular weight (Mw) of three bio-oils increased gradually with increasing aging time. The Mw of cellulose bio-oil increased from 281 to 473 Da (68%) after 24 hours aging. The Mw of lignin bio-oil and corn stover bio-oil increased from 386 to 480 Da (24%) and 388 to 481 Da (24%), respectively. Figure 6 shows the molecular weight distributions of each bio-oil. For cellulose bio-oil, the low molecular weight peak around 95 Da, which could correspond to light oxygenates, noticeably decreased with aging while concentrations at the high molecular weight range (> 300 Da) increased. Similar behavior was observed for the lignin and cornstover bio-oil with some differences in peak locations. The low molecular weight peaks (corresponding to phenolic monomers and dimers derived from lignin) for lignin bio-oil and corn stover bio-oil occurred at 72 Da and 180 Da and, 90 Da and 181 Da, respectively. Clearly, all three bio-oils underwent repolymerization during the aging tests.

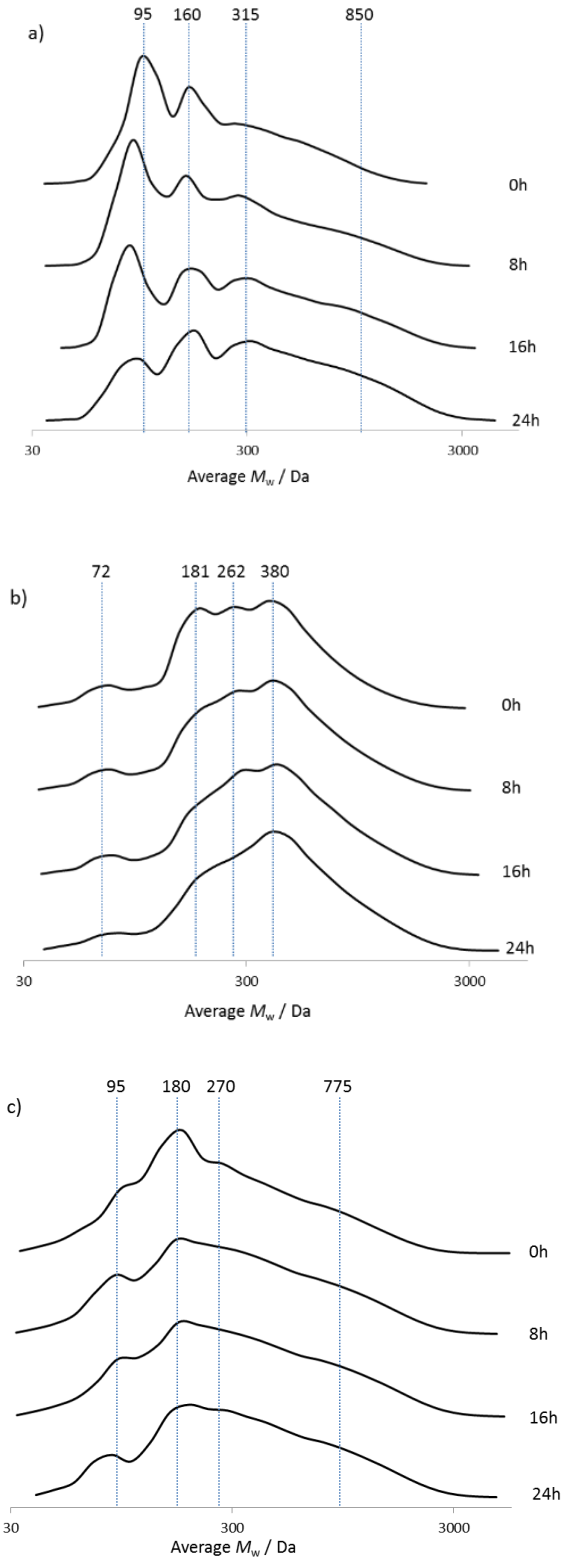

Figure 6. Gel permeation chromatograms of a) cellulose bio-oil, b) lignin bio-oil and c) corn stover bio-oil.

The free radical concentrations as a function of time for the three bio-oils during the aging tests are plotted in Figure 7. The concentrations of radicals were relatively constant during the aging tests for all three bio-oils. For example, radical concentration in lignin bio-oil remained almost constant at approximately 7.4×10^{20} spins g^{-1} even while M_w increased 24% over 24 hours. If radicals participated in coupling reactions to form large molecular weight compounds, the concentration of radicals would have been expected to decrease as radical termination reactions occurred. The absence of a correlation between the extent of polymerization and free radical concentrations in bio-oil implies that free radicals do not participate in secondary repolymerization reactions in the condensed phase. It seems unlikely that the constancy of radical concentration during polymerization of the bio-oil was due to perfectly balanced radical propagation in the polymerization reaction networks, which normally would include significant radical termination reactions as well.

We also analyzed the chemical composition of aged bio-oils using GC/MS-FID (see Tables S2 – S4). For lignin bio-oil (Table S2), the most distinctive change was a decrease in vinylphenols. For example, the yield of 4-vinylphenol decreased from 4.3 to 2.6 wt% over the 24 hours of the accelerated aging test. In previous work, we have found that unsaturated C = C bonds in vinylphenol are highly reactive toward polymerization [47]. Hosoya et *al*.[48] also reported that unsaturated C = C bonds on side chains of aromatic rings are the most reactive structure responsible for repolymerization. Clearly, highly reactive functional groups such as vinyl play an important role in repolymerization of lignin bio-oil. For cellulose bio-oil (Table S3), light oxygenates, including hydroxy acetone and 2,5-dimethoxytetrahydrofuran decreased with aging time. These oxygen containing light compounds are somewhat reactive, thus the repolymerization of cellulose derived light

oxygenates in the bio-oil to form large molecular weight compounds is plausible [49]. For corn stover bio-oil (Table S4), concentrations of derivatives from both carbohydrates and lignin derivatives decreased with aging time. This is not surprising considering the results for bio-oils produced from cellulose and lignin. Whether there was a synergistic effect between these two components in the corn stover bio-oil was not clear.

We performed tests to explicitly evaluate the stability of free radicals in bio-oil upon addition of a compound with a reactive functional group. In this experiment, we combined 2-methoxy-4-vinylphenol with lignin bio-oil samples as a 1:2 mixture, and then conducted accelerated aging tests to see whether any reaction occurs between radical species and reactive functionality. If radical species take part in reactions with vinyl group, C = C double bonds are converted into C – C single bonds by a radical chain mechanism, forming large molecular weight compounds without a net change in radical concentration. Figure S1 displays the gel permeation chromatograms obtained from the mixture of lignin bio-oil and 2-methoxy-4-vinylphenol. There was no significant change with molecular weight distribution over time compared to the control case (24 hr aging without 2-methoxy-4-vinylphenol addition). Neither did the concentration of radicals change in the bio-oil during the aging test (Figure S2). These results imply that radical species in lignin bio-oil are stable toward secondary reactions with reactive functionalities.

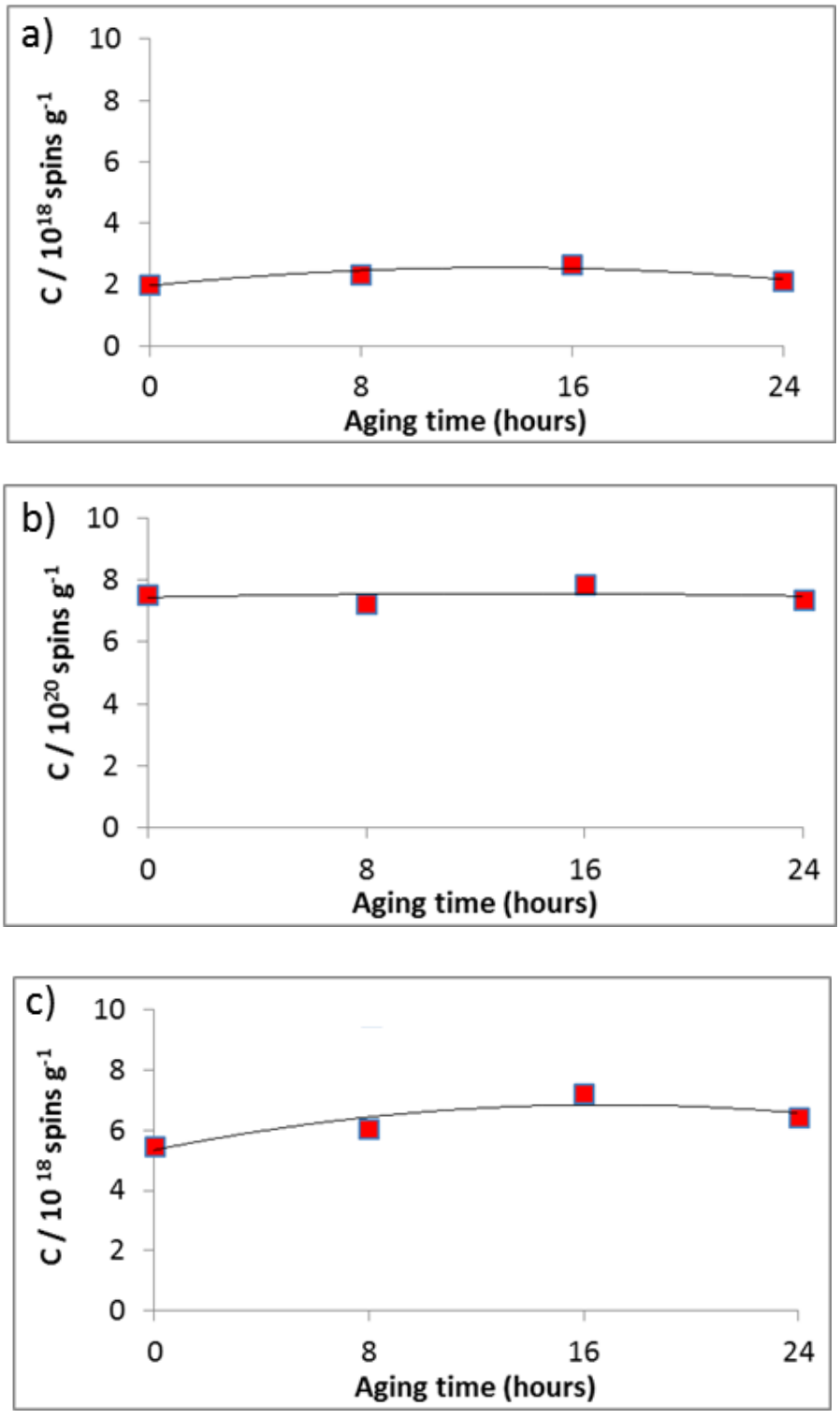

Figure 7. The concentrations of free radical in a) cellulose bio-oil, b) lignin bio-oil and c) corn stover bio-oil as a function of aging time.

Conclusion

The free radicals in bio-oils obtained from the pyrolysis of cellulose, lignin and corn stover were analyzed using an EPR spectroscopy to investigate thermal behavior in condensed pyrolysis products. The quantitative analysis of free radical in each bio-oil sample revealed that the free radicals were highly concentrated in lignin bio-oil and the lignin fraction (pyrolytic lignin) of whole bio-oil. It was confirmed from our observation of free radicals in cellulose bio-oil that homolytic cleavage is involved in cellulose pyrolysis. From accelerated aging tests, we found no relationship between changes in molecular weight of the bio-oil samples and the concentration of radicals. Lignin-derived radicals seemed to be stable in aromatic environments due to the mesomeric effect. And the stability of radicals in cellulose bio-oil might be attributed to structural steric hindrance. Clearly, radicals are produced during pyrolysis of both the carbohydrate and lignin fractions of lignocellulosic biomass. These are transformed into stable radicals in bio-oil either during pyrolysis or upon condensation to liquid.

Experimental Section

Materials

Corn stover used in this study was obtained from the BioCentury Research Farm (Boone, IA). The corn stover was ground and sieved to obtain the desired size range of 250 – 850 μm. Cellulose (50 μm) was purchased from Sigma-Aldrich. Organosolv lignin was obtained from Archer Daniels Midland (Decatur, IL). Prior to pyrolysis test, lignin samples were washed using dilute acid to remove minerals and residual carbohydrates.

Bio-oil preparation

Fast pyrolysis of cellulose, lignin and corn stover was performed using a continuous free-fall reactor. A schematic diagram of the reactor is shown in Figure S3 (See Supporting Information). The reactor consisted of a feeder, a 35 mm diameter stainless steel reactor of 3.05 m height, a char collection system, and a bio-oil collection system. For the all pyrolysis tests, nitrogen sweep gas was introduced into the reactor at 60 standard L min^{-1} biomass fed at 2 kg h^{-1}. All heaters were set at 600 °C and the pyrolysis vapors inside the reactor maintained around 550 °C as monitored by type K thermocouples. Bio-oils produced from the pyrolysis tests were stored at -20 °C until analyzed. Pyrolytic lignin was extracted from corn stover bio-oil using the method described by Scholze and Meier [38]. Accelerated aging test for the bio-oils was conducted at 80 °C for 24 hours.

EPR, GPC and GC analysis

Approximately 100 mg of each bio-oil sample was dissolved in 1 mL of 1,4-dioxane. After mixing the solution, a 300 μL aliquot was transferred to an EPR quartz tube for EPR analysis. EPR spectra were recorded on a Bruker ELEXYS E580 FT-EPR spectrometer at the X-band (9.5 GHz) microwave frequency with a magnetic field modulation of 100 kHz at room temperature. 2,2-diphenyl-1-picrylhydrazyl (DPPH) was used as a radical standard. The EPR parameters were: center field of 3340 G, sweep width of 200 G, sweep time of 83.9 sec, receiver gain of 30 – 50 dB and modulation amplitude of 2 G. For quantitative analysis of radicals, double integration of the defined region of 3310 – 3370 G was made using Xepr software.

Gel permeation chromatography (GPC) of samples was carried out using the Dionex Ultimate 3000 series high performance liquid chromatography (HPLC) equipped with a Shodex Refractive Index detector and Diode Array Detector. Two GPC columns (3 μm, 100 Å, 300 × 7.5 mm; PLgel, Agilent) were connected in series and kept at 25 °C. Tetrahydrofuran (THF) with a flow rate of 1 ml/min was used as the eluent. The GPC column was calibrated using six polystyrene standards. Approximately 0.02 g bio-oil sample was dissolved in a 10 mL of THF, with the solution filtered using a syringe filter prior to the GPC analysis.

Identification and quantification of chemical compounds in bio-oil were performed using a Varian CP-3800 gas chromatograph equipped with Saturn 2200 mass spectrometry and mass spectrometry (MS)/flame ionization detector (FID). Bio-oil sample was first analyzed using GC/MS to identify its composition. The chemicals identified by GC/MS were calibrated in GC/FID using pure compounds. After identification, GC/FID was performed for quantification of chemical species using a Phenomenex ZB-1701 (60 m × 0.25 mm × 0.25 μm) capillary column. Injection temperature was 275 °C and oven temperature was programmed to hold at 35 °C for 3 min, ramp to 280 °C at 3 °C min^{-1} and then hold for additional 4 min.

Acknowledgements

This work was supported by the National Advanced Biofuel Consortium through a subcontract with the National Renewable Energy Laboratory. The authors would like to thank Joseph Polin of the Bioeconomy Institute for valuable discussions.

Supporting Information

Table S1. Elemental composition and molecular weight of pyrolytic lignin extracted from corn stover bio-oil.

Elemental composition (wt. %)	
Carbon	60.3
Hydrogen	5.8
Oxygen	33.9
Mw (g/mol)	408
Calculated molecular formula	$C_{21}H_{23}O_9$

Table S2. Compositional analysis of lignin bio-oil determined by GC/MS-FID.

Lignin bio-oil	Aging time			
	0h	8h	16h	24h
Phenol	0.16±0.01	0.17±0.01	0.15±0.01	0.13±0.01
Guaiacol	0.06±0.01	0.06±0.01	0.07±0.01	0.05±0.00
p-cresol	0.11±0.01	0.13±0.01	0.12±0.01	0.10±0.01
2-methoxy-4-mehylphenol	0.06±0.01	0.06±0.01	0.07±0.00	0.05±0.00
4-ethylphenol	0.18±0.04	0.20±0.02	0.18±0.00	0.15±0.03
4-vinylphenol[1)]	4.31±0.35	3.64±0.20	3.18±0.40	2.63±0.09
Eugenol	0.01±0.00	0.02±0.00	0.02±0.00	0.02±0.00
Syringol	0.07±0.01	0.09±0.01	0.09±0.01	0.08±0.00
Isoeugenol	0.03±0.01	0.04±0.01	0.05±0.01	0.04±0.00
2,6-dimethoxy-4-methylphenol	0.07±0.01	0.08±0.01	0.07±0.03	0.06±0.03
Vanillin	0.02±0.00	0.02±0.01	0.02±0.01	0.02±0.01
2,6-dimethoxy-4-ethylphenol	0.04±0.00	0.04±0.00	0.05±0.00	0.04±0.00
Acetoguaiacone	0.05±.001	0.07±0.01	0.09±0.01	0.08±0.01
2,6-dimethoxy-4-vinylphenol	0.03±0.01	0.03±0.00	0.03±0.01	0.03±0.00
guaiacyl acetone	0.04±0.00	0.05±0.00	0.06±0.01	0.05±0.00
2,6-dimethoxy-4-(2-propenyl) phenol	0.00±0.01	0.01±0.00	0.01±0.00	0.01±0.00
2,6-dimethoxy-4-(1-propenyl) phenol	0.03±0.00	0.03±0.01	0.04±0.02	0.04±0.01
3,5-dimethoxy-4-hydroxybenzaldehyde	0.02±0.01	0.02±0.00	0.04±0.03	0.03±0.01
acetosyringone	0.19±0.02	0.26±0.02	0.34±0.06	0.28±0.02
syringyl acetone	0.01±0.00	0.02±0.00	0.02±0.00	0.02±0.00
Sum	**5.50±0.48**	**5.03±0.30**	**4.70±0.58**	**3.92±0.01**

[1)] Peaks of 4-vinylphenol and 2-methoxy-4-vinylphenol on chromatogram slightly overlapped each other, the peaks were treated as one and quantified using the calibration of 4-vinylphenol.

Table S3. Compositional analysis of cellulose bio-oil determined by GC/MS-FID.

Cellulose bio-oil	Aging time			
	0h	8h	16h	24h
methyl cyclopentane	0.04±0.01	0.04±0.00	0.02±0.01	0.03±0.01
1,1-dimethoxy propane	0.17±0.00	0.13±0.01	0.13±0.02	0.16±0.03
hydroxy acetone	1.20±0.15	1.04±0.04	0.91±0.08	0.80±0.06
furan compound[1)]	0.40±0.08	0.33±0.03	0.28±0.07	0.23±0.04
glycolaldehyde	0.08±0.02	0.05±0.00	0.05±0.00	0.04±0.01
2,5-dimethoxytetrahydrofuran	0.73±0.06	0.37±0.01	0.21±0.07	0.17±0.07
1,2-cyclopentendione	0.33±0.08	0.25±0.04	0.23±0.02	0.17±0.01
furfural	0.07±0.01	0.08±0.00	0.06±0.02	0.07±0.01
pyran compound[2)]	0.43±0.14	0.14±0.04	0.07±0.00	0.06±0.00
2(5H)-furanone	0.18±0.02	0.14±0.01	0.13±0.02	0.13±0.00
butanedionic acid, dimethyl ester	0.11±0.02	0.11±0.00	0.10±0.02	0.08±0.01
methyl cyclopentenolone	0.10±0.02	0.07±0.00	0.07±0.01	0.06±0.00
5-HMF	0.14±0.05	0.13±0.00	0.16±0.03	0.18±0.01
levoglucosan	16.64±0.68	16.83±1.02	17.11±1.03	16.64±0.45
Sum	20.62±1.48	19.72±1.20	19.52±1.40	18.82±0.71

[1)] Quantified using a calibration of 2,5-dimethoxytetrahydrofuran.
[2)] Quantified using a calibration of 2H-pyran-2-one.

Table S4. Compositional analysis of corn stover bio-oil determined by GC/MS-FID.

Corn stover bio-oil	Aging time			
	0h	8h	16h	24h
acetic acid	3.75±0.38	3.77±0.35	3.72±0.44	3.88±0.33
hydroxy acetone	2.97±0.3	2.84±0.18	3.00±0.23	3.06±0.20
1-hydroxy butanone	0.24±0.02	0.23±0.02	0.23±0.02	0.23±0.01
furfuryl alcohol	0.04±0.00	0.01±0.00	-	-
1-(acetyloxy)-2-propanone	0.03±0.00	0.03±0.00	0.03±0.00	0.03±0.00
2-methyl-2-cyclopentenone	0.27±0.03	0.23±0.01	0.27±0.02	0.25±0.01
furfural	0.01±0.00	0.01±0.00	0.01±0.00	0.01±0.00
5-methyl furfural	0.01±0.00	0.01±0.00	0.01±0.00	0.01±0.00
4-hydroxy butanoic acid	0.33±0.03	0.31±0.01	0.31±0.02	0.29±0.01
phenol	0.18±0.02	0.15±0.01	0.17±0.01	0.15±0.00
guaiacol	0.01±0.00	0.01±0.00	0.02±0.00	0.02±0.00
p-cresol	0.13±0.01	0.11±0.01	0.13±0.00	0.11±0.01
2-methoxy-4-methyl phenol	0.03±0.00	0.02±0.00	0.03±0.00	0.02±0.00
4-ethylphenol	0.10±0.01	0.07±0.00	0.10±0.00	0.08±0.00
4-vinylphenol[1)]	0.42±0.04	0.15±0.01	0.15±0.00	0.11±0.00
eugenol	0.02±0.00	0.01±0.00	-	-
5-HMF	0.01±0.00	0.01±0.00	-	0.01±0.00
syringol	0.06±0.01	0.06±0.00	0.06±0.00	0.05±0.00
isoeugenol	0.03±0.00	0.02±0.00	0.01±0.00	0.01±0.00
2,6-dimethoxy-4-methylphenol	0.03±0.00	0.02±0.00	0.02±0.00	0.02±0.00
acetoguaiacone	0.05±0.01	0.05±0.00	0.05±0.00	0.04±0.00
2,6-dimethoxy-4-(1-propenyl) phenol	0.04±0.00	0.02±0.00	0.02±0.00	0.01±0.00
Levoglucosan	1.20±0.12	1.08±0.04	1.13±0.00	1.09±0.06
Sum	9.96±1.00	9.22±0.64	9.48±0.75	9.48±0.65

[1)] Peaks of 4-vinylphenol and 2-methoxy-4-vinylphenol on chromatogram slightly overlapped each other, the peaks were treated as one and quantified using the calibration of 4-vinylphenol.

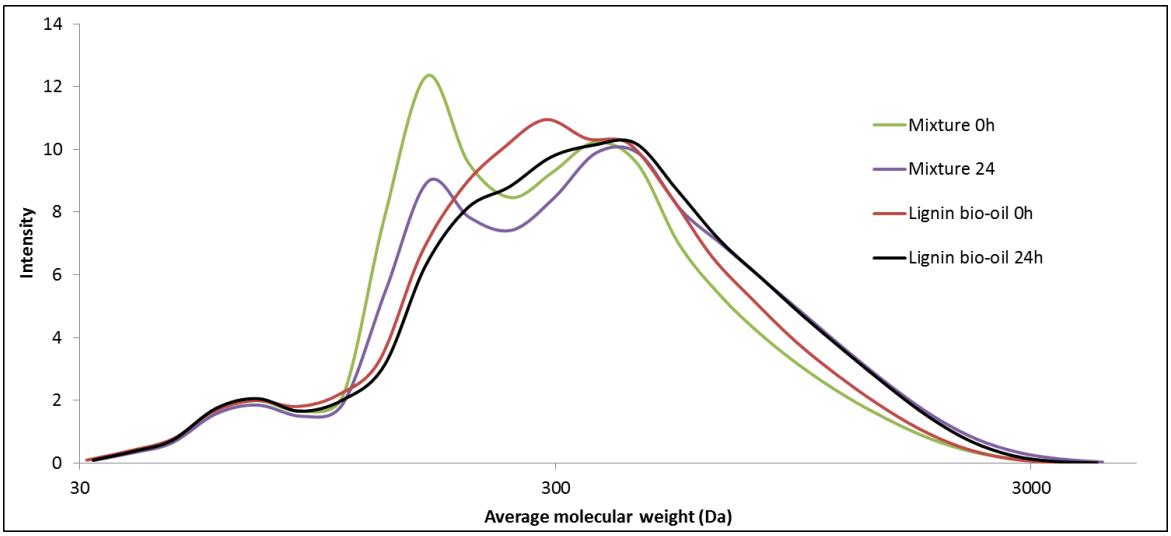

Figure S1. Gel permeation chromatograms of lignin bio-oil and a mixture of lignin bio-oil and 2-methoxy-4-vinylphenol.

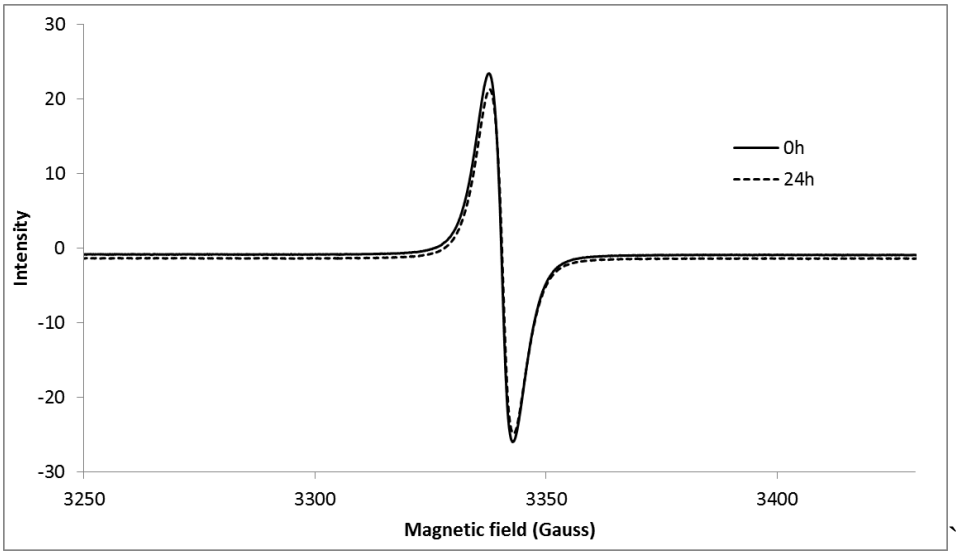

Figure S2. EPR spectra of mixture of lignin bio-oil and 50 wt% of 2-methoxy-4-vinylphenol. EPR parameters: 100 kHz, X-band; microwave frequency, 9.5 GHz; modulation amplitude, 2 G; sweep time, 83.9 seconds; number of scans, 4; sweep width, 200 G; receiver gain 30 .

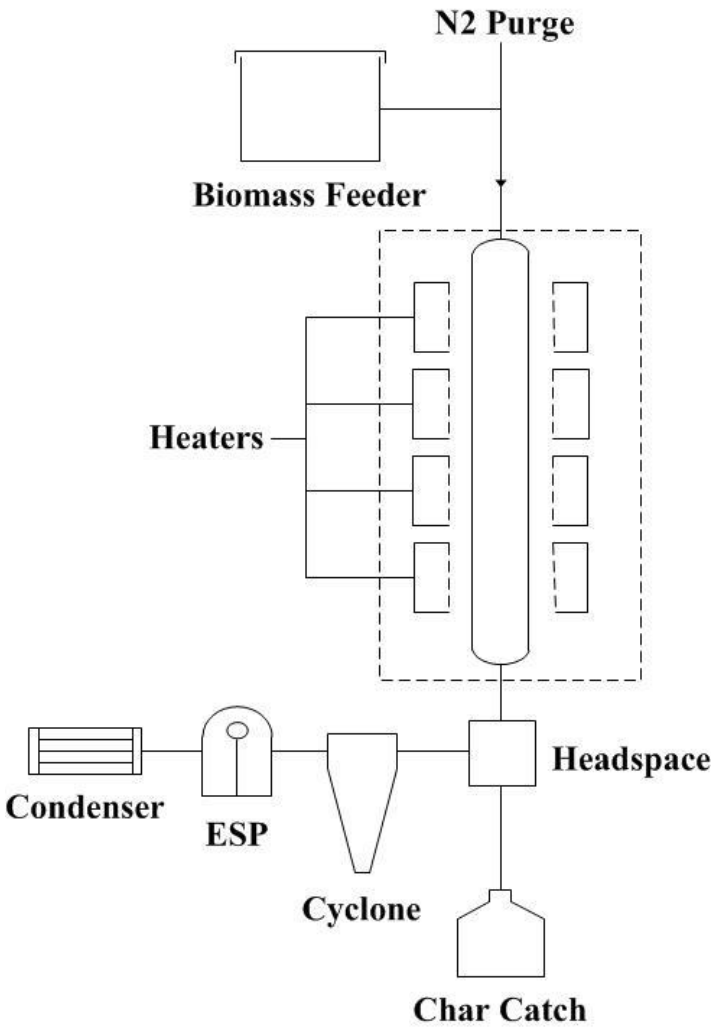

Figure S3. A schematic diagram of freefall reactor.

REFERENCES

[1] A.J. Ragauskas, C.K. Williams, B.H. Davison, G. Britovsek, J. Cairney, C.A. Eckert, W.J. Frederick, J.P. Hallett, D.J. Leak, C.L. Liotta, J.R. Mielenz, R. Murphy, R. Templer, T. Tschaplinski, The path forward for biofuels and biomaterials, Science 2006;311:484-89.

[2] A. Demirbas, Biomass resource facilities and biomass conversion processing for fuels and chemicals, Energ Convers Manage 2001;42:1357-78.

[3] M. Van de Velden, J. Baeyens, A. Brems, B. Janssens, R. Dewil, Fundamentals, kinetics and endothermicity of the biomass pyrolysis reaction, Renew Energ 2010;35:232-42.

[4] T.S. Kim, J.Y. Kim, K.H. Kim, S. Lee, D. Choi, I.G. Choi, J.W. Choi, The effect of storage duration on bio-oil properties, J Anal Appl Pyrol 2012;95:118-25.

[5] M.E. Boucher, A. Chaala, C. Roy, Bio-oils obtained by vacuum pyrolysis of softwood bark as a liquid fuel for gas turbines. Part I: Properties of bio-oil and its blends with methanol and a pyrolytic aqueous phase, Biomass Bioenerg 2000;19:337-50.

[6] M.S. Mettler, S.H. Mushrif, A.D. Paulsen, A.D. Javadekar, D.G. Vlachos, P.J. Dauenhauer, Revealing pyrolysis chemistry for biofuels production: Conversion of cellulose to furans and small oxygenates, Energ Environ Sci 2012;5:5414-24.

[7] X.L. Zhang, J. Li, W.H. Yang, W. Blasiak, Formation Mechanism of Levoglucosan and Formaldehyde during Cellulose Pyrolysis, Energ Fuel 2011;25:3739-46.

[8] P.R. Patwardhan, R.C. Brown, B.H. Shanks, Product Distribution from the Fast Pyrolysis of Hemicellulose, ChemSusChem 2011;4:636-43.

[9] P.R. Patwardhan, J.A. Satrio, R.C. Brown, B.H. Shanks, Product distribution from fast pyrolysis of glucose-based carbohydrates, J Anal Appl Pyrol 2009;86:323-30.

[10] H.B. Mayes, L.J. Broadbelt, Unraveling the Reactions that Unravel Cellulose, J Phys Chem A 2012;116:7098-106.

[11] C. Amen-Chen, H. Pakdel, C. Roy, Production of monomeric phenols by thermochemical conversion of biomass: a review, Bioresource Technol 2001;79:277-99.

[12] J. Kibet, L. Khachatryan, B. Dellinger, Molecular Products and Radicals from Pyrolysis of Lignin, Environ Sci Technol 2012;46:12994-3001.

[13] C. Bährle, V. Custodis, G. Jeschke, J.A. van Bokhoven, F. Vogel, In situ Observation of Radicals and Molecular Products During Lignin Pyrolysis, ChemSusChem 2014;7:2022-29.

[14] R. Bayerbach, D. Meier, Characterization of the water-insoluble fraction from fast pyrolysis liquids (pyrolytic lignin). Part IV: Structure elucidation of oligomeric molecules, J Anal Appl Pyrol 2009;85:98-107.

[15] M. Bardet, S. Hediger, G. Gerbaud, S. Gambarelli, J.F. Jacquot, M.F. Foray, A. Gadelle, Investigation with C-13 NMR, EPR and magnetic susceptibility measurements of char residues obtained by pyrolysis of biomass, Fuel 2007;86:1966-76.

[16] J.J. Meng, T.I. Smirnova, X. Song, A. Moore, X.Y. Ren, S. Kelley, S. Park, D. Tilotta, Identification of free radicals in pyrolysis oil and their impact on bio-oil stability, Rsc Adv 2014;4:29840-46.

[17] G.R. Eaton, S. Eaton, S, D.P. Barr, R.T. Weber, Quantitative EPR, 1st ed., Springer, New York, 2010.

[18] L. Petrakis, D.W. Grandy, Formation and Behavior of Coal Free-Radicals in Pyrolysis and Liquefaction Conditions, Nature 1981;289:476-77.

[19] L. Petrakis, D.W. Grandy, Electron-Spin Resonance Spectrometric Study of Free-Radicals in Coals, Anal Chem 1978;50:303-08.

[20] R.F. Sprecher, H.L. Retcofsky, Observation of Transient Free-Radicals during Coal Pyrolysis, Fuel 1983;62:473-76.

[21] M.S. Seehra, B. Ghosh, S.E. Mullins, Evidence for Different Temperature Stages in Coal Pyrolysis from Insitu Electron-Spin-Resonance Spectroscopy, Fuel 1986;65:1315-16.

[22] N.S. Qiu, H.L. Li, Z.J. Jin, Y.K. Zhu, Temperature and time effect on the concentrations of free radicals in coal: Evidence from laboratory pyrolysis experiments, Int J Coal Geol 2007;69:220-28.

[23] G.L. Squadrito, R. Cueto, B. Dellinger, W.A. Pryor, Quinoid redox cycling as a mechanism for sustained free radical generation by inhaled airborne particulate matter, Free Radical Bio Med 2001;31:1132-38.

[24] C.L.B. Guedes, E. Di Mauro, V. Antunes, A.S. Mangrich, Photochemical weathering study of Brazilian petroleum by EPR spectroscopy, Mar Chem 2003;84:105-12.

[25] B. Dellinger, S. Loninicki, L. Khachatryan, Z. Maskos, R.W. Hall, J. Adounkpe, C. McFerrin, H. Truong, Formation and stabilization of persistent free radicals, P Combust Inst 2007;31:521-28.

[26] H. Sivonen, S.L. Maunu, F. Sundholm, S. Jamsa, P. Viitaniemi, Magnetic resonance studies of thermally modified wood, Holzforschung 2002;56:648-54.

[27] L. Petrakis, D.W. Grandy, Free-Radicals in Coals and Coal Conversion .3. Investigation of the Free-Radicals of Selected Macerals Upon Pyrolysis, Fuel 1981;60:115-19.

[28] M. Ohtani, S. Ohkoshi, M. Kajitani, T. Akiyama, A. Sugimori, S. Yamauchi, Y. Ohba, M. Iwaizumi, Direct Observations of the Intermediate Species in the Photodissociation of Bis(S-Benzyl-1,2-Diphenyl-1,2-Ethylenedithiolato)Nickel by Time-Resolved Epr and Uv-Vis Absorption-Spectroscopy, Inorg Chem 1992;31:3873-74.

[29] F. Graf, K. Loth, H.H. Gunthard, Chlorine Hyperfine Splittings and Spin-Density Distributions of Phenoxy Radicals - Esr and Quantum Chemical Study, Helv Chim Acta 1977;60:710-21.

[30] E. Vejerano, S. Lomnicki, B. Dellinger, Formation and Stabilization of Combustion-Generated Environmentally Persistent Free Radicals on an Fe(III)(2)O-3/Silica Surface, Environ Sci Technol 2011;45:589-94.

[31] G. Dobele, T. Dizhbite, G. Rossinskaja, G. Telysheva, D. Mier, S. Radtke, O. Faix, Pre-treatment of biomass with phosphoric acid prior to fast pyrolysis - A promising method for obtaining 1,6-anhydrosaccharides in high yields, J Anal Appl Pyrol 2003;68-9:197-211.

[32] K.H. Kim, X. Bai, R.C. Brown, Pyrolysis mechanisms of methoxy substituted α-O-4 lignin dimeric model compounds and detection of free radicals using electron paramagnetic resonance analysis, J Anal Appl Pyrol 2014.

[33] P.F. Britt, A.C. Buchanan, M.J. Cooney, D.R. Martineau, Flash vacuum pyrolysis of methoxy-substituted lignin model compounds, J Org Chem 2000;65:1376-89.

[34] H. Kawamoto, M. Ryoritani, S. Saka, Different pyrolytic cleavage mechanisms of beta-ether bond depending on the side-chain structure of lignin dimers, J Anal Appl Pyrol 2008;81:88-94.

[35] J. Fossey, D. Lefort, J. Sorba, Free radicals in organic chemistry, Wiley, Paris, 1995.

[36] R.W. Rex, Electron Paramagnetic Resonance Studies of Stable Free Radicals in Lignins and Humic Acids, Nature 1960;188:1185-86.

[37] C. Steelink, G. Tollin, Stable Free Radicals in Soil Humic Acid, Biochim Biophys Acta 1962;59:25-&.

[38] B. Scholze, D. Meier, Characterization of the water-insoluble fraction from pyrolysis oil (pyrolytic lignin). Part I. PY-GC/MS, FTIR, and functional groups, J Anal Appl Pyrol 2001;60:41-54.

[39] M.M. Tang, R. Bacon, Carbonization of Cellulose Fibers .1. Low Temperature Pyrolysis, Carbon 1964;1:390-90.

[40] Shafizad.F, Y.L. Fu, Pyrolysis of Cellulose, Carbohyd Res 1973;29:113-22.

[41] Shafizad.F, R.A. Susott, G.D. Mcginnis, Pyrolysis of Substituted Phenyl Beta-D-Glucopyranosides and 2-Deoxy-Alpha-D-Arabino-Hexopyranosides, Carbohyd Res 1972;22:63-&.

[42] H. Kameya, M. Ukai, Analysis of Relaxation Behavior of Free Radicals in Irradiated Cellulose Using Pulse and Continuous-Wave Electron Spin Resonance, in: T. van de Ven (Ed.) Celllulose - Fundamental Aspects, InTech, 2013.

[43] T. Hosoya, Y. Nakao, H. Sato, H. Kawamoto, S. Sakaki, Thermal Degradation of Methyl beta-D-Glucoside. A Theoretical Study of Plausible Reaction Mechanisms, J Org Chem 2009;74:6891-94.

[44] X.L. Zhang, W.H. Yang, C.Q. Dong, Levoglucosan formation mechanisms during cellulose pyrolysis, J Anal Appl Pyrol 2013;104:19-27.

[45] G.R. Ponder, G.N. Richards, T.T. Stevenson, Mechanisms of Pyrolysis of Polysaccharides .6. Influence of Linkage Position and Orientation in Pyrolysis of Polysaccharides - a Study of Several Glucans, J Anal Appl Pyrol 1992;22:217-29.

[46] M.J. Antal, G. Varhegyi, Cellulose Pyrolysis Kinetics - the Current State Knowledge, Ind Eng Chem Res 1995;34:703-17.

[47] X. Bai, K.H. Kim, R.C. Brown, E. Dalluge, C. Hutchinson, Y.J. Lee, D. Dalluge, Formation of phenolic oligomers during fast pyrolysis of lignin, Fuel 2014;128:170-79.

[48] T. Hosoya, H. Kawamoto, S. Saka, Secondary reactions of lignin-derived primary tar components, J Anal Appl Pyrol 2008;83:78-87.

[49] A. Demirbas, Mechanisms of liquefaction and pyrolysis reactions of biomass, Energ Convers Manage 2000;41:633-46.

CHAPTER 7

CONCLUSIONS AND FUTURE WORK

Conclusions

Thermochemical conversion of biomass was studied to understand its pyrolytic behavior and finally to overcome biomass recalcitrance for its utilization. Fast pyrolysis and solvolysis are promising thermochemical conversion technologies offering advantages over several other advanced technologies. They can convert the entire biomass into fuel and value-added products which can more economically be upgraded. There is still room to improve the performance and thus help thermochemical conversion technologies stand above other pathways. These processes require further optimization to produce products with the highest possible yields as well as value. Thus, in-depth understanding of the fundamentals behind thermochemical conversion technologies is necessary.

First, it was revealed that partial oxidative pyrolysis can improve the yield of monomeric sugar contents in bio-oil. It is believed that oxygen can break down the lignin sheath surrounding cellulose fibers, allowing levoglucosan produced from depolymerizing cellulose to escape. When it comes to passivated biomass, the effect of partial oxidation on the yield of hydrolyzable sugar yield was more significant. Additionally the presence of oxygen prevented reactor clogging by reducing the char agglomeration, which allowed the rector to run at a steady state without a pressure buildup. Heavy fraction (Stage Fraction 1) of bio-oil contained up to 67 wt% hydrolyzable sugars.

Secondly, this study focused on solvolytic conversion of lignin to alkylphenol with assistance of hydrogen-donor solvents. It was found that the solvolytic conversion of lignin

involves thermal cleavage of lignin macromolecules, followed by secondary reactions, including cracking and repolymerization among the primary products. Also, the presence of hydrogen donor solvents was found to suppress repolymerization reactions by stabilizing the primary products to alkyl-substituted phenols and promoting demethoxylation.

This study also discussed pyrolysis mechanisms of lignin using methoxy substituted α-O-4 lignin dimeric model compounds. We detected free radicals using electron paramagnetic resonance analysis. From the analysis of pyrolysis products, it was found that the reaction pathways of methoxy substituted α-O-4 dimers were complex as methoxy substitution has higher reactivity toward C – O homolysis. It was revealed that methoxy substitution promoted the formation of large molecular weight products, possibly by radical coupling reaction.

Lastly, the effort was given to elucidate the existence of free radical from condensed bio-oil and to understand its potential role in condensed-phase polymerization. From the quantitative analysis of free radicals in bio-oil, it was found that free radicals were highly concentrated in lignin bio-oil and the lignin fraction of whole bio-oil. The results clearly demonstrated that radicals are produced during pyrolysis of both carbohydrates and lignin fractions of biomass. These radicals are transformed into stable radicals in bio-oil either during pyrolysis or upon condensation to liquid.

Overall it was proven that thermochemical conversion of biomass can be affected and controlled by an external environment and its inherent nature of materials. These can be considered to improve performance of biomass conversion technologies, such as increasing the yield of value-added products or stabilizing products. These improvements should help to

make thermochemical conversion technologies a more feasible pathway to produce advanced products.

Future work

As discussed above, it was found that free radicals are present in condensed bio-oil and they are stable toward secondary repolymerization. However, the analysis of condensed products cannot provide information on the initial stage of pyrolysis. Thus, uncertainties of pyrolysis still remain, implying that a different approach is required to elucidate the pyrolytic behavior of reactive radicals. Spin trapping technique can be used to investigate the primary radical species during pyrolysis. Once the unstable radical intermediate met spin trapping reagent, for example DMPO (5,5-Dimethyl-1-Pyrroline-N-Oxide), it is transformed into stable nitroxyl radical which is detectable by EPR analysis. This can be quantified and identified, which could provide the structural information of free radical species. Study of radicals produced in pyrolysis vapor via spin trapping will be considered for future work.